Primary Production by Phytoplankton in Lake Simcoe 2010-2011

by

Tae Yeon Kim

A thesis
presented to the University of Waterloo
in fulfillment of the
thesis requirement for the degree of
Master of Science
in
Biology

Waterloo, Ontario, Canada, 2013

© Tae Yeon Kim 2013

AUTHOR'S DECLARATION

I hereby declare that I am the sole author of this thesis. This is a true copy of the thesis, including any required final revisions, as accepted by my examiners.

I understand that my thesis may be made electronically available to the public.

Abstract

Degradation of water quality, introduction of dreissenid mussels (notably *Dreissena polymorpha*) and depletion of oxygen concentrations in the hypolimnion in Lake Simcoe, Ontario prompted a study of phytoplankton primary production to inform efforts to improve the lake conditions. The characterization of algal production is critical since, as primary producers, their biomass is positively correlated with production at higher trophic levels in pelagic food webs and oxygen levels. This study was conducted from August 2010 to August 2011, including the winter season (Dec-Mar). Temporally, the lake displayed a unimodal pattern with late summer to fall production maxima. For all seasons considered, the pelagic daily areal primary production (P_{int}) was lower in the nearshore than offshore, consistent with the nearshore shunt hypothesis that mussels should be able to deplete phytoplankton more effectively in the nearshore. The sensitivity analysis revealed that chl *a* and the photosynthetic parameter P^B_{max} were the most influential variables for explaining such spatial differences. The size distribution of chl *a* and production varied where both netplankton (>20µm) and nanoplankton (2-20µm) were greatest in fall and picoplankton (<2µm) was highest in summer and early fall. A large chl *a* peak of nanoplankton was also found in late-winter (Mar) at offshore stations. The seasonal areal primary production (SAPP; May-Oct) and chl *a*:TP were significantly lower nearshore than offshore, consistent with grazing impacts from the large nearshore dreissenid mussel community. The lake as a whole is quite productive comparable to other large lakes with comparable total P concentrations and dreissenid mussel populations. The latter part of the study showed that the deep chlorophyll layer (DCL) was not as frequent as expected and was detected only 28% of time during late-spring to summer when the lake was thermally stratified (Aug-Sept 2010 and

May-Aug 2011). The percent dissolved oxygen (%) did not show any indications of elevated primary production in the DCL although the production estimates suggested that there is a substantial (an average of 55%) amount of primary production occurring below thermocline when a DCL exists. Whether or not the DCL has potential to nourish the benthic filterers (dreissenids) and has ecological significance in the lake remains unclear. Overall, the factors that control phytoplankton primary production in Lake Simcoe seem to operate somewhat differently from other large lakes and further investigation is needed to elucidate them. The analysis of primary production and biomass has improved knowledge of non-summer production and can provide guidance to site-specific P and oxygen remediation.

Acknowledgements

I would really like to thank:

Dr. Ralph Smith-For being a supportive and kind supervisor

Dr. Bill Taylor- For always giving me helpful hints and insights

Dr. Roland Hall and Jenny Winter- For their time and suggestions

Rebecca North-For being always helpful

Emilija Cvetanovska and Bianca Liang- For their assistance in the field and all the fun times in the lab

Christina Quinn- For sampling and data sharing

Joanna Majarreis (JoJo/Salmon/"Poo"h cup)- For emotional support and sitting through thousands of my practice presentations.

Laura Beecraft-For letting me borrow coffee cups when I desperately needed one

Quinn's Marina-For logistical support

Ontario Ministry of Environment, Ontario Ministry of Natural Resources, and Environment Canada-For helping out with sampling especially in winter

University of Waterloo Aquatic Ecology Group (UWEG)-For insights and useful suggestions

Environment Canada (Lake Simcoe Cleanup Fund)

NSERC (R. Smith Discovery Grant)

Dedication

This thesis is dedicated to my Father, family (Son, Julie, Derek, Erin and Soon-Young) and friends (Hanna and David) for their support and encouragement.

Table of Contents

List of Figures

Figure 2.9 Panels a-c (top) show monthly plots of ^{14}C size production (P_{opt}, µg C $\cdot L^{-1}$ h^{-1}) by size class (net, nano and pico). Panels d-f (bottom) show monthly plots of chl *a* (µg/L) by size class. August 2010 data was excluded from the analysis due to poor experimental results. Points identified as outliers (>2 standard deviations) were removed from the analysis. The solid lines represent nearshore stations (•) and WTP (□) while the dashed lines represent offshore stations (o). Each error bar is one standard error.

Figure 2.10 A modification from Smith et al. (2005). The plot shows relationship of log_{10} transformed chl *a* against TP. The arrows locate average offshore (SIO), nearshore (SIN) and total (SIT) chl *a*:TP for open water seasons (May-Oct). The solid, dashed, and broken lines represent dreissenids-present, -absent and NOLSS trend lines. Refer to table 2.6 for appropriate symbols on the plot.

Figure 2.11 Stations with SAPP estimates for May-Oct 2010-11 using 100% theoretical cloud free conditions. The units are expressed in g C m^{-2}.

Figure 2.12 A modification from Smith et al. (2005). The plot illustrates log_{10} transformed SAPP and TP for post-dreissenid Lake Erie and Lake Simcoe and pre- dreissenid NOLSS and the Great Lakes excluding Lake Erie. The arrows indicate offshore (SIO), nearshore (SIN) and total (SIT) average SAPP vs. TP over May-Oct. Refer to table 2.6 for appropriate abbreviations.

Figure 3.1 An OLS regression of extracted chl *a* vs. YSI chl *a* values for all seasons (n=94). As indicated by the *p* value on the graph, the correlation was significant and moderately strong (R^2=0.61). The middle solid line represents the slope (0.74) and the two bands around the slope are lower and upper 95% confidence interval. Prior to the analysis, the data was log_{10} transformed to stabilize the variances.

Figure 3.2 An OLS regression of log_{10} extracted and log_{10} YSI chl *a* (µg/L) for winter (Dec-Mar) except January. The two outer lines show upper and lower 95% confidence interval bands and the solid middle line shows the slope of the line. The regression equation of the model is y=0.80x + 0.14 where R^2 and *p*-value were 0.72 and <0.05 respectively.

Figure 3.3 An OLS regression of extracted chl *a* vs. YSI chl *a* values for thermally stratified seasons (Aug-Sept 2010 and May-Aug 2011; n=52). As indicated by the *p* value on the graph, the correlation was significant but weak (R^2=0.40). The middle solid line is the slope (0.50) and the two bands around the slope are lower and upper 95% confidence interval. Prior to the analysis, the data was log_{10} transformed to satisfy the variances.

Figure 3.4 An OLS regression of extracted chl *a* vs. YSI chl *a* values from Sep 2010 and May-Aug 2011 (n=41). As indicated by the *p* value on the graph, the correlation was significant (<0.05) and moderately strong (R^2=0.70). The middle solid line represents the slope (0.75) and the two bands around the slope are lower and upper 95% confidence interval. Prior to the analysis, the data was log_{10} transformed to normalize the variances. An outlier was detected and removed from the analysis.

Figure 3.5 Vertical distribution of dissolved oxygen (% saturation; solid line), chl *a* (µg/L; long-dash line) and temperature (°C; short-dash line) over depth (m) for station K42 May 2011.

Figure 3.6 Vertical distribution of % dissolved oxygen (% DO; solid line), chl *a* (µg/L; long-dash line) and temperature (°C; short-dash line) over depth (m) for station M66 July 2011.

Figure 3.7 An example of subsurface chl *a* maximum in well-mixed shallow water. Vertical profiles of % dissolved oxygen (% DO; solid line), chl *a* (µg/L; long-dash line) and temperature (°C; short-dash line) over depth (m) is shown for station N32 August 2010.

Appendix Figure 1.1 A plot of predicted P_{int} (mg C m^{-2} d^{-1}) and P_{avg} (mg C m^{-3} d^{-1}) for the WTP samples. Most of the samples were sampled on a monthly basis except for March (n_{Mar}=2) and April (n_{Apr}=3). A total of 12 WTP samples were collected over the course of the study.

Appendix Figure 1.2 WTP PI parameters. a) The left figure shows light utilization efficiency (α^B; (mgC/(mg chl Ein m-2)) plotted against the sampled date b) The right figure shows the rate of light saturation (P^Bmax; mgC/(mg chl hr)) versus the sampled date. The PI parameters were derived using the program, PSPARMS.

Appendix Figure 1.3 Extracted chl *a* (µg/L) values for WTP across the sampled dates.

Appendix Figure 1.4 A plot of P_{int} (mg C m^{-2} d^{-1}) and P_{avg} (mg C m^{-3} d^{-1}) for transitional sites (S15 and C9). The station S15 (•) was collected throughout the study period (n_{S15}=7) except October, January, April, June and August. Similarly, station C9 (x) was sampled 7 times over the course of the study except October, January, March, April, June and August.

Appendix Figure 1.5 PI parameters for transitional stations a) The left figure shows light utilization efficiency (α^B; (mgC/(mg chl Ein m-2)) against the sampled date b) The right figure shows the rate of light saturation (P^Bmax; mgC/(mg chl hr)) against the sampled date. The PI parameters were generated using the Fee program (1990), PSPARMS. Station S15 was represented by the solid dot (•) and the station C9 as "x".

Appendix Figure 1.6 Extracted chl *a* values (µg/L) for transitional sites- C9 (•) and S15 (x).

Appendix Figure 2.1 A plot of $\log_{10}$ transformed fluoroprobe chl *a* vs. YSI chl *a* (µg/L) for all the available seasons (n=73). The equation of the line is y=1.20x-0.40 and the R^2 is 0.62. The middle line represents the slope and the other two lines show upper and lower 95% confidence interval. The *p*-value that the slope of the regression line is zero was <0.05.

Appendix Figure 2.2 The model I linear regression of $\log_{10}$ transformed fluoroprobe and extracted chl *a* (n=73). The slope is 1.05 and the y-intercept is -0.34 (y=1.05x-0.34). The R^2 was 0.41 and the significance of the slope of the regression line being zero was p<0.05.

List of Tables

Table 3.5 The parameters from the model I regression for the thermally stratified months only (Aug-Sep 2010 and May-Aug 2011). These parameters include the coefficient (slope (0.50) and intercept (0.07)), the std error and the lower and upper 95% of confidence interval. All of the data is $\log_{10}$ transformed prior to the analysis.

Table 3.6 Analysis of variance of YSI and extracted chl *a* values for the thermally stratified period (Aug-Sep 2010 and May-Aug 2011). The parameters include sum-of-squares, degrees of freedom (df), mean-square, F-ratio as well as *p*-value. All of the data is $\log_{10}$ transformed.

Table 3.7 The parameters from the model I regression for the thermally stratified months excluding August 2010 (Sep 2010 and May-Aug 2011). The coefficients (slope (0.75) and intercept (0.052)), the std error and the lower and upper 95% of confidence interval are provided. All of the data is $\log_{10}$ transformed. One outlier was omitted from the analysis.

Table 3.8 Analysis of variance of YSI and extracted chl *a* values for the thermally stratified period from Sep 2010 and May-Aug 2011. The parameters include sum-of-squares, degrees of freedom (df), mean-square, F-ratio as well as *p*-value. All of the data is $\log_{10}$ transformed. Also, an outlier was taken out from the analysis.

Table 3.9 Major axis, a type of model II regression was used to test the significance of slope based on the model log(y)=blog(x)+*a* where *a*=intercept, b= slope of the line and x=dependent variable (YSI chl *a*) and y=independent variable (extracted chl *a*). The coefficient of determination (R^2) and the lower and upper 95% confidence intervals of the OLS (ordinary least squares) and MA slopes and intercepts are provided below.

Table 3.10 Summary of all offshore stations (K42, K45 and M66) sampled from Aug-Sept 2010 and May-Sept 2011. The seasonal thermocline was defined as >1.0 C m^{-1} temperature gradient and the Z_{eu} (m) is the depth of photic zone (1% light level). DCL:SML is the ratio of average chl *a* concentration measured in DCL and SML.

Table 3.11 The offshore stations (Z_{max}= >15m; Aug-Sept 2010 and May-Aug 2011) with DCL identified by vertical water column profiles using YSI. The surface mixed layer (SML) chl *a* represents the average epilimnetic chl *a* (µg/L) taken from YSI vertical profiles of chl *a*. The top depth of DCL (m) is the starting depth at which the subsurface chl *a* levels exceed two times of epilimnetic concentrations, usually below or at thermocline. The bottom depth of DCL (m) is the depth where DCL no longer exists (SML chl *a* ≥DCL chl *a*). Then, the chl *a* concentration in DLC is determined by averaging the chl *a* over the depth in which DCL is present, and the DCM is the maximum average chl *a* concentration (µg/L) over a meter found within DCL. The percentage of dissolved oxygen (%DO) is also included in the table, as taken from YSI.

Table 3.12 Using the Fee model, P_{int} (mg C m^{-2}) and P_{avg} (mg C m^{-3}) for offshore stations (Z_{max}= >15m; Aug-Sept 2010 and May-Aug 2011) were estimated based on 100% theoretical cloud free condition. All the parameters were kept the same as the epilimnetic samples and chl *a* values

were entered below surface mixed layer to Z_{max}. Percent Epilimnion (% Epi) is the percent of daily primary production occurring in the epilimnion. The outputs from the model also include mean PAR (µEin m^{-2} sec^{-1}) up to and below Z_{mix} and the onset of light saturation (I_k, µmol m^{-2} sec^{-1}).

Appendix Table 1.1 Summary of linear mixed effects model output of different variables (Aug 2010-Jul 2011). The bolded numbers indicate significance ($P<0.05$).

Appendix Table 1.2 Summary of predicted production (P_{int} and P_{avg}) for Beaverton water treatment plant (WTP) based on the incident irradiance, theoretical 75%- and 100% cloud-free model. Photosynthesis-irradiance (PI) parameters were generated using the program PSPARMS; however, other parameters (Kd_{PAR}, Z_{mix}) were based on other stations ("assumed station", E50, E51, T2) located close to WTP that were sampled within the same month. Throughout the calculation, the production model assumed that the extracted chl *a* values from the WTP samples were same throughout the depth. Also, the Z_{max} for WTP was assumed to be 7.6m. Otherwise, the units for the variables are: α^B (mgC/(mg chl Ein m-2)); P^B_{max} (mgC/(mg chl hr)); chl *a* (µg/L); P_{int} (mg C m^{-2}); P_{avg} (mg C m^{-3}).

Appendix Table 1.3 Daily areal and volumetric productions for transitional site (~15m; S15, C9). The production estimates were based on the incident irradiance, theoretical 75%- and 100% cloud-free model. The programs DTOTAL and DPHOTO were used to generate P_{int} (mg C m^{-2} d^{-1}) and P_{avg} (mg C m^{-3} d^{-1}). The production was calculated using the integrated epilimnetic samples except in February (station C9) and March (station S15) when the sampled were collected within a meter from the surface ('surface'). The units for the variables were: Z_{samp} (m); Z_{mix} (m); α^B (mgC/(mg chl Ein m-2)); P^B_{max} (mgC/(mg chl hr)); chl *a* (µg/L).

Appendix Table 2.1 Summary table of the coefficients (slope and intercept), standard error of the estimate (Std error) and 95% confidence interval from the model I linear regression of $\log_{10}$ transformed fluoroprobe and YSI chl *a*. Two outliers were identified and were removed from the analysis.

Appendix Table 2.2 Table of analysis of variance. The list of parameters (sum-of-squares, degree of freedom (df), mean square, F-ratio and *p*-value) are summarized. All values remained $\log_{10}$ transformed. Two outliers were omitted from the analysis.

Appendix Table 2.3 Table of coefficients (slope and intercept), standard error of the estimate (Std error) and 95% confidence interval from the model I linear regression of $\log_{10}$ transformed fluoroprobe and extracted chl *a*. Two outliers were excluded from the analysis.

Appendix Table 2.4 Analysis of Variance**.** The list of parameters (sum-of-squares, degree of freedom (df), mean square, F-ratio and *p*-value) are summarized. The values remained $\log_{10}$ transformed. Also, two outliers were omitted from the analysis.

Chapter 1- General Introduction

Lake Simcoe

Lake Simcoe is the largest lake in southern Ontario (722 km^2) after the Laurentian Great Lakes. The lake is a valuable resource to the province where the coldwater fishery alone yields $100 million annually (Evans et al. 1996, Eimers et al. 2005) contributing to about 15% of the angling effort in Ontario. Other recreational pursuits are worth $200 million in annual revenue and Lake Simcoe is a source of drinking water to eight municipalities (Nicholls 1992, Palmer et al. 2011). However, after the European settlement in the 1790s (North et al. 2012), the ecological health of Lake Simcoe has been continuously degrading. Some of the main concerns about the lake include excessive loading of phosphorus (P), oxygen (O_2) depletion in the hypolimnion, degradation of water quality and introduction of invasive species notably zebra mussels (*Dreissenia polymopha*). The concerns over water-quality degradation by multiple stressors in the lake prompted Ontario Ministry of the Environment (OME) to initiate water sampling during 1971 to 1974 in an attempt to manage and improve the conditions of lake (Nicholls 1995). Since then, the work was further extended as a collaborative initiative involving the Ministry of Natural Resources (MNR) and the Lake Simcoe Region Conservation Authority (LSRCS) under the program, Lake Simcoe Environmental Management Strategy (LSEMS) (Nicholls 1995). Consequently, the early 1990's saw a marked reduction in external P loading from an average of 114 tonnes/yr to 67 tonnes/yr (Winter et al. 2007). Managing anthropogenic P input is crucial because excessive P loading is often linked with coldwater fish stock failure (as occurred in the 1960s) and also enhances the growth and biomass of phytoplankton. The increase in the

phytoplankton can be problematic for the lake because they can eventually settle and decompose consuming substantial O_2, resulting in hypoxia during late-summer.

In Lake Simcoe, zebra mussels were first sighted in the fall of 1992, and they expanded abundantly in numbers by 1995 (Evans et al. 2011). Based on data from 2008, the average dreissenids biomass was 27.2 g shell-free dry mass (SFDM/m^2) in the main basin of Lake Simcoe and 12.4 g SFDM/m^2 in nutrient-rich Cook's Bay (Ozersky et al. 2011).

Primary production and its measurement in plankton communities

The energy flow in an ecosystem is essential to organisms in that system. A widely accepted definition of 'production' is an energy flow or flux of mass and/or energy in an area over time (Wetzel 2001). The term refers to the formation of new organic materials over a period of time, and also includes any losses from respiration, secretion, excretion, grazing and death (Wetzel 2001). Primary production is thus based primarily on photosynthesis, which can be schematically summarized as:

$$6CO_2+12H_2O + \text{light} \rightarrow C_6H_{12}O_6 + 6H_2O + 6O_2$$

Gross photosynthesis refers to the rate of photosynthesis before any losses, including respiration (Bender et al. 1999). It is a rate of light dependent reactions where electrons flow from water to terminal electron acceptors (Lawlor 2001, Falkowski and Raven 2007), the net result being the reduction of CO_2 to organic matter. Respiration is a process that converts organic

carbon (e.g. glucose) into inorganic carbon (CO_2) (Cole and Pace 1995). Thus, gross photosynthesis includes all photosynthetic carbon fixation without considering any losses such as excretion or respiration (Falkowski and Raven 2007).

Gross primary production is the community-level equivalent to gross photosynthesis and is defined as the total amount of electron equivalents generated from the photochemical oxidation of water (Falkowski and Raven 2007). Net primary production is gross primary production minus respiratory losses of carbon (Falkowski and Raven 2007) and is defined as the net formation of organic carbon by photosynthetic processes in autotrophic organisms over a period of time that has an ecological relevance (Lindeman 1942, Williams 1993). In sum, primary production is a rate at which organic substances are produced from photosynthetic activities to be used by the community (Kalff 2002). It is imperative to study phytoplankton primary production since the production represents a major input of organic matter in aquatic systems (Wetzel 2001). Phytoplankton primary production supports aquatic food webs and contributes to a considerable input of organic matter and potential energy that drives the ecosystem (Wetzel 2001). As a result, phytoplankton production has been extensively studied and measured in different ecosystems, especially in large lakes and oceans (e.g. Fahnenstiel and Scavia 1987, Fee et al. 1992, Smith et al. 2005, Depew et al. 2006, Bocaniov and Smith 2009).

Despite the need to understand primary production, measurements in nature can be difficult primarily because the effects of respiratory losses are virtually impossible to measure accurately on a routine basis (Li and Maestrini, 1993). One widely accepted method involves using radioactive ^{14}C-labelled bicarbonate to measure values that can be close to gross

production (Smith et al. 2005; Depew et al. 2006, Falkowski and Raven 2007). However, some investigators suggested that ^{14}C tracer methods measure values intermediate between gross and net production (Beardall et al. 2009). Fahnenstiel and Scavia (1987) argued that the ^{14}C uptake method may yield an underestimation of gross production and an overestimation of net production. However, such problems are minimized by shortening the incubation time (~1 hour) to redue respiration losses (Fahnenstiel et al. 1987, Beardall et al. 2009). Another issue is that experiments are commonly conducted under artificial light that differs from nature and among investigators (Boney 1989), creating discrepancies between studies (e.g. Millard 1996, Smith et al. 2005). Nonetheless, ^{14}C methods have allowed primary production to be extensively studied and measured in different lakes including the eastern (e.g. Smith et al. 2005, Depew et al. 2006) and western basin of Lake Erie (e.g. Smith et al. 2005), Lake Ontario (e.g. Millard et al. 1996), Lake Michigan (e.g. Fahnenstiel et al. 1987, Fahnenstiel et al. 2010) and Oneida Lake (Idrisi et al. 2001) because it is precise, sensitive and efficient.

Environmental controls on phytoplankton production

Light and temperature

Approximately 50% of incoming solar radiation is the photosynthetically active radiation (PAR) which is a segment of the solar spectrum that is visible to the human eye (400-700nm, Kirk 1994). Solar radiation is crucial to aquatic ecosystems partly because absorption and dissipation of heat have profound impact on the circulation and thermal structure in lakes (Wetzel 2001). Light also has taxon-specific influences on photosynthesis and algal growth

(Wetzel 2001). In nature, incoming solar radiation experiences scattering and absorption in the atmosphere (Kirk 1994). Scattering by air and dust particles, and absorption by ozone, $CO_{2,}$ oxygen molecules and most of all, water vapour significantly attenuate solar radiation and alter the incident spectrum (Kirk 1994). Cloud cover also influences light penetration where a small amount of cloud cover can increase up to 5-10% of the total extraterrestrial irradiance that reaches Earth (Kirk 1994). Once in the water, attenuation and spectral modification is much stronger, with the blue and green wavelengths typically penetrating better than violet or red (550nm) (Kirk 1994).

Once light is available for photosynthesis, light harvesting complexes (LHC) in phytoplankton cells act as antennae in absorbing the incoming photons and transmitting much of the energy to the photosynthetic electron transport systems (Falkowski and Raven 1997). Under low light (e.g. turbid water) the rate of plankton photosynthesis is limited by the rate of photon absorption (Falkowski and Raven 1997). It is governed by photochemical reactions that are largely temperature independent except at temperatures below <5℃ (Kalff 2002). At high saturating light conditions, on the other hand, the rate of photon absorption exceeds the electron transfer in the electron transport rate (ETR) (Falkowski and Raven 2007), and the rate-limiting step is temperature-regulated biochemical reactions rather than photochemical reactions (Kalff 2002). In some cases, combinations of high light and excessive exposure to ultraviolet (UV) radiation at the surface of the lake (within a few meters on a summer day) can cause photooxidative damage in the cell, leading to photoinhibition (Hiriart et al. 2001).

In temperate zone lakes there is a pronounced annual cycle of heat content and thermal structure. Many lakes, including Lake Simcoe (Stainsby et al. 2011), have a temperate dimictic cycle of thermal stratification with two mixing periods (spring and fall) separated by two periods of thermal stratification (winter and summer). Winter stratification is possible in Lake Simcoe because it forms ice cover. The annual cycle of solar radiation input and thermal structure produces strong seasonal variations in light availability for primary production, with particularly low values under ice and snow cover in winter (e.g. Twiss et al. 2011). Higher irradiance values in the water column in spring and summer are accompanied by higher temperatures, which can accelerate photosynthetic enzyme function (Falkowski and Raven 2007). The depth of surface mixing in summer (which defines the epilimnion thickness) affects light availability during the summer stratified season, with deeper mixing producing lower average irradiance for the epilimnetic phytoplankton (e.g. Guildford et al. 2005). Mixing depths increase during autumn until stratification breaks down, creating a season of strongly diminishing light availability as well as falling temperatures. The annual cycle of stratification and mixing is important not only for light and temperature environments, but also for nutrient availability.

Nutrients

Nutrients are crucial to phytoplankton for their growth and survival. The main nutrients essential to phytoplankton cells include phosphorus (P), nitrogen (N) and iron (Fe) (e.g. Schindler 1977) and are categorized as either macro- (e.g. nitrogen, phosphorus) and micronutrients (e.g. iron). The availability of nutrients depends on factors such as the initial

loading (e.g. point sources), mixing energy of a lake (e.g. resuspension, recycling), amount of organic matter, and algal biomass (e.g. competition).

In a given system, the element supplied at the lowest rate relative to the rate of demand is the limiting nutrient for phytoplankton (Wetzel 2001) but the limitation is naturally expected to vary between phytoplankton given that nutrient requirements differ among species. In any case, if phytoplankton experience nutrient limitation, the overall performance (metabolism and production) may be reduced.

The major source of nutrients for phytoplankton during much of the growing season is internal recycling, so there is a strong correlation between the rate of nutrient recycling and primary production (Essington and Carpenter 2000). This means that the processes that influence the magnitude and the rate of nutrient recycling can exert a dramatic effect on the plankton production. The deeper mixed layer of a lake can promote and enhance nutrient retention and, hence, availability of nutrients that would increase the primary production (Fee et al. 1994). Organisms such as zooplankton and dreissenid mussels contribute to regeneration of nutrients via excretion (Arnott and Vanni 1996)

Phosphorus is a limiting nutrient in many temperate lakes (Wetzel 2001, Kalff 2002). The source of P in lake systems is primarily through direct atmospheric deposition, run-off waters, and regeneration of P from the benthos, although most of total P is not bioavailable (Wetzel 2001). Phosphorus is needed in the cell for production of RNA and DNA (Bjorkman and Karl 2003), structural components such as phospholipids, and energy intermediates such ATP and

ADP (Wetzel 2001). In low nutrient (oligotrophic) and unproductive lakes, a pulse of P input (e.g. effluents) can significantly increase algal production for a certain period of time until P is available again (Wetzel 2001).

Nitrogen (N) is also a crucial nutritional component of algae. Some of the nitrogen sources include atmospheric deposition, lightning, sediments, precipitation, effluents and groundwater drainage (Wetzel 2001). The most bioavailable form of nitrogen is NH_4^+, and nitrogen is used for the production of proteins and amino acids (Wetzel 2001).

Iron can be also limited in freshwater lakes and it is used as a cofactor of enzymes in phytoplankton (Wetzel 2001). Iron is biologically available in the epilimnion when it can form complexes with organic matter.

Availability of all nutrients is affected by annual stratification and mixing cycles. In spring and fall when the denser and cooler surface water of the epilimnion gradually mix with the other lower strata, nutrients are relatively high (Wetzel 2001) compared to stratified seasons because nutrients are mixed in from deeper waters and from the sediments. As summer approaches, on the other hand, thermal stratification develops and nutrients (in particulate form) sink to the bottom, no longer available for phytoplankton in the surface layer. In winter, an inverse thermal stratification forms that isolates suspended phytoplankton from sediment sources of nutrient, but there tend to be relatively high concentrations of inorganic nutrients thoughout the water column due to diminished demand (Wetzel 2001).

Temporal and spatial patterns of phytoplankton production

Phytoplankton production rates show strong seasonality and differences between depth zones (nearshore and offshore) in large lakes due to differences in light, temperature and nutrient environments and to variations in the biotic environment (e.g. parasites, predators). In typical temperate dimictic lakes, it is generally accepted that the planktonic seasonal succession pattern involves spring and fall biomass maxima that consist of large, fast-sinking cells such as diatoms (Fahnenstiel and Scavia 1987, Carrick et al. 2001, MacDougall et al. 2001). The spring bloom is an essential feature of the seasonal algal production contributing significantly to the total annual production (Sommer and Lewandowska 2011). In some cases, low nutrient lakes that are situated at high latitude appear to have a single spring peak that supports the pelagic food webs (Sommer and Lewandowska 2011). However, at times, a chl *a* peak in fall is observed, as seen in Lake Simcoe (Nicholls 1995) and the eastern basin of Lake Erie (MacDougall et al. 2001). In winter, in contrast to spring and fall, often low production are observed consisting of small flagellates that are adapted to low light and temperature conditions (Wright 1964, Wetzel 2001, Vehmaa and Salonen 2009). In summer when the water is thermally stratified, the production is typically higher than winter but lower than other seasons mainly due to nutrient limitation and sedimentation (Hecky et al. 1986, Jensen et al. 1994, Wetzel 2001).

The nearshore shunt as proposed by Hecky et al. (2004) is a conceptual model that describes the dynamics of nutrients and energy as a consequence of re-engineering of Great Lakes ecosystems by dreissenids. The model postulates that dreissenids have retained nutrients (e.g. N and P) at the nearshore where they are retained and readily consumed by benthic algae such as the nuisance *Cladophora* sp (e.g. Higgins and Vander Zanden 2011). Spatially, some of

the measurements conducted in the 1970s (Lakes Ontario, Erie and Michigan) suggested higher phytoplankton production and biomass in the nearshore of the lake, rather the offshore (Glooschenko et al. 1973, Rousar 1973). Some recent findings after the invasion of mussels, however, show support for higher production in the offshore compared to the nearshore such as in the eastern basin of Lake Erie (e.g. Depew et al. 2006). Other than the direct primary production measurements from Lake Erie, selective decreases of chl *a* in nearshore of Lakes Michigan (Carrick et al. 2001) and Ontario (Hall et al. 2003) were observed after the mussel invasion.

Dreissena polymorpha

Although not all introduced species are regarded as invasive, approximately 10% of the non-indigenous species that arrive in an ecosystem become invasive and pose severe threats to that system (Mill et al. 1993). Amongst the successful biological invaders of North American freshwater are zebra mussels (*Dreissena polymorpha*). Due to their rapid expansion throughout the North American freshwaters, the total cost for repairing drinking water intakes, power facilities and other infrastructures were estimated to be ~267 million dollars, with an ongoing cost of ~11-16 million dollars per year (Higgins and Vander Zanden 2010). In addition, the dreissenids often pose a threat to the biological integrity (Hecky et al. 2004, Fahnenstiel et al. 2010) through altering the light regime (e.g. Fishman et al. 2000; Stasio et al. 2007), nutrient dynamics (e.g. Fahnenstiel et al. 1995, Karatayev et al. 1997, Hecky et al. 2004) and other trophic effects such as an increase in the littoral benthic community (Idrisi et al. 2001, Higgins and Vander Zanden, 2010). At times, the selective filtering behavior of dreissenids is associated

with shifts in phytoplankton community as observed in some inland freshwater bodies, such as the Saginaw Bay, Lake Huron (Fishman et al. 2009) and Lake Simcoe (Winter et al. 2011). Dreissenids are capable of filtering a wide size spectrum (0.7-450 µm) (Lavrentyev et al. 1995) and have preferences for different phytoplankton size groups (Smith et al. 1998, Nicholls et al. 2002, Barbiero et al. 2006, Winter et al. 2011). During open water season, when it is optimal for dreissenid growth (8-25 ℃), nanoplankton (2-20 µm) are more readily grazed than smaller and larger cells (Barbiero et al. 2006). Sometimes, the consumed larger cells may be unpalatable to mussels and are largely excreted as a form of pseudofeces via exhalant siphon where the discharged cells survive and continue to contribute to the production and biomass (Baker et al. 1998; Vanderploeg et al. 2001, Naddafi et al. 2007). During thermally stratified seasons, the larger cells (>20 µm) are lower in numbers compared to the other seasons, because lower surface to volume ratio allows the netplankton to be more prone to sinking.

Based on the observations from other large comparable lakes, the mussel effects on phytoplankton should vary both seasonally and spatially (e.g. Carrick et al. 2001, Depew et al. 2006). The nearshore shunt proposes that dreissenids can especially exert strong impact in the shallow nearshore waters, where mixing facilitates access to phytoplankton (Hecky et al. 2004). Some studies also reported that the establishment of zebra mussels is strongly related to lower chlorophyll *a* (chl *a*) to total P ratio (chl *a*/TP) as seen in the nearshore of Lake Erie, western Lake Ontario and the Detroit River (Nicholls et al. 1999). A lower chl *a*:TP is observed when zebra mussels exert high grazing rates that significantly decrease the phytoplankton population (Nicholls et al., 1999). In Lake Erie, after the arrival of the mussels, chl *a*:TP was found to be 2-6 times lower than the pre-mussel period (Nicholls et al. 1999). However, trends in chl *a*:TP after

dreissenid invasion remains controversial because some lakes including Oneida Lake (Idrisi et al. 2001), Lake Huron, central and eastern Lake Ontario and upper St. Lawrence River showed no clear trend in chl *a*:TP reduction (Nicholls et al. 1999). Based on the re-evaluation of the empirical relationship, Young et al. (2011) found an increase in chl *a*:TP in Lake Simcoe after the arrival of dreissenids, which differ from some of the observations made in the Great Lakes.

The Deep Chlorophyll Maximum (DCM)

Biomass is the mass or weight of biological material expressed as mass per unit area or volume (Wetzel 2001). Often, chl *a* concentration is a proxy for phytoplankton biomass because all photosynthetic organisms contain the pigment (Cullen 1982). However, the interpretation of chl *a* concentration needs care because chlorophyll is a small (average 1%) but variable part of the dry weight of phytoplankton cells (Cullen 1982).

The deep chlorophyll maximum (DCM) and deep chlorophyll layer (DCL) are features that have been widely documented across different aquatic environments including oceans, estuaries and freshwater lakes (Fahnenstiel and Scavia 1987, Barbiero and Tuchman 2001).DCL is defined as a region that show elevated levels of chl *a* below or at the thermocline. Development of DCM and DCL typically occur from early to late summer when thermal stratification is present. In late summer, as the thermocline gradually dissipates, a deepening of the DCM and DCL is often observed (Fahnenstiel and Scavia 1987, Smith et al. 2005). The formation of DCM and DCL is also dependent on the water quality. For example, Lake Michigan experienced a larger DCL in the 1980s due to enhanced water quality associated with

zooplankton grazing (Fahnenstiel and Scavia 1987). At times, upwelling of nutrients from the lake bottom may help sustain the DCM and DCL as well (Klaumeier and Litchman 2001).

The importance of seasonal DCM and DCL is recognized in transparent, oligotrophic lakes because often DCM can constitute a significant portion to the total production (Fahnenstiel and Scavia 1987) and influence trophic transfer in the system (Malkin et al. 2012). However, in some systems, the contribution of DCM and DCL to total production is less important (Millard 1996) such as in east basin of Lake Erie (Smith et al. 2005). In some cases, the presence of a DCM is accompanied by production and biomass maxima provided that there is sufficient light and nutrients to support it (Fahnenstiel and Scavia 1987). More recent studies, on the other hand, show that the DCM could be a result of elevated levels of chl *a* without having high production or biomass (Barbiero and Tuchman 2001). For instance, elevation of chl *a* may be present near the pycnocline under low light conditions because of high phytoplankton chl *a* content per cell (Cullen 1982).

The DCL is viewed as an important food resource for mussel growth at shallow depths (Malkin et al. 2012, Schwab et al. submitted). In Lake Ontario, for instance, DCM supported significant mussel growth at intermediate depths (10-15m) in early summer but no growth was detected in late summer when DCM dissipated (Malkin et al. 2012). At times, however, mussels may also affect the DCL. In recent years, mussel-impacted lake Lake Michigan experienced a significant reduction in its spring bloom primarily due to increased number of mussels which was also coincident with diminished DCL (Fahnenstiel et al. 2010).

Objectives

In Lake Simcoe, many collaborative efforts led to reductions in the external P loading (Winter et al. 2007). Controlling and managing P input is crucial because excessive amounts of P can lead to increased phytoplankton production and biomass, which are largely sedimented and decomposed consuming O_2 in the process. In Lake Simcoe, fishing is an important recreational pursuit and the oxygen depletion in the deeper waters can negatively affect the coldwater fishery. In recent years, several attempts were made in order to meet the target of minimum volume-weighted hypolimnetic dissolved oxygen concentration (MVWHDO) of 7 mg/L to restore the self-sustaining coldwater fish population (Eimers et al. 2005). However, the oxygen level is still low (average 4.3 mg/L 1998/99-2003/04) and can potentially pose threat to coldwater fish such as Lake Trout and whitefish (Winter et al. 2007).

Despite the fact that phytoplankton primary production is strongly associated with oxygen depletion, no previous primary production measurements have been reported. The phytoplankton production that leads to hypoxia can occur outside of summer when mussel effects are less; so for example, Lake Simcoe may experience a large amount of planktonic production composed of large rapidly sinking cells in winter to early spring. Thus, analysis of primary production and biomass (chapter 2 and 3) will help to understand the contribution of non-summer production and provide guidance to site-specific P and oxygen remediation, leading to more effective management in the future. In Chapter 2, a primary objective was to define the annual cycle of primary production and chl *a* biomass with particular attention to whether spring and summer dominate (as they do in many comparable lakes) or whether fall and winter production may be important as well. In parts of Lake Erie, MacDougall et al. (2001) noticed

summer-fall peaks in some years of the study, and Nicholls (1995) reported a fall phytoplankton biovolume peak in Lake Simcoe that may suggest significant fall production, possibly extending into winter. The possibility of high production events during the ice-covered season (Twiss et al. 2011) has not been examined in Lake Simcoe.

The second major objective was to obtain insight into the effects of zebra mussels on phytoplankton productivity through analysis of nearshore versus offshore differences and comparisons against other lakes. Provided that zebra mussels are abundant, especially in the nearshore, the spatial differences (nearshore and offshore) can help elucidate the affects of dreissenids as seen in other lakes (Smith et al. 2005, Depew et al. 2006). Often, examining the yield of chl *a* and primary production relative to TP can further discriminate any differences that might reflect the impacts of dreissenids (e.g. Smith et al. 2005). In general, lakes without dreissenids have some tendency to yield higher chl *a*:TP compared to mussel-impacted lakes (Cha et al. 2012), especially when zebra mussels exert high grazing pressure on phytoplankton population (Nicholls et al. 1999). An inter-lake (non-mussel and mussel-impacted) comparative analysis of chl *a*:TP and primary production:TP between Lake Simcoe and other large oligotrophic and mesotrophic lakes will be conducted in order to better understand the role of mussels in a broader context (e.g. Smith et al. 2005).

The third major objective (addressed in chapter two) was to test how the seasonal and zonal abundance and production of different phytoplankton size classes may reflect the influence of mussels and other environmental factors, while affecting the rate of export of organic matter through sedimentation or grazing. In particular, I sought to determine whether production peaks

(especially in spring) were also peaks for abundance and production of the larger sized phytoplankton (e.g. Fahnenstiel et al. 2010) and whether there was evidence for preferential consumption of certain size classes by zebra mussels.

Chapter three has the major objective of determining the concentrations and frequency of the DCM and DCL during thermally stratified seasons to provide guidance as to whether the DCM and DCL may be important for primary production and food webs in Lake Simcoe. In clear, oligotrophic lakes including Lakes Michigan, Ontario and Superior, DCM and DCL can contribute significantly to the total primary production (Fahnenstiel and Scavia 1987, Malkin et al. 2012) and recent studies show that DCL may be important in nourishing the mussels (Malkin et al. 2012). There are no previously published reports of a DCM or DCL for Lake Simcoe.

Chapter 2- Spatial and temporal dynamics of phytoplankton production and size distribution in a large oligo-mesotrophic lake (Lake Simcoe)

Overview

Lake Simcoe has received a substantial amount of attention in recent years due to concerns over water quality, hypoxia and invasive species, notably dreissenid mussels. Phytoplankton are directly connected to such issues but their primary production rates have never been reported for Lake Simcoe. This study used ^{14}C methods to determine the temporal and spatial variations, and size distributions, of phytoplankton primary production in the lake. From August 2010 to July 2011, including the winter season (Dec-Mar), the daily areal primary production (P_{int}) ranged from 0.1 to 814.3 mg $C \cdot m^{-2}$ d^{-1} and the average volumetric production in the photic zone (P_{avg}) from 0 to 146.9 mg $C \cdot m^{-3}$ d^{-1}. A fall maximum was detected in both production and chlorophyll *a* concentration (chl *a*), and the nearshore sites (<15m) had lower values than offshore (>15m) except in summer. Chl *a* concentrations and the photosynthetic parameter P^B_{max} accounted for most of the difference in production between nearshore and offshore. Netplankton (>20µm) and nanoplankton (2-20µm) production was maximal in fall and nanoplankton also dominated production from late winter through early summer. Picoplankton (<2µm) production was greatest in summer and early fall. Nanoplankton and especially netplankton were more important offshore than nearshore. Winter production was low but a large pulse of nanoplankton chl *a* occurred in late-winter at offshore sites. Seasonal (May-Oct.) areal primary production and chl *a*:total P ratios were lower nearshore than offshore, consistent with grazing impacts from the large nearshore dreissenid mussel community. The

lake as a whole had primary production rates comparable to, or higher than, other large lakes with comparable total P concentrations and dreissenid mussel populations.

Introduction

Lake Simcoe is the second largest lake in southern Ontario (722 km^2) next to the Laurentian Great Lakes. The lake is a valuable resource to the province, with the recreational coldwater fishery alone yielding $100 million annually (Eimers et al. 2005, Palmer et al. 2011) and contributing to about 15% of the angling effort in Ontario. Other recreational pursuits are worth $200 million in annual revenue and Lake Simcoe is also a source of drinking water to eight municipalities (Nicholls 1992, Palmer et al. 2011). However, after the European settlement in the 1790s, the ecological health of Lake Simcoe has been continuously degrading (North et al. 2012). Some of the main concerns of the lake include excessive nutrient loading of phosphorus (P), oxygen depletion in the hypolimnion with consequent loss of cold water fish habitat, degradation of water quality and introduction of invasive species, notably zebra mussels (*Dreissena polymorpha*).

The lake possesses a relatively large area of nearshore water with high mussel biomass (Ozersky et al. 2011), and there is sufficient mixing in nearshore that mussels have access to the phytoplankton in most of the water column much of the time. Considering experience in other large mussel-colonized lakes (e.g. Vanderploeg et al. 2002, Fishman et al. 2009, Fahnenstiel et al. 2010), we anticipate that mussels should have considerable impact on phytoplankton in Lake Simcoe. The evidence supporting a strong and sustained impact of mussels on phytoplankton biomass and chl *a* is nonetheless mixed or absent (Winter et al. 2011, Young et al. 2011). A decrease in phytoplankton biovolume was observed immediately after the establishment of mussels (Eimers et al. 2005) but was not sustained (Winter et al. 2011). Furthermore, chl *a*:TP ratios increased for several years after the colonization of mussels before declining again, and a

chl *a*:TP model derived from mussel-free inland lakes made good predictions of chl *a* in Lake Simcoe despite presence of mussels (Young et al. 2011). At the same time, Winter et al. (2011) noted changes in phytoplankton community composition coincident with mussel colonization. A trend to decreased ice cover and delayed onset of thermal stratification (Stainsby et al. 2011) has likely contributed to the changes in phytoplankton community structure (Hawryshn et al. 2012), yet the timing and sustained nature of the changes suggests a connection to the mussels.

Based on the observations from other large comparable lakes, the mussel effects on phytoplankton should vary both seasonally and spatially (e.g. Carrick et al. 2001, Depew et al. 2006). The nearshore shunt proposes that dreissenids can especially exert strong impact in the shallow nearshore waters, where mixing facilitates access to phytoplankton (Hecky et al. 2004). In Lake Simcoe, the difference of effect between nearshore and offshore should be particularly strong because mussels are essentially confined to the nearshore (<20m) at present (e.g. Ozersky et al. 2011). In fact, there is evidence from surveys in summer months for lower chl *a* biomass at nearshore than offshore stations in Lake Simcoe (Guildford et al. in review). Even in nearshore waters, however, stratification can impede mussel assess to phytoplankton during some seasons (Ackerman et al. 2001, Boegman et al. 2008) and the activity of zebra mussels is thought to be inhibited by temperatures below 8°C (Schneider 1992, Mills et al. 1996). While temporal and spatial variation of mussel effects in Lake Simcoe should be strong, most analyses to date have focused on average conditions from spring through fall, and with little systematic attempt to differentiate nearshore from offshore conditions.

Different measures of phytoplankton biomass, notably phytoplankton biovolume and chl *a*, have shown some discrepancies in Lake Simcoe (Eimers et al. 2005). While biovolume is arguably the most direct and accurate measure of phytoplankton biomass in natural plankton samples (Conroy et al. 2005), neither chl *a* nor biovolume is truly a direct measure of biomass or carbon content. Deriving biomass and carbon contents entails conversion factors (e.g. of mass or carbon content per volume of phytoplankton cells) that are often extrapolated from limited calibration studies and assumed constant, even though environmental variation and taxon-specific properties can affect the stoichiometry and energy density of phytoplankton material (Falkowski and Raven 2007). Trends detected in chl *a* or biovolume may not always reflect accurately on the potential of phytoplankton to generate new organic material, even though such primary production is key to issues of oxygen cycling and demand, and of food web functioning. Measurements of primary production in some lakes have shown that rates and patterns of production can differ significantly from those suggested by chl *a* (Smith et al. 2005), but direct measurement of C^{14} primary production has not been measured in Lake Simcoe.

In temperate lakes, including Lake Michigan, there has historically been a planktonic seasonal succession involving a spring maximum (Fahnenstiel et al. 2010) followed by a second maximum in fall that consist of relatively large, fast-sinking cells such as diatoms (Sommers and Lewandowska 2011). These large spring diatoms are, or were (Fahnenstiel et al. 2010) important agents in consuming inorganic nutrients and transporting both nutrients and organic carbon to the benthos and sediments (e.g. Higgins and Vander Zanden 2010). During stratified seasons, typically very small phytoplankton (picoplankton) may dominate abundance and production, with tight coupling between consumption and production in the epilimnion. In some lakes, such

as the eastern basin of Lake Erie, there can be a single summer-fall maximum of phytoplankton production (MacDougall et al. 2001), and there is historical evidence for a fall phytoplankton maximum in Lake Simcoe (Nicholls et al. 1995). After the arrival of dreissenids, both Lake Michigan and eastern Lake Erie have shown a significant decrease in the magnitude of the spring bloom and diminished importance of large spring diatoms (Barbiero et al. 2009, Fahnenstiel et al. 2010). Dreissenid mussels can graze on a wide range of particle sizes but are believed to prefer the 2-60 μm range and to be capable of altering phytoplankton community composition through selective feeding (Vanderploeg et al. 2002, Fishman et al. 2009, Vanderploeg et al. 2010). To date, no published reports have addressed the seasonal patterns of production rates and size distributions of phytoplankton in Lake Simcoe, or whether there might have been any change consequent to dreissenid colonization.

This study is the first to report on the rates of phytoplankton primary production in Lake Simcoe and seeks to assess how productivity of the lake compares to other large oligo-mesotrophic lakes, with or without dreissenid mussels. The present work was also designed to determine whether chl *a* and primary production, using temporally and spatially resolved sampling, provide evidence of mussel effects as postulated by the nearshore shunt hypothesis. The study also asks whether the spatial and temporal patterns of primary production differ from those of chl *a*, and what the size distribution of chl *a* and primary production may reveal of dreissenid mussel effects and the role of phytoplankton in hypoxia and food web issues.

Methods

Sites and sampling methods

Lake Simcoe (44°2N, 79°2W) is the second largest lake (722 km^2 surface area) in the Laurentian Great Lakes catchment, after the Great Lakes themselves. This large, mesotrophic lake has been described in several recent publications (e.g. Eimers et al. 2005, Winter et al. 2007, Palmer et al. 2011). The lake (Figure 2.1) comprises three major regions: the main basin to the northeast (surface area= 643 km^2, Z_{avg}= 14m, Z_{max}= 33m), Cook's Bay to the south (surface area= 44 km^2, Z_{avg} =13m, Z_{max} =15m) and Kempenfelt Bay to the west (surface area=34 km^2, Z_{avg} =20m, Z_{max} =42m). This study focuses on results from four nearshore (Z_{max}<15m; Figure 2.1: E50, E51, N32, T2) and three offshore (Z_{max} >15m, Figure 2.1: K42, K45, M66) stations.

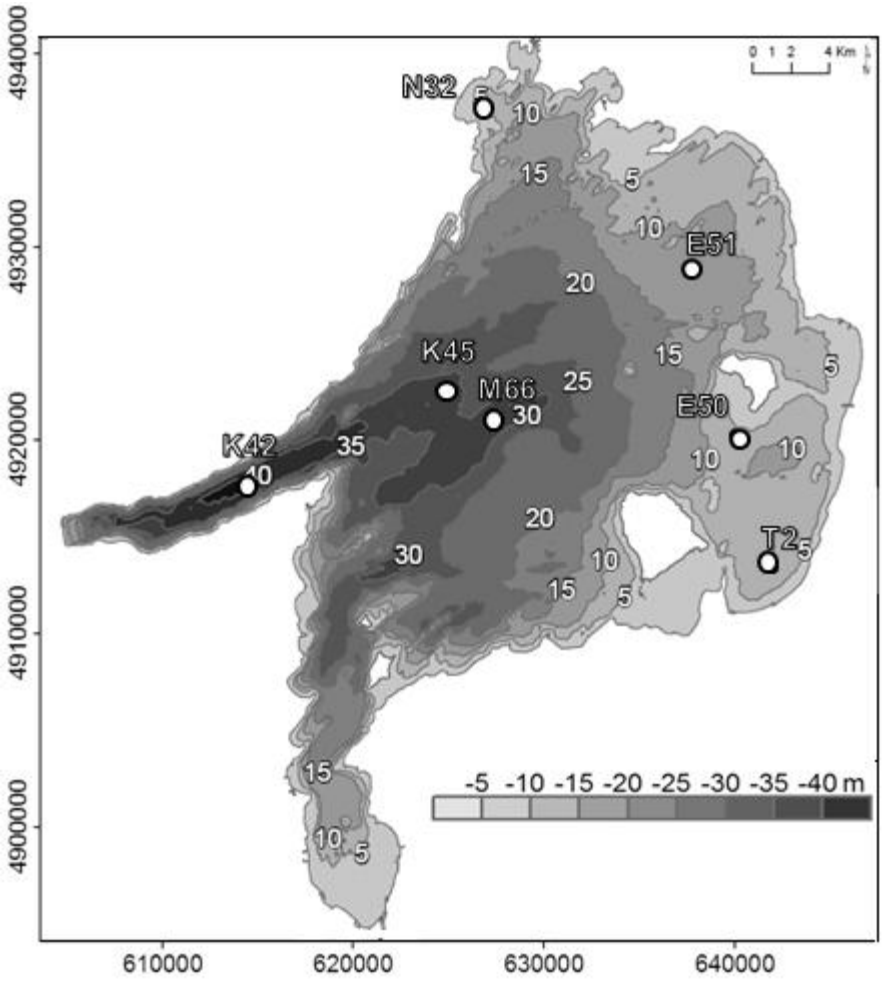

Figure 2.1 Map of Lake Simcoe, Ontario, Canada with bathymetric information. Original bathymetric data derived from Canadian Hydrographic Service by OMNR with scale 1:36 000. The map was further modified with appropriate stations (K42, K45, M66, T2, E51, E50, N32) as described in this study. This map should not be used for navigation, as OMNR will not be legally responsible for the use of any information indicated on the map and the map itself.

Sampling was conducted from August 2010 to August 2011. During the open water season (Apr to early Dec) surveys were conducted monthly and usually included all stations, but sampling during the ice-covered season was more opportunistic and less complete. Results discussed here are mainly for epilimnetic water samples, normally obtained with an integrating tube sampler to a depth of 1m above the thermocline or to a depth of 10 m if the thermocline was deeper or absent. The only exception was in August 2011 when a Niskin bottle (General Oceanics, Miami, Florida) was used to sample water at a discrete depth of 2m to a depth of 10m, and samples were mixed together. Temperature profiles measured with a YSI (YSI-6600V2-4, YSI Inc, Yellow Spring, OH) were used to determine whether a thermocline (defined as >1.0 C m^{-1} temperature gradient) was present and its location. No samples were collected in January 2011. The depth of under-ice sampling (Feb-Mar) was based on the chl *a* peak observed with the YSI and a van Dorn sampler was used to sample water depths ranging from 1-5 m assuming isothermal conditions under ice. Only one sample was taken from the surface during winter (<1m) at station K45 on 9 Feb 11. For all seasons, the large volume samples (in 2 polyethylene carboys) were kept dark and within 2℃ of lake temperature pending analysis at University of Waterloo.

Other than the regular water quality stations, additional samples from the Beaverton water treatment plant (WTP, Figure 2.1) were collected from January to July 2011 on a monthly basis except for some winter samples (Mar-early Apr) which were collected more intensively (Table 2.1). Since these samples were directly taken from the water intake pipes, it was assumed to have uniform chl *a* with respect to depth when estimating the production rates. The intake pipes are located near the station E50, so Z_{max} was kept same as the nearshore station E50.

Table 0.1 Sampled station, Z_{max}**,** date and spatial classification of Lake Simcoe 2010-2011.

Stations	Latitude	Longitude	Zone	Average Z_{max} (m)	Sampled Months
Main Basin					
E50	44° 24' 31	79° 14' 16	Nearshore	10	Aug, Sep, Oct, Nov, Feb, Mar, May, Jun, Jul
E51	44° 14' 35	79° 30' 43	Nearshore	12	Aug, Sep, Oct, Nov, Dec, May, Jul
N32	44° 34' 41	79° 24' 5	Nearshore	6	Aug, Sep, Oct, Nov, May, Jun
T2	44° 21' 50	79° 13' 36	Nearshore	8	Aug, Sep, Oct, Nov, Apr, May, Jun, Jul, Aug11
M66	44° 25' 18	79° 25' 32	Offshore	32	Aug, Sep, Oct, Nov, Apr, May, Jun, Jul, Aug11
S15	44° 21' 52	79° 23' 16	Transitional	20	Aug, Sep, Nov, Dec, Mar, May, Jul, Aug11
Cook's Bay					
C9	44° 17' 38"	79° 30' 2"	Transitional	18	Aug, Sep, Nov, Dec, Feb, May, Jul, Aug
C6	44° 14' 35"	79° 30' 43"	Nearshore	14	Aug, Sep, Nov, Feb, May, Jul, Aug11
Kempenfelt Bay					
K42	44° 23' 57	79° 34' 14	Offshore	39	Aug, Sep, Oct, Nov, Dec, Feb, Mar, May, Jun, Jul, Aug11
K45	44° 26' 34	79° 26' 40	Offshore	33	Aug, Sep, Oct, Nov, Dec, Feb, May, Jun, Jul, Aug11
Beaverton water treatment plant (WTP)*			Nearshore*	N/A*	Jan, Feb, Mar (n=2), Apr (n=3), May, Jun, Jul

*WTP samples are collected to represent nearshore station (E50) and Z_{max} is unavailable. Refer to methods and materials for more information.

^{14}C Primary production experiments

The ^{14}C tracer method used here is intended to measure a rate close to gross photosynthesis, including both dissolved and particulate production, using a short incubation period (1 hour) that minimizes the respiration losses (e.g. Beardall et al. 2009, Depew et al. 2006, Smith et al. 2005, Halsey et al. 2010). The stored water samples were screened through 200 µm nylon mesh to remove larger zooplankton and 110 ml from each sample was inoculated with 80 microcuries of ^{14}C bicarbonate (ICN Biomedicals, Irvine, California). In each experiment, 18 samples of 5 ml from the ^{14}C spiked water sample were placed into borosilicate glass scintillation vials and immediately incubated in a light gradient chamber for an hour at a temperature close to in vivo. The light source was a tungsten halogen lamp providing sample irradiance ranging from 0.91 to 1084 µmol photons $\cdot m^{-2} s^{-1}$. At the beginning of the incubation, duplicate samples for time zero and total activity were taken to provide corrections for background activity and to identify the total ^{14}C activity in the spiked sample. The duplicate total activity samples were fixed using ethanolamine.

After an hour of incubation, 3 subsamples from medium to high irradiance were combined and 5 ml aliquots filtered in parallel through polycarbonate filters of 2 and 20 µm pore size, as well as GF/F filters, to determine the size distribution of ^{14}C uptake. Retention on GF/F (nominal pore size 0.8µm) filters was assumed to represent essentially all of the particulate uptake. The remaining 15 subsamples as well as the GF/F filtrate were acidified with 6M hydrochloric acid (HCl) to terminate further carbon assimilation and left uncovered for approximately 24 h to release unfixed $^{14}CO_2$. Samples were analyzed by liquid scintillation using EcoLume (MP biomedicals, Solon, OH, USA) scintillation cocktail.

Chlorophyll a (chl a) and dissolved inorganic carbon (DIC) measurements

One of the main sources of variation when estimating phytoplankton areal primary production is related to the amount and distribution of the photoautotrophic biomass (Falkowski and Raven 2007). At times, normalizing areal primary production to biomass can help reduce this variation by an order of magnitude (Falkowski and Raven 2007) and hence chl *a*, a proxy for phytoplankton biomass, was used to normalize primary production (Fee et al. 1990). Chl *a* was chosen as an index for phytoplankton biomass because chl *a* is a pigment that is universally present in all algal types except for some of the marine algae and higher aquatic plants (Falkowski and Raven 2007).

To measure chl *a*, raw water was first screened through a nylon (Nitex) mesh (nominal 200 µm pore size). Aliquots (200 ml) of the screened water and of filtrate from 2 and 20 µm polycarbonate filters were filtered on GF/F filters and stored in the dark at -20°C pending further analysis. Filters were extracted in 90% acetone for 18-24 hours and chl *a* was determined using a Turner Designs 10-AU fluorometer (Turner Designs, Sunnyvale, California, USA) that had been calibrated against pure chl *a* (Smith et al. 1999, Depew et al. 2006). The dissolved inorganic carbon (DIC) concentration, which was used to calculate the photosynthetic assimilation, was measuring using the Gran titration method.

Primary production and other calculations

Photosynthetic parameters (P^B_{max}, α^B, I_k) and daily integrated production were calculated using software developed by Fee (1990) modified into Windows format. The program (PSPARMS) determines two major parameters of the photosynthesis-irradiance (PI) curve (Jassby and Platt 1976): light saturated rate of photosynthesis (P^B_{max}) and the slope of the PI curve (α^B) where the subscript 'B' denotes chl *a* normalization. When photoinhibition was evident, a model by Platt et al. (1980) was used to fit the curve instead. Over the course of the field work, vertical profiles of photosynthetically active radiation (PAR), including the PAR above the water, were measured using a Li-COR cosine underwater quantum sensor with Li-COR 1000 data logger (Lincoln, Nebraska). Then, the daily areal production (P_{int}, mg C m^{-2} d^{-1}) and the daily volumetric production (P_{avg}, mg C m^{-3} d^{-1}) over the photic zone were computed using surface PAR information collected in the field. When the maximum station depth exceeded the euphotic depth (1% light depth), the program truncated the depth accordingly.

The vertical attenuation coefficient, Kd_{PAR} which is one of the required input parameter in the Fee programs DPHOTO and DTOTAL, was calculated from the linear regression of natural logarithm of irradiance versus depth (Kirk 1994). Then, the mean PAR within epilimnion was obtained by using a function of Kd_{PAR} and Z_{mix}, similar to the method employed by Depew et al. (2006):

(1) $$Ia = \frac{Io}{-kd_{PAR} \times Ze}\left(e^{-Kd_{PAR} \times Ze} - 1\right)$$

Where I*a* is the epilimnetic mean PAR expressed as a percentage of Io, and Ze is the depth of the mixed layer. Note that all of terms and their corresponding units used throughout the study are summarized in Table 2.2.

Table 2.2 List of terms and their corresponding units used throughout the study. The computer models (Fee 1990) used for calculating *in situ* phytoplankton photosynthesis is also summarized below.

Description	Abbreviation	Unit
Daily areal primary production	P_{int}	mg C m^{-2} d^{-1}
Daily volumetric primary production	P_{avg}	mg C m^{-3} d^{-1}
Chlorophyll a	Chl *a*	µg/L
Dissolved inorganic carbon	DIC	µg/L
Photosynthetically Active Radiation	PAR	µmol photons m^{-2} s^{-1}
Vertical light attenuation	Kd_{PAR}	m^{-1}
Mixing depth	Z_{mix}	m
Maximum depth	Z_{max}	m
Maximum rate of photosynthesis at light saturation	P^B_{max}	mg C mg chl a^{-1} h^{-1}
Light utilization efficiency	α^B	mg C/(mg chl *a* Ein m^{-2}))
Rates of carbon assimilation at light saturation	P_{opt}	mg C m^{-3} h^{-1}
Seasonal areal primary production	SAPP	g C m^{-2}
Total phosphorus	TP	mg m^{-3}
Calculates (P)hoto(S)ynthesis (PAR)a(M)eter(S) from photosynthesis versus PAR	PSPARMS	--
Stimulation of (PHOTO)synthesis as a function of depth at a single place for a singly (D)ay	DPHOTO	--
Calculation of integral and mean photosynthesis and mean PAR above and below the thermocline based on the DPHOTO output	DTOTAL	--
Simulation of (PHOTO)synthesis as a function of depth at a single place for a range of dates (an entire (Y)ear or ice-free season)	YPHOTO	--
Estimation of integral and mean photosynthesis and mean PAR above and below thermocline based on the YPHOTO outputs	YTOTAL	--

Chl a:TP, SAPP and sensitivity analysis

In order to better understand the effects and role of mussels (Smith et al. 2005, Depew et al. 2006), relationships between chl *a* and TP (May-Oct 2010-2011) were plotted using SYSTAT ver. 10.0 (SYSTAT Software Inc., Point Richmond, California). The method was modified from Smith et al. (2005) where chl *a* and TP of nearshore, offshore and total (nearshore and offshore) in Lake Simcoe were added along with other comparable systems. The inter-comparison of chl *a* versus TP included systems with dreissenids present (Lakes Erie, Simcoe) and absent (Saginaw Bay, Georgian Bay, Bay of Quinte and Lakes Huron, Michigan, Ontario, Erie) as well as NOLSS (Northwest Ontario Lake Size series; Fee and Hecky 1992) which includes Lake Superior.

Seasonal Areal Primary Production (SAPP) was calculated in order to standardize the comparisons of primary production among lakes (Millard et al. 1999). The P_{int} results from May, June and July 2011 were combined with those from August, September and October 2010 to generate seasonal areal primary production over the standardized time of 1 May-31 Oct. All the calculations were done using the programs DPHOTO, DTOTAL, YPHOTO and YTOTAL (Fee 1990). Although 100% cloud free model can exaggerate the estimates, it was selected in order to standardize the comparisons among lakes (Millard et al. 1999).

A sensitivity analysis similar to Fahnenstiel et al. (1995) was employed in order to elucidate the possible effects of variables that influence the changes in the nearshore and offshore SAPP. The parameters in the model included chl *a*, Kd_{PAR}, P^B_{max}, α^B, Z_{max} and $Z_{mix.}$ Z_{mix} was defined as the depth above the thermocline. For each simulation run (DPHOTO, DTOTAL), a parameter from offshore stations, averaged over the period of May-Oct, was substituted for its

nearshore counterpart while keeping the other parameters at their nearshore values (Fahnenstiel et al. 1995, Smith et al. 2005, Depew et al. 2006). The output from the model was then used to determine the change in calculated productivity for the nearshore.

Statistical analysis

The linear mixed effects model (LME) is a statistical model modified from the generalized linear model (GLM) (Bolker et al. 2009). By definition, LME is a model that helps to describe the response variable considering both random and fixed effects. The model is mathematically described as (Pinheiro and Bates 2000):

$$(2) \qquad y_{ij}=\beta_1 x_{1ij} + \beta_2 x_{2ij} \ldots \beta_n x_{nij} + b_{i1} z_{1ij} + b_{i2} z_{2ij} \ldots b_{in} z_{nij} + \varepsilon_{ij}$$

where y_{ij} is the value of the outcome variable for a particular ij case, and β_1 through β_n are the fixed effect coefficients. The cases x_{1ij} through x_{nij} are the fixed effect variables (predictors) for observation j in group i whereas b_{i1} through b_{in} represent random effect coefficients. The random effect variables (predictors) are z_{1ij} through z_{nij} and ε_{ij} is the 'within-individual' measurement error (e.g. measurement or sampling errors) with the assumption that each of the group's error is multivariate normally distributed (Pinheiro and Bates 2000).

More simply put in the context of this study:

$$(3) \qquad y_{ij}= \beta_o + b_{oi} + \beta_1 \text{season2} + \beta_2 \text{season3} + \beta_3 \text{season4} + \beta_4 \text{zone2} + \beta_5 \text{season2zone2} + \beta_6 \text{season3zone2} + \beta_7 \text{season4zone2} + \varepsilon_{ij}$$

where y_{ij} is the value of the outcome variable (e.g. $P_{int,}$ chl *a*, Kd_{PAR}) with respect to season (1-spring, 2-summer, 3- fall, 4-winter) and zone (1-nearshore and 2-offshore). β_o is the average dependent variable ('y') when the season and zone is 1. β_1 to β_3 are the differences in the average dependent variable between the rest of the seasons (season 2 (β_1), season 3 (β_2) and season 4 (β_3)) to season 1 when controlling for zone. Then, β_4 to β_7 is the average difference in dependent variable between the two zones when controlling for season. The term 'b_{oi}' is the random intercept and ε_{ij} is the within-individual measurement error.

The main goal of the model was to statistically describe the spatial and temporal patterns of production and other variables (e.g. P_{int}, P_{avg}, P_{opt}) by testing whether the two categorical variables (season and zone) have a significant association with the variables of interest. The validation of the model output was further tested by a Wald test, to see if the two zones are 'true' significant predictors of outcome variable when controlling for season (e.g. Ho= β_4= β_5=0, β_4=0, β_5=0). Throughout the study, the level of significance (α) was set to <0.05. So, if the *p*-value was <0.05 detected by the Wald's test, the null hypothesis was rejected, which meant that season was not significantly associated with the response variable. If the significance level was <0.05 for given season and/or zone, then the analysis was followed with pairwise comparisons provided by the output of the model in R.

The LME model was chosen because the model includes both random (repeated measures) and fixed effects and accounts for the temporally autocorrelated data. LME is advantageous for longitudinal data since the model handles the covariance due to repeated measures and does assume independence of data (Pinheiro and Bates 2000). Unlike repeated

measures of analysis of variance (ANOVA), the model does not require same number of observation for each of the subjects and uniform measurement interval is not necessary (Pinheiro and Bates 2000). In this study, the two categorical factors were season (spring-winter) and zone (nearshore and offshore) and the dependent variables were P_{int}, P_{avg}, P_{opt}, K_{PAR},α^{B}, P^{B}_{max}, chl *a*/TP, mean PAR, ^{14}C and chl *a* size fractions. The months were grouped into: spring (Apr-May), summer (Jun-Aug), fall (Sep-Nov) and winter (Dec-Mar) which were decided based on the temperature profiles. To meet the requirements of parametric statistics, the following data were transformed prior to the test to achieve normality-(P_{int} ,chl *a*,^{14}C net- sized production, nanoplankton chl *a*: cube transformation; P_{avg}, chl *a*:TP, ^{14}C nano- sized production, α^{B}, picoplankton chl *a*: square-root transformation; $P^{B}_{max,}$ Kd_{PAR}: $\log_{10}$ transformation; mean PAR, P_{opt}, ^{14}C pico-sized plankton: no transformation).

When investigating SAPP:TP among different systems, the data (total, nearshore and offshore) was $\log_{10}$ transformed to stabilize the variance prior to using analysis of covariance (ANCOVA). The null hypothesis is that there is no significant difference of SAPP between lake sets (pre- and post- dreissenids) when controlling for differences in TP, which is the continuous covariate. All statistical analysis used the software R or SYSTAT ver. 10.0 (SYSTAT Software Inc., Point Richmond, California).

Results

On average, the nearshore sites were warmer than offshore sites in spring (Apr-May) and slightly colder in winter (Dec-Mar), but no temperature difference was found in summer (Jun-Aug) and fall (Sept-Nov) (Table 2.3). A weak but persistent thermocline was evident at most of the nearshore stations in early summer (Jun-Jul, e.g. Figure 2.2a) but it became very weak in August and disappeared during the fall. In mid to late- winter (Feb-Mar), both nearshore and offshore stations formed an inverse thermal stratification under the ice cover. For deeper offshore stations, thermal stratification was present in early to late summer (Jun-Sept, Z_{mix}= 5.3 (station M66, June) -13.5m (station M66 August)) but started to breakdown in mid-fall (Oct) and essentially disappeared by November (e.g. Figure 2.2b). An absence of thermal stratification was also seen in December and April to May (e.g. Figure 2.2b).

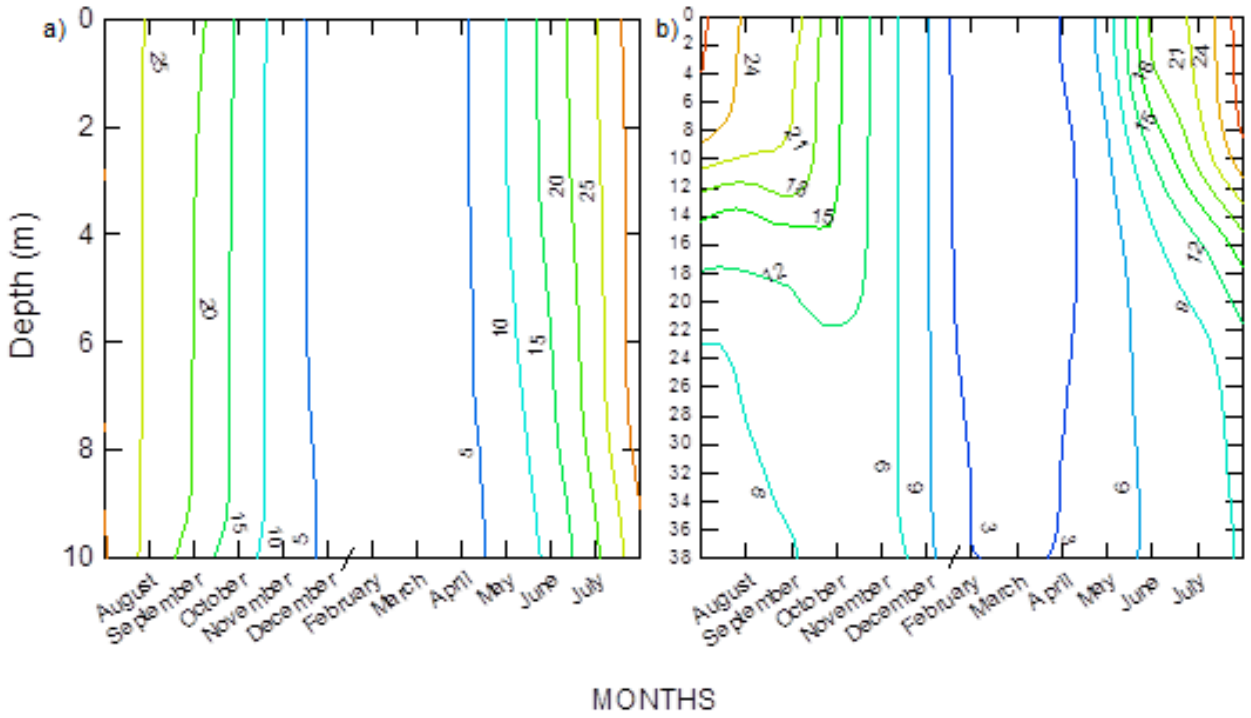

Figure 2.2 a (left) and b (right) Temperature and depth isopleth of a) E50 nearshore station b) K42 offshore station. The data are from August 2010 to July 2011. No samples were collected in December, January and April for E50 station (Z_{max}=10.5m) and January and April for K42 station (Z_{max}=38m).

Table 2.3 Summary of primary production and other variables from August 2010- July 2011.

SEASON	ZONE	TEMP	Kd_{PAR}	Z_{mix}	MeanPAR	Chla	P^B_{max}	α^{B*}	P_{int}	P_{avg}	P_{opt}	Chla/TP
Spring	NS	8.79	0.28	9.63	39.8	0.77	0.86	2.81	52.4	7.8	0.64	0.091
	(n=4)	(1.52)	(0.026)		(3.82)	(0.14)	(0.16)	(0.38)	(7.39)	(1.59)	(0.14)	(0.014)
(Apr-	OS	5.85	0.24	32.3	13.5	2.30	1.55	5.19	268.9	14.6	3.12	0.288
May)	(n=4)	(0.95)	(0.020)		(1.57)	(0.93)	(0.25)	(0.41)	(63.2)	(4.75)	(0.91)	(0.13)
			0.26	8.3	26.7	1.53	1.20	4.00	160.6	11.2	1.88	0.19
	Total		(0.017)		(5.33)	(0.52)	(0.19)	(0.52)	(50.4)	(2.65)	(0.63)	(0.071)
Summer												
	NS	22.2	0.32	7.13	41.7	2.08	2.48	6.78	255.3	48.7	3.22	0.16
	(n=10)	(0.63)	(0.024)		(4.03)	(0.42)	(0.95)	(2.99)	(51.7)	(10.1)	(0.54)	(0.042)
(Jun-	OS	21.4	0.28	10.1	35.2	1.49	4.24	5.46	392.2	37.3	3.61	0.18
Aug)	(n=9)	(0.52)	(0.011)		(2.78)	(0.32)	(1.60)	(1.17)	(61.7)	(7.17)	(0.71)	(0.035)
		21.7	0.30	8.52	38.6	1.80	3.31	6.20	320.1	43.3	3.41	0.17
	Total	(0.47)	(0.014)		(2.55)	(0.27)	(0.90)	(1.70)	(42.0)	(6.29)	(0.43)	(0.027)
Fall												
	NS	14.4	0.34	8.3	34.7	1.89	2.48	7.51	302.6	48.2	4.71	0.22
	(n=11)	(1.93)	(0.018)		(2.14)	(0.15)	(0.37)	(1.02)	(55.2)	(12.5)	(0.83)	(0.012)
(Sep-	OS	15.9	0.36	21.8	15.2	3.97	2.47	9.26	597.0	46.2	9.49	0.387
Nov)	(n=9)	(1.74)	(0.028)		(1.70)	(0.35)	(0.14)	(0.97)	(39.4)	(5.53)	(0.50)	(0.035)
		15.1	0.35	14.4	26.0	2.82	2.48	8.30	435.1	47.3	6.86	0.30
	Total	(1.30)	(0.016)		(2.62)	(0.29)	(0.21)	(0.72)	(48.0)	(7.16)	(0.74)	(0.025)
Winter												
	NS	1.44	0.34	7.5	38.9	1.00	1.09	3.80	36.0	5.65	1.06	0.12
(Dec-	(n=4)	(1.24)	(0.057)		(3.34)	(0.27)	(0.17)	(0.49)	(24.3)	(4.45)	(0.30)	(0.027)
Mar)												
	OS	2.33	0.34	25.1	13.7	6.09	0.94	4.32	85.4	5.83	4.32	0.66
	(n=6)	(1.25)	(0.036)		(2.11)	(2.66)	(0.25)	(0.78)	(28.6)	(1.93)	(1.80)	(0.28)
		1.97	0.34	18.0	23.8	4.06	1.00	4.11	65.6	5.76	3.02	0.44
	Total	(0.86)	(0.030)		(4.47)	(1.74)	(0.16)	(0.49)	(20.4)	(1.97)	(1.17)	(0.18)

Note: Each of the parentheses represents one standard error. The stations E51 May and September was omitted for P_{int} and other variables. Please refer to the method section for units for each of the variables.

*The parameter α^B was (Station K45 July) was recognized as an outlier (Cook's distance) and was excluded from the seasonal average

In Lake Simcoe, Kd_{PAR} ranged from 0.20 (station M66, 5 October 2010) to 0.51 m^{-1} (station K45, 9 February 2011). A linear mixed effects model detected no significant interaction between season and zone (p=0.80) and only seasons were significantly different for Kd_{PAR} (LME, p=0.0065). Temporally, the average Kd_{PAR} was highest in fall followed by winter (p<0.0001) but lowest in spring especially in the offshore stations (Table 2.3, Figure 2.3). The pairwise comparisons in the LME model suggested that average Kd_{PAR} values in winter were not significantly different from the values reported in summer (LME, p=0.35) and likewise, spring was not different from summer (p=0.12) (Table 2.3, Figure 2.3). The Kd_{PAR} in fall, on the other hand, was greater than the rest of the seasons (p<0.05).

For mean PAR within the epilimnion, the linear mixed effects model identified a significant interaction between season and zone (LME, p=0.016) and both categorical variables were also significant predictors for mean PAR (LME, p<0.05). Overall, the mean PAR was greatest in summer followed by spring, fall and winter (Table 2.3). For all seasons, the average mean PAR in the nearshore was up to 55% higher than the offshore but the difference was only statistically significant in spring (LME, p<0.0001), fall (LME, p<0.0001) and winter (LME, p<0.0001). The spatial significance was associated with the trends in Z_{mix}. In summer, for instance, when the difference in Z_{mix} between nearshore (Z_{mix}=7.13) and offshore (Z_{mix}=10.1) was relatively small, LME did not detect any significance in the average zonal difference in mean PAR (LME, p=0.058).

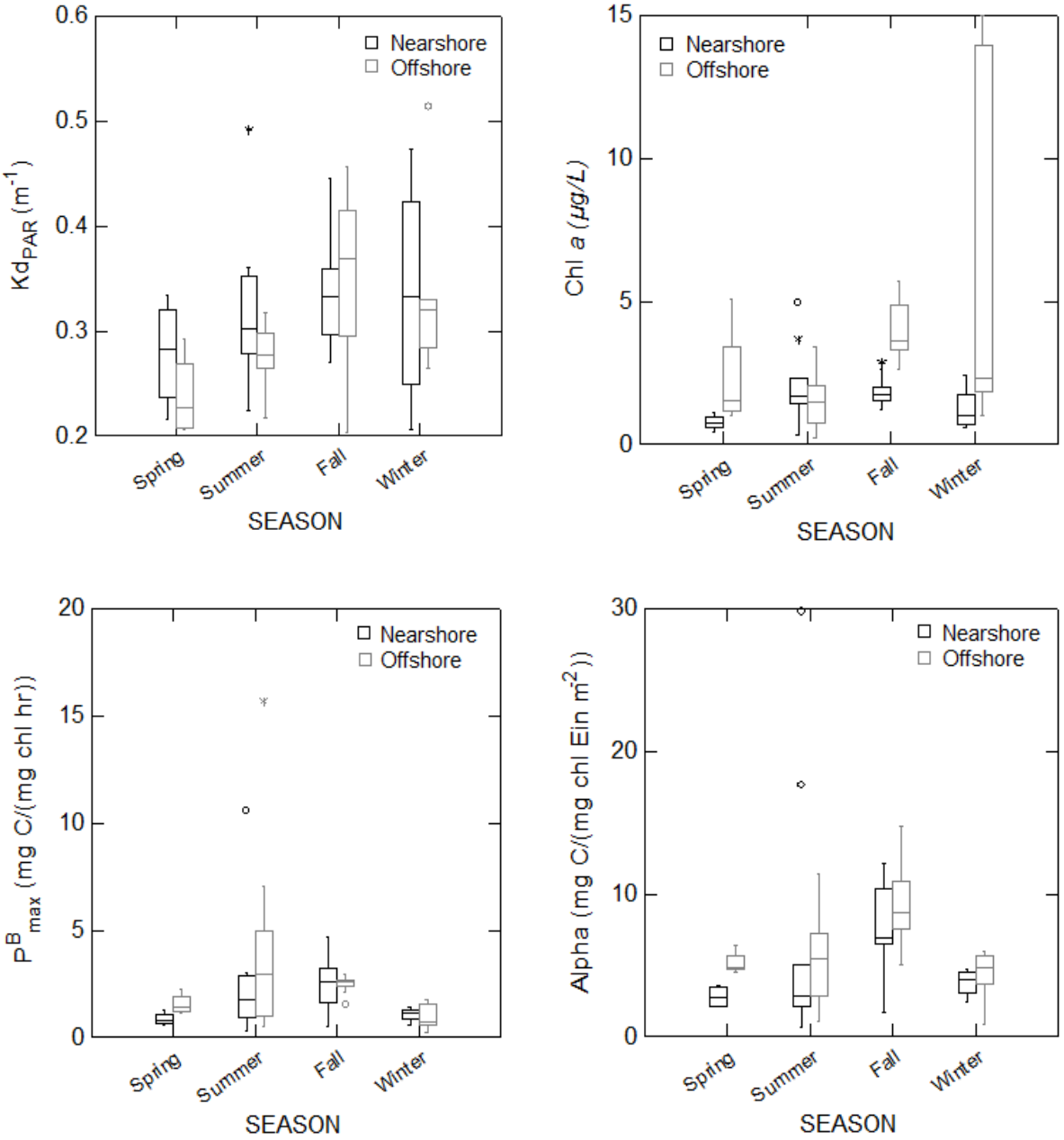

Figure 2.3 Box and whisker plot of (a) Left top: Kd_{PAR} (m^{-1}) (b) Right top: Chl *a* (µg/L) (c) Left bottom: P^{B}_{max} (mg C/(mg chl hr)) (d) Right bottom: α^{B} (mg C/(mg chl Ein m^{-2})). Solid black and gray boxes are all nearshore and offshore respectively for each season. Outliers are indicated by * or °.

Temporal and spatial patterns of primary production, chl a, and photosynthetic parameters

Over the course of the study, daily areal integrated production estimates ranged from 0.1 mg C $\cdot m^{-2} \cdot d^{-1}$ (station K42, 9 Feb 11) to 814.3 mg C $\cdot m^{-2} \cdot d^{-1}$ (station M66, 31 Aug 10). P_{int} displayed no interaction (LME, p=0.85) but season and zone were significant predictors for production (LME, p<0.0001). Contrary to the classical seasonal pattern of a typical dimictic lake, P_{int} was highest in fall followed by summer, spring and winter (Table 2.3, Figure 2.4) but there was no significant difference between seasonal averages for summer and fall (LME, p=0.51). In general, the average P_{int} was lower in the nearshore stations than offshore stations (Table 2.3, Figure 2.4). The production remained relatively high during summer and fall especially in the offshore but declined dramatically during winter months (Dec-Mar, Figure 2.5). In April, one offshore station (M66) showed a sudden increase in March, but only one sample was available for the analysis due to undesirable field sampling conditions in that month. Chl *a*, which is used as a proxy for phytoplankton biomass, had a significant association with P_{int} (Spearman's rho=0.46, n=57, p=0.0021).

In contrast to patterns in P_{int}, no significant interaction or zonal effect was detected for the average production rate in the photic zone, P_{avg}. The P_{avg} ranged from ~0 (station E50, 3 Feb 11) to 146.9 (station K42, 8 Nov 10) mg $\cdot C \cdot m^{-3}$ d^{-1}, while the highest seasonal average was for fall and lowest for winter (Table 2.3, Figure 2.4). There were significant differences in P_{avg} between all seasons (LME, p<0.0001) except for spring and winter (LME, p=0.13). Although zone was not a significant predictor for P_{avg}, the absolute mean of P_{avg} for offshore stations was generally lower than nearshore stations in both summer and fall (Table 2.3, Figure 2.4),

reflecting the deeper photic zone and greater relative importance of light-limited production at offshore sites.

The rate of carbon assimilation at light saturation (P_{opt}) provides a measure of volumetric production when light is saturating. The range in P_{opt} was from 0.34 (station K42, 21 Jun 11) to 12.8 (station K42, 9 Mar 11). The highest average P_{opt} was observed in fall (LME, $p<0.0001$) and lowest in spring where the differences of the two seasons were approximately 3.5 fold (Table 2.3, Figure 2.4). Additionally, for all seasons, P_{opt} was significantly higher in offshore than nearshore waters ($p=0.011$). The largest difference in mean P_{opt} between nearshore and offshore stations was in spring and winter (Table 2.3, Figure 2.4).

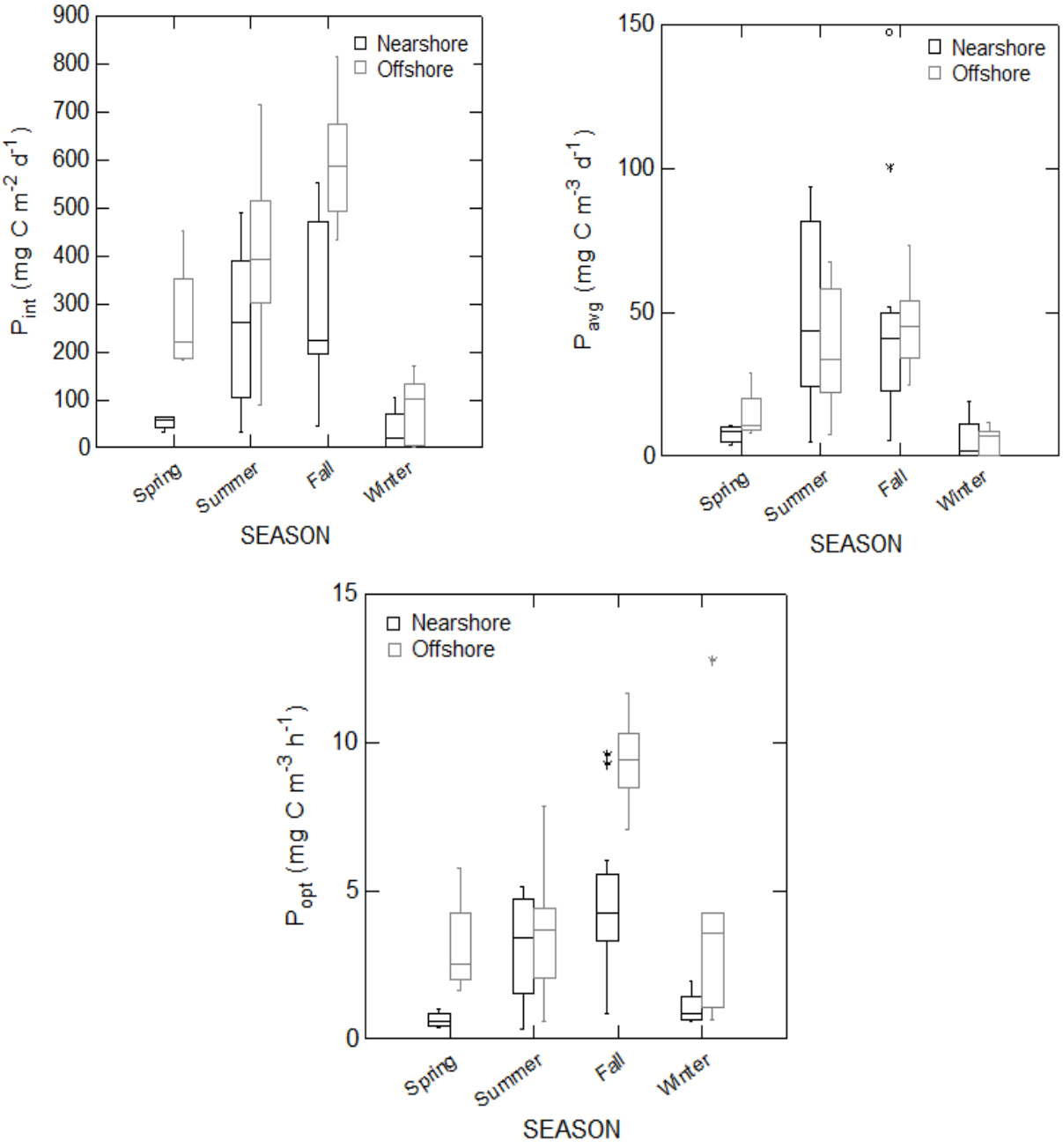

Figure 2.4 Box and whisker plot of (a) Left top: P_{int} (mg C m^{-2} d^{-1}) (b) Right top: P_{avg} (mg C m^{-3} d^{-1}) (c) Left center: P_{opt} (mg C m^{-3} h^{-1})). The black boxes are all nearshore stations and gray boxes are all offshore station in a given season. Note that outliers are denoted by * or °.

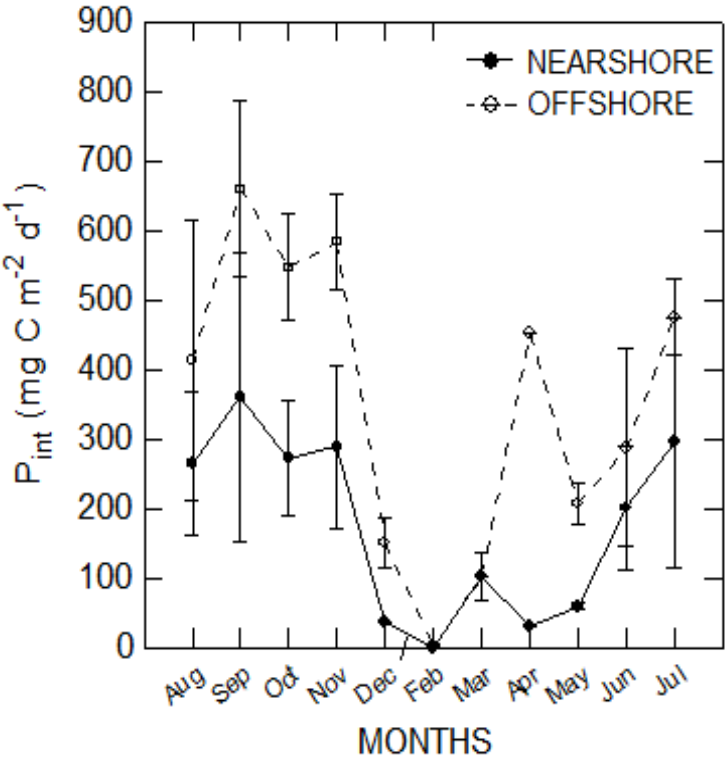

Figure 2.5 A monthly plot of P_{int} (mg C·m^{-2} d^{-1}) and chl *a* (µg/L) from August 2010-July 2011. The solid line represents the average nearshore P_{int} (•) and the dashed line represents average offshore stations (o). Each of the error bars are adjusted to one standard error. Refer to the methods for seasonal groupings. None of the stations were collected in January.

The temporal and spatial variations of chl *a* on a monthly basis are illustrated in figure 2.6 but all statistical analysis were based on seasonal groupings of the data. From August 2010 to July 2011, chl *a* ranged from 0.23 (station K45, 14 July 2011) to 15.0 µg/L (station K42, 9 March 2011). On average, chl *a* concentration was highest in the offshore stations during winter and fall (Figure 2.3) and chl *a* concentrations in spring were generally lower than other seasons, especially in the nearshore stations (Table 2.3, Figure 2.3). Chl *a* values in winter were quite variable between samples (n=10, Table 2.3, Figure 2.3) while values in fall were less variable and remained relatively high (n=2, Table 2.3, Figure 2.3). The total chl *a* in early winter was fairly low (1.4 ±0.3 µg/L, Dec 2010-Feb 2011) and remained lower in mid-February (1.1 ±0.3 µg/L) before attaining very high values in March (10.2 ± 4.2µg/L, Figure 2.6). These unusual high chl *a* values were only observed in one offshore station (e.g. 13-14µg/L; station K42, 9 Mar 11, Figure 2.6) and none in the nearshore stations (e.g. 1.8µg/L; station E50, 1 Mar 11). Chl *a* in samples from the WTP was higher than the average of the nearshore sites during March and April, but was always far less than the March peak observed offshore (Figure 2.6).Vertical profiles of chl *a* fluorescence at station K42 (Dec-Mar) showed that chl *a* concentrations were generally low in early winter (Dec 2.42µg/L; Feb 1.38µg/L) but increased in March (Figure 2.7). In mid-March, the average chl *a* above the thermocline (Z_{mix}=15m) reached up to 23.8 µg/L (Figure 2.7). The TP concentration in February (station K42 and K45) ranged from 0.25-0.27 µg/L at the surface (~1m) and slightly increased to 0.29 and 0.32 µg/L (station K42) at 2 and 4m in March respectively. This slight increase in TP may have supplied nutrients to the chl *a* biomass. Most likely, however, these "pulses" of chl *a* seem to be related to light conditions, with ice and snow in February producing strong light attenuation of the relatively low incident irradiance (Table 2.4). The surface incident irradiance in March was much higher than in early

February and transmission was greater (Table 2.4). Of the surface incident irradiance, only 1.8% of light was transmitted through snow and ice in February compared to 3% and 8% in March 9th and 14th respectively (Table 2.4). The sunrise was occurring an hour or so earlier in March as the sunset time much later (Table 2.4) suggesting increased photoperiod.

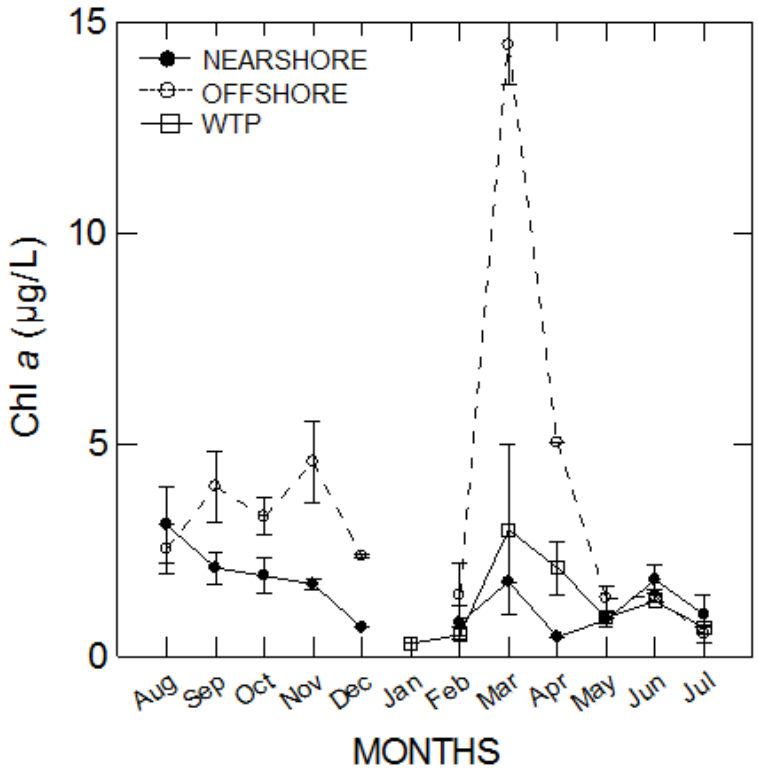

Figure 2.6 A monthly plot of chl *a* (µg/L) from August 2010-July 2011. The solid line represents the average nearshore chl *a* (•) and the dashed line represents average offshore stations (o). Note that samples from the Beaverton water treatment plant (WTP) were also plotted from January to July 2011and are represented by unfilled squares (□). Each of the error bars are adjusted to one standard error.

Table 2.4 Snow and ice thickness data for K42 station in 2011. The light transmission was obtained by determining the percentage of surface incident irradiance (spot measurements) and the penetration of light underneath ice. The sunrise and sunset was estimated by the Fee model.

Date	**Snow thickness (cm)**	**Ice thickness (cm)**	**Surface Incident Irradiance ($\mu E/m^2s$)**	**Light Transmission (%)**	**Sunrise**	**Sunset**
09-Feb-11	12.7	25.4	177.9	~1.8	7:25	17:37
09-Mar-11	Spotty covering	35.6	821	~3	6:40	18:15
14-Mar-11	Patchy and thin	45.7	1850	~8	6:31	18:22

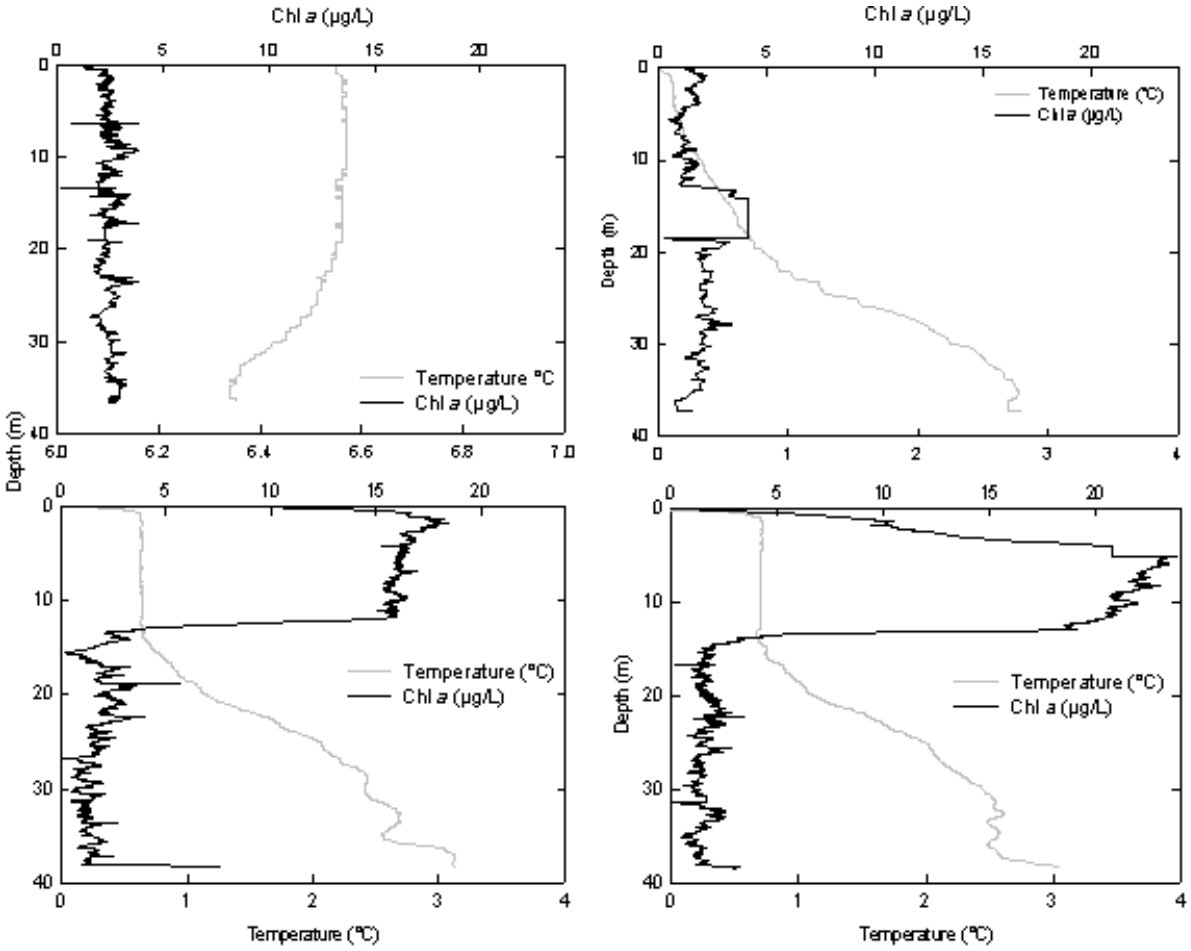

Figure 2.7 In vivo profile of depth and chl *a* (µg/L) for K42 winter 2011. The left top panel shows the depth profile for K42 in December as the adjacent graph on right shows the profile for early February. The bottom profiles are from early(left) and mid March (right). The Z_{mix} for K42 for December, February and March was 36.5m, 37m, and 15m respectively.

When all seasons were considered, the mean chl *a* at offshore stations (chl a_{total}=3.4 µg/L) was approximately two times higher than nearshore stations (chl a_{total}=1.7µg/L). In fact, the chl *a* was up to six times higher in offshore compared to nearshore (winter, Table 2.3). The only exception was in summer when the average chl *a* in nearshore sites was higher than at offshore sites (Table 2.3), but this was not statistically significant (p=0.26). Only the seasons fall (p=0.0035) and winter (p=0.0001) shared significant differences between nearshore and offshore.

Season, but not zone or interaction, was a significant predictor for the photosynthetic parameters P^B_{max} and α^B (p=0.003 and 0.007 respectively). Throughout the seasons, P^B_{max} ranged from 0.25mg C·mg chl h^{-1} (station K42, 14 Mar 2011) to 15.7mg C·mg chl h^{-1} (station K42, 14 Jul 2011) and α^B was from 0.66 (station K42, 5 Aug 2010) to 29.8 (station E50, 14 Jul 2011) as one station was detected as an outlier and removed from the analysis (95.1 mg C/(mg chl *a* Ein m^{-2})); station K45, 14 Jul 2011). The highest average of P^B_{max} was found in the summer, followed by fall, spring and winter (Table 2.3, Figure 2.3). α^B, on the other hand, showed a slightly different pattern, where fall was highest then summer, winter and spring (Table 2.3, Figure 2.3). Fall was the only season that displayed significant differences with respect to other seasons (LME, p<0.05).

The monthly plot of chl *a*:TP showed a gradual increase in chl *a*:TP from August to November, and the ratio started to decrease in December. In March, a transient but high ratio in was found (Figure 2.8), due to a peak in chl *a* biomass (Figure 2.6). Chl *a*:TP was usually higher in the offshore than nearshore (LME, p=0.0084), except for June and July (Figure 2.8). In winter, a large difference (5.5 fold) was found between nearshore and offshore accounting for

high biomass in mid-March (Table 2.3, Figure 2.8). A spatial difference of up to three-fold (nearshore <offshore) was found in other seasons (Table 2.3). No interaction was found (LME, p=0.19) but season was a significant predictor of chl *a*:TP (LME, p=0.016). Although winter had the highest chl *a*:TP, it was not significantly different from values in fall (LME, p=0.88; Table 2.3, Figure 2.8) due to the large variability of winter values.

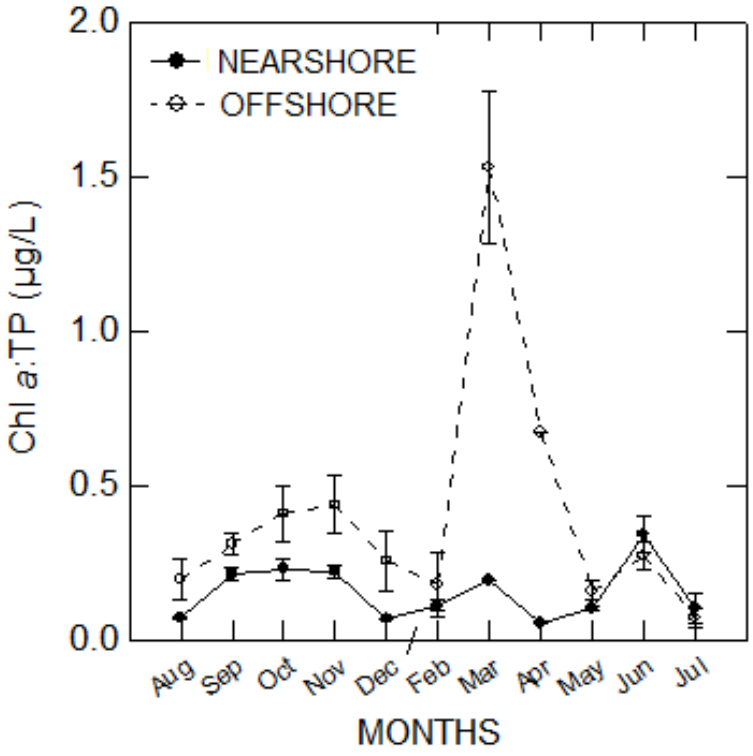

Figure 2.8 A monthly plot of chl *a*:TP from August 2010-July 2011. Each of the error bars are one standard error. The solid line is nearshore stations (•) and the dashed line is offshore stations (o). No samples were collected in January.

Size distribution of production and chl a

Netplankton production showed a maximum in November and August, with a smaller peak in April, and was higher offshore than nearshore in most months particularly from August to December and in April (Figure 2.9). A significant effect of season (LME, p=0.0065) and zone (p=0.0001) was detected but no significant interaction effect was reported (LME, p=0.92). The offshore net-sized production ranged from 0.015 (station M66, 21 Jun 11) to 4.24µg C·L^{-1}h^{-1} (station K45, 12 August 11) and the nearshore from ~0 (station T2, 12 Aug 11) to 1.88µg C·L^{-1}h^{-1} (station E51, 10 Nov 11). In total (nearshore and offshore), the mean netplankton production was highest in fall (1.18 ±0.26µg C·L^{-1}h^{-1}) and lowest in spring (0.31 ±0.11 µg C·L^{-1}h^{-1}). Seasonally, fall was significantly higher than all other seasons (LME, p<0.05) and the values in spring were not significantly different from summer and winter (LME, p>0.05). In April, however, only two samples were collected in the field, (station M66 and T2) and one (nearshore T2) was rejected as an outlier, so the lake was not well-sampled at this time. Samples from the WTP nonetheless supported the impression that netplankton production was relatively low in spring and early summer (Figure 2.9).

The maximum production for nanoplankton was found in September and decreased from then until early March (Figure 2.9). In March and April, nanoplankton production attained some relatively high values, especially offshore. It was lower again in May and variable through the summer. Similar to the netplankton production, nanoplankton displayed no interaction effects (LME, p=0.82) while both season (LME, p=0.001) and zone (LME, p=0.0062) were significant factors. The nanoplankton production reached up to 8.9 µg C·L^{-1}h^{-1} (station K42, 9 Mar 11) where the highest production was approximately twice higher than that of netplankton

production. The lowest nanoplankton production was found in station T2 in August 2011 (~0 µg $C \cdot L^{-1}h^{-1}$). By seasonal average, fall (2.33 ± 0.27µg $C \cdot L^{-1}h^{-1}$) was highest followed by winter (1.50 ±0.83µg $C \cdot L^{-1}h^{-1}$), summer (1.44 ±0.27µg $C \cdot L^{-1}h^{-1}$) and spring (0.78 ±0.30µg $C \cdot L^{-1}h^{-1}$). The average nanoplankton production in nearshore sites (1.19 ±0.20 µg $C \cdot L^{-1}h^{-1}$) was about half of offshore site values (2.22 ±0.36 µg $C \cdot L^{-1}h^{-1}$) (Figure 2.9). For picoplankton size production, no significant trends were detected for interaction, season or zone (LME, $P>0.05$) (Figure 2.9).

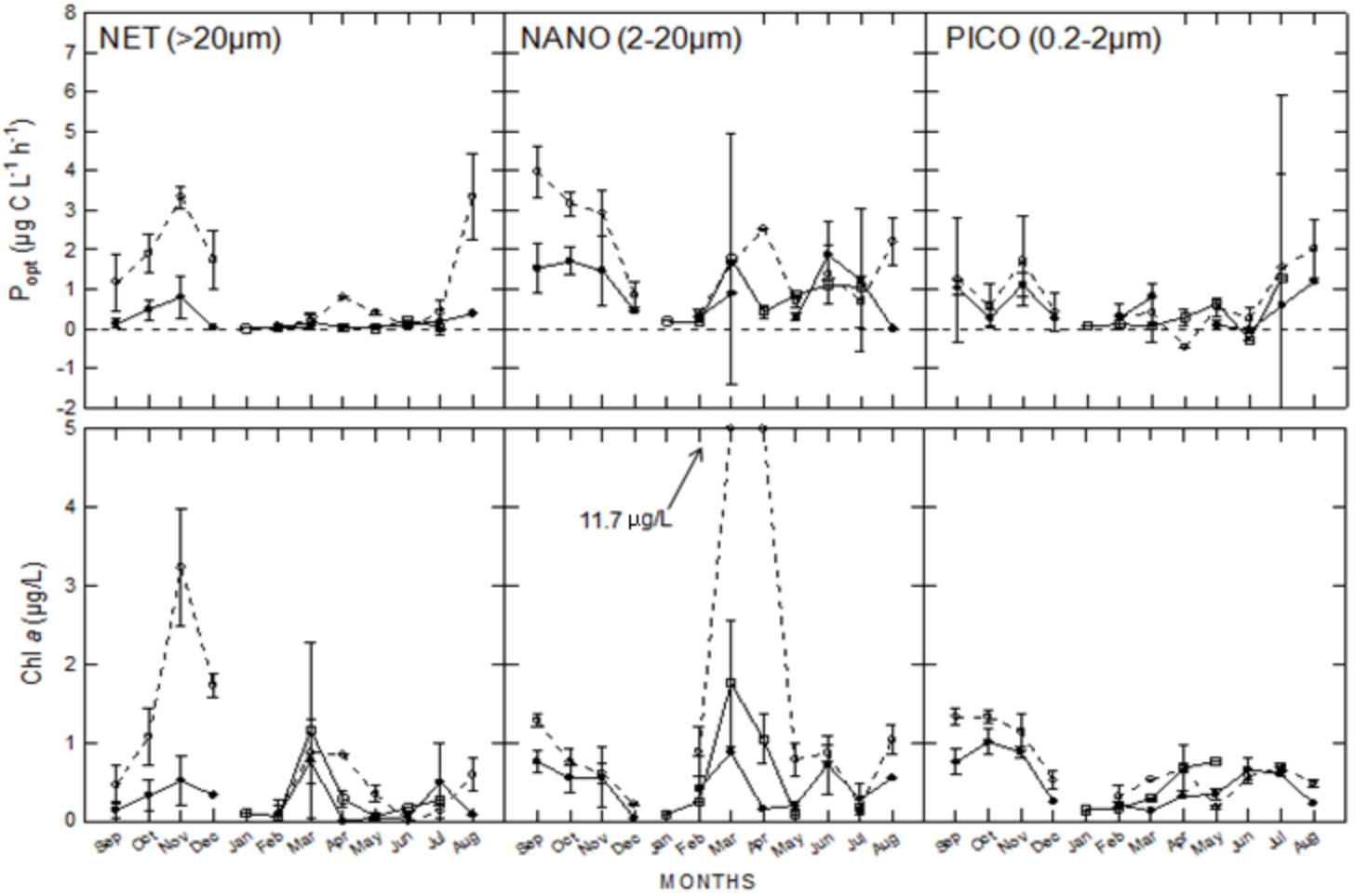

Figure 2.9 Panels a-c (top) show monthly plots of ^{14}C size production (P_{opt}, µg C $\cdot L^{-1}$ h^{-1}) by size class (net, nano and pico). Panels d-f (bottom) show monthly plots of chl *a* (µg/L) by size class. August 2010 data was excluded from the analysis due to poor experimental results. Points identified as outliers (>2 standard deviations) were removed from the analysis. The solid lines represent nearshore stations (•) and WTP (□) while the dashed lines represent offshore stations (o). Each error bar is one standard error.

The seasonal and spatial patterns of chl *a* size fractions were similar to the trends (Figure 2.9) in the ^{14}C size-fractionated production but with some important differences. In November, the netplankton production was reflected in an even greater peak of chl *a* as well as in August where the production was also seemingly higher with respect to chl *a* (Figure 2.9). An appreciable peak of chl *a* in March was not reflected in a comparable production peak. Netplankton chl *a* showed no interaction (LME, p=0.10) between season and zone but both season (LME, p=0.0073) and zone (LME, p=0.0014) were significant predictors (Figure 2.9).The seasonal average patterns in chl *a* differed slightly from ^{14}C production where fall (0.87 ±0.24µg/L) was highest followed by winter (0.66 ±0.2µg/L), summer (0.28 ±0.08µg/L) and spring (0.23 ±0.10µg/L). The difference between fall and winter was not significant (LME, p>0.05) but fall was significantly higher than summer and spring (LME, p<0.05). All seasons combined, the net chl *a* was about one third times lower in the nearshore (0.25 ±0.060µg/L) than offshore (0.82 ±0.18 µg/L). Also, the average netplankton chl *a* was higher in the offshore for each individual season compared to nearshore. Although the on-lake sampling was sparse in winter and spring, WTP samples gave results similar to the nearshore sites.

The seasonal and spatial patterns of nanoplankton chl *a* were similar to production (Figure 2.9) except the large winter chl *a* peak did not translate into a comparably large production peak while the fall peak of offshore production did not translate into as large a peak of chl *a*. The seasonal average chl *a* values were highest in winter (2.74 ±1.49µg/L), followed by spring (0.94 ±0.52µg/L), fall (0.75 ±0.085µg/L), and summer (0.53 ±0.085µg/L). Unlike the production, the differences in seasonal means for chl *a* were not significant (LME, p=0.063), owing to large within-season variability. No interaction effect was detected by the statistical

model (LME, p=0.40). The spatial trends, on the other hand, showed higher offshore chl *a* with zone a significant predictor for nano chl *a* (LME, p=0.023). In winter, for instance, the chl *a* was nine times higher in the offshore (4.27 ±2.34µg/L) than nearshore (0.45 ±0.19µg/L). WTP samples suggested that nanoplankton chl *a* may have been higher than suggested by on-lake sampling in March and April, but values were still lower than for offshore sites (Figure 2.9).

The monthly plot of picoplankton chl *a* showed highest average values in fall months (Sep-Nov), and a second maximum in summer (Jun-Aug, Figure 2.9). The offshore stations were relatively high in March to April, comparable to summer months but nearshore values were lower (Figure 2.9). WTP samples suggested that nearshore picoplankton chl *a* could be substantially higher than indicated by the sparse on-lake sampling. The relatively large fall chl *a* values were not reflected in comparably large production values, while the late summer production peak was not accompanied by as pronounced a maximum of chl *a* (Figure 2.9). The seasonal (LME, p<0.0001) and spatial (LME, p=0.0068) effects on pico-sized chl *a* were significant, and no significant interaction was identified (LME, p=0.13). The pairwise comparisons indicated no significant difference between average values for spring and winter (LME, p=0.88) but seasons were significantly different from each other (LME, p<0.05). For all seasons except spring, the mean for offshore stations was significantly higher than for nearshore stations (LME, p<0.05).

Seasonal areal primary production and inter-lake comparisons

The May to Oct. average chl *a* for Simcoe fell below the chl *a* vs TP trend line for values observed in other large north temperate lakes (Figure 2.10). The yield of chl *a* was especially low in the nearshore (average chl *a*:TP of 0.131) and was the lowest in the data set. The yield of chl *a* at offshore sites (average chl *a*:TP of 0.315) was, by contrast, almost exactly on the trend lines, suggesting little difference from the comparison systems. Additional years of observation would be required to allow statistical assessment of any apparent differences between Lake Simcoe and other lakes.

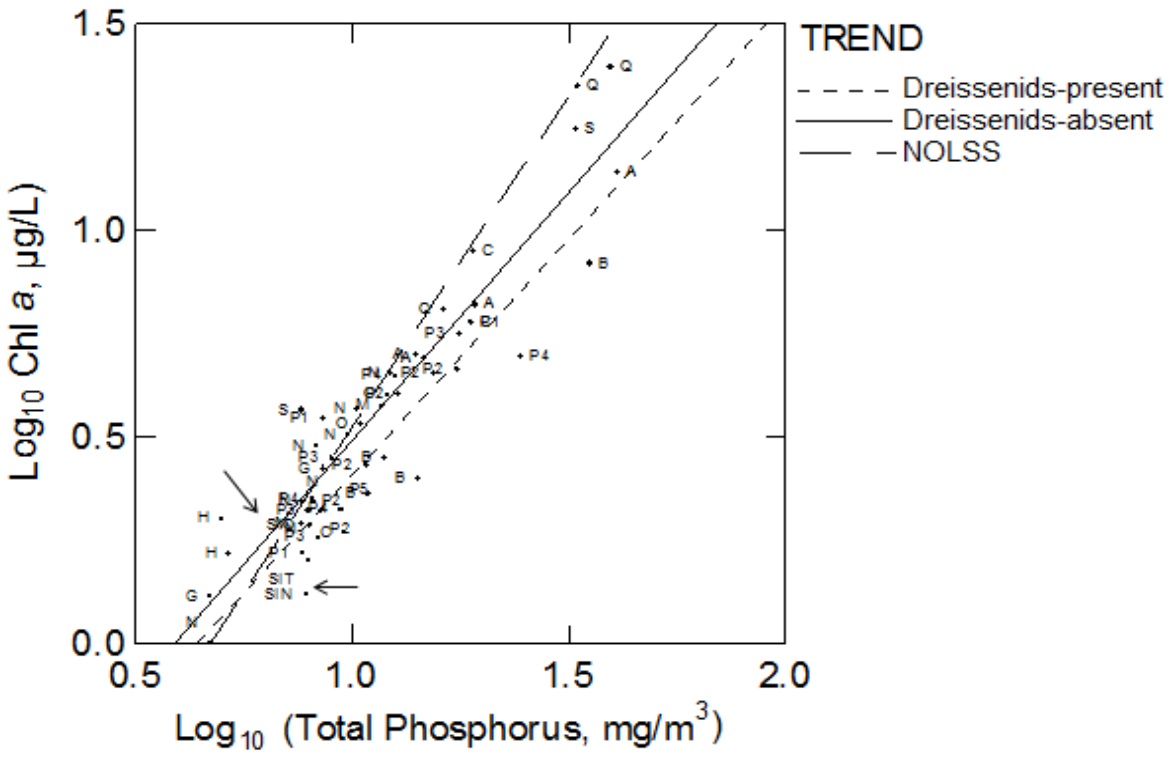

Figure 2.10 A modification from Smith et al. (2005). The plot shows relationship of $\log_{10}$ transformed chl *a* against TP. The arrows locate average offshore (SIO), nearshore (SIN) and total (SIT) chl *a*:TP for open water seasons (May-Oct). The solid, dashed, and broken lines represent dreissenids-present, -absent and NOLSS trend lines. Refer to table 2.6 for appropriate symbols on the plot.

The seasonal areal production (SAPP) ranged from 29.2 (station T2) to 151.1 g C·m^{-2} (station K42) (Table 2.5, Figure 2.11). The nearshore SAPP (61.2 g C·m^{-2}) was approximately 55% lower than offshore SAPP (135 g C·m^{-2}) (Table 2.5, Figure 2.11). This difference between nearshore and offshore was significant (ANOVA, p=0.0003). Figure 2.12 illustrates the relationship between TP and SAPP in various dreissenid present and absent locations (Table 2.6). ANCOVA indicated that TP was a significant (p=0.0001) predictor of SAPP, explaining 75% of the variation with the exclusion of the NOLSS lakes. The presence or absence of dreissenids was not a significant factor (p=0.09) but the average trend for dreissenid-present systems was, if anything, to higher SAPP than for dreissenid-present systems over the low to intermediate range of TP. The Lake Simcoe lakewide (SIT), and nearshore (SIN) averages were centered among other dreissenid-present and absent systems with comparable TP. The Lake Simcoe offshore average (SIO) was by comparison relatively high and above any of the trend lines.

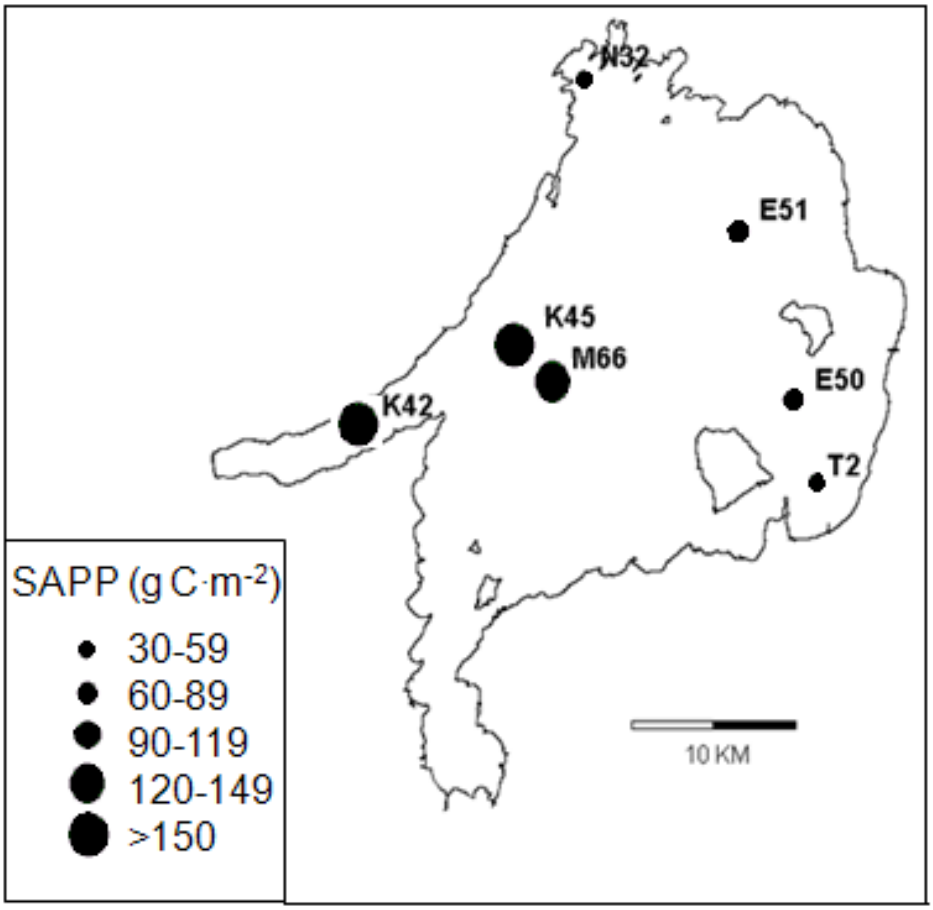

F**igure 2.11** Stations with SAPP estimates for May-Oct 2010-11 using 100% theoretical cloud free conditions. The units are expressed in g C m^{-2}.

Table 2.5 May-Oct 2010-2011 SAPP (g C·m^{-2}) values for each individual station. The average of all stations as well as the average nearshore and offshore SAPP were also computed. The SAPP was based on 100% free cloud model.

Station	SAPP (g C·m^{-2})
E50	61.5
E51	86.9
K42	151.1
K45	150.2
M66	130.1
N32	49.3
T2	29.2
Nearshore	61.2
Offshore	135
Total Stations	90

Table 2.6 Data used in figure 2.10 and 2.12. *Note that NOLSS stands for Northwest Ontario Lake Size Series. The table also shows the years that each point was taken along with the presence of *Dreissena*. Modified from Smith et al. (2005).

Lake	Years	Presence of Dreissena	Plot Symbol	Reference
Lake Erie	1968-72average	No	A	Charlton et al. 1999
Lake Erie	1984-86average	No	B	Charlton et al. 1999
Lake Erie	1985-88average	No	C	Makarewicz et al. 1999
Georgian Bay	1976	No	G	Kwiatkowski 1984
Lake Huron	1975	No	H	Kwiatkowski 1984
Lake Michigan	1970 and 1977	No	M	Carrick et al. 2001
NOLSS*	1986-1991	No	N	Millard et al. 1999
Lake Ontario	1987-92average	No	O	Millard et al. 1999
Lake Erie	1990-93average	Yes	P1	Makarewicz et al. 1999
Lake Erie	1993 and 1994	Yes	P2	Millard et al. 1999
Lake Erie	1994-96average	Yes	P3	Charlton et al. 1999
Lake Erie	1997	Yes	P4	Smith et al. 2005
Lake Erie	1998	Yes	P5	MacDougall et al. 2001
Bay of Quinte	1989-94average	No	Q	Millard et al. 1999
Saginaw Bay	1970-1980average	No	S	Fahnenstiel et al. 1995
Lake Simcoe (Nearshore)	2010-2011average	Yes	SIN	Present study
Lake Simcoe (Offshore)	2010-2011average	Yes	SIO	Present study
Lake Simcoe (All stations)	2010-2011average	Yes	SIT	Present study

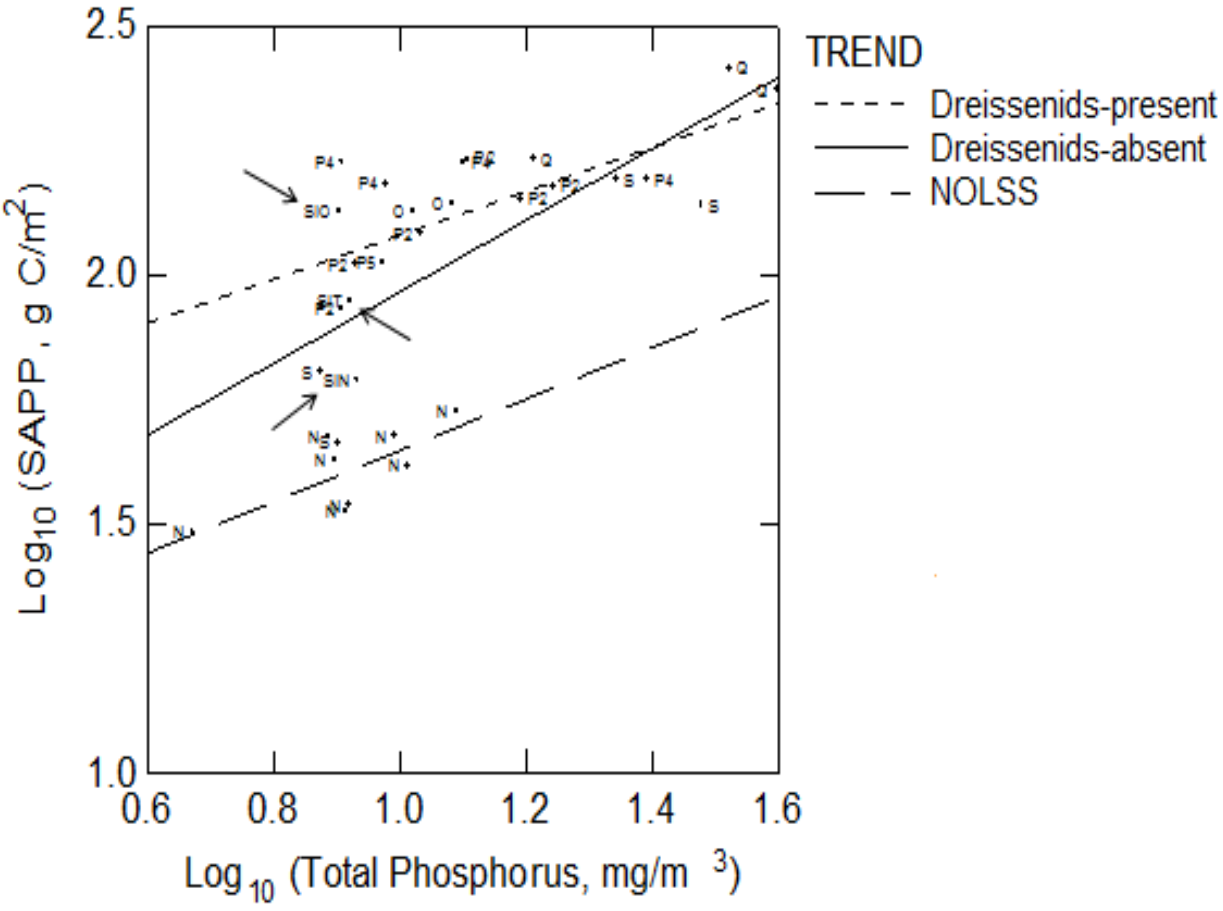

Figure 2.12 A modification from Smith et al. (2005). The plot illustrates $\log_{10}$ transformed SAPP and TP for post-dreissenid Lake Erie and Lake Simcoe and pre- dreissenid NOLSS and the Great Lakes excluding Lake Erie. The arrows indicate offshore (SIO), nearshore (SIN) and total (SIT) average SAPP vs. TP over May-Oct. Refer to table 2.6 for appropriate abbreviations.

The results from the sensitivity test suggested that chl *a* and P^B_{max} were the most influential variables explaining lower primary production in nearshore than offshore zones (Table 2.7). Substituting the offshore values for either parameter produced a 26% increase of nearshore production (ratio of 1.26). Despite the fact that Z_{max} (average station depth) had the greatest difference between zones (285%), it increased productivity up to only 20% (Table 2.7). Likewise, Z_{mix} had a difference of 102.7% between zones, but its effect on productivity was minimal (Table 2.7). The percentage differences in α^B and Kd_{PAR} were 28.2 and -10.8% respectively, resulting in a difference of production of close to 5%. The difference in SAPP with all offshore parameter values relative to all nearshore parameters (Total effect) was 2.03, similar to the average difference in observed SAPP between nearshore and offshore.

Table 2.7 Sensitivity analysis to determine which parameters are important in explaining the difference in average areal primary production between nearshore and offshore. The difference in average parameters is expressed as a percentage of the average value across both zones.

Parameters	**% difference in parameters (offshore-nearshore)**	**Proportional effect on nearshore production of substituting offshore parameter value**
Chl *a*	27.8	1.26
Kd_{PAR}	-10.8	1.05
P^B_{max}	56.9	1.26
α^B	28.2	1.05
Z_{mix}	102.7	0.99
Z_{max}	285	1.20
Total effect		2.03

Discussion

Lake Simcoe displayed large seasonal and shorter-term variations of chl *a* and primary production over the one year study period, and the pattern deviated from the classical bimodal pattern of spring and fall peaks. Lower chl *a* concentrations and primary production rates were detected in nearshore than offshore stations, consistent with the nearshore shunt hypothesis that mussels should be able to deplete phytoplankton more effectively in the nearshore (Hecky et al. 2004). The size distribution of chl *a* and primary production also varied, with netplankton and nanoplankton relatively more abundant and productive offshore than nearshore, and with annual production of potentially fast-sinking netplankton occurring mainly in the fall. Apart from mussels, the abundance of macrophytes in the nearshore may have played a role in nearshore production. Some of the potential impacts of macrophytes on phytoplankton production include alleopathy, enhanced of grazing pressure from zooplankton, increased sedimentation and shading. Overall, the results suggested that controls on phytoplankton production may operate somewhat differently in Simcoe than some other large lakes, and that the impacts of mussels in the natural environment may be different from expectations based on laboratory assessments of mussel energetics. Since the establishment of dreissenids, however, some trends (e.g. chl *a*:TP; Young et al. 2011) measured in the lake varied over the years and the results for this study may not necessarily represent the trends in past years or for the years to come.

Seasonal and spatial distribution of ^{14}C primary production and chl a biomass

Other large lake systems, including the eastern basin of Lake Erie (e.g. Depew et al. 2006) and Lakes Ontario (Millard et al. 1996) and Michigan (e.g. Fahnenstiel and Scavia 1987), have displayed bimodal patterns of primary production with spring and fall peaks. However, a unimodal pattern with a single production peak was documented in some stations in the eastern basin of Lake Erie (MacDougall et al. 2001), suggesting that patterns can vary among years and locations even in the same system. In the present study, Lake Simcoe displayed a unimodal pattern with a dominant peak in late summer-fall and the strong dominance of the fall peak seems unlike historic patterns in the Great Lakes. While the present study spanned only one year, sampling of water treatment plant intakes in years prior to dreissenid mussel colonization (1982-1992; Nicholls (1995)) showed that the highest phytoplankton densities occurred mostly in fall. Nicholls (1995) suggested the fall maxima might be supported by the internal loading of P from the sediment and this mechanism may still be an important driver.

Overall, the P_{int} was higher in the offshore compared to the nearshore, as observed in the eastern basin of Lake Erie (2001-2002) where dreissenids were suggested to be key agents in such spatial distribution (Depew et al. 2006). No previous data are available in Lake Simcoe to assess how P_{int} and P_{opt} respond to colonization by zebra mussels but studies conducted elsewhere (e.g. eastern basin of Lake Erie) reported higher nearshore P_{avg} or P_{opt} than offshore prior to dreissenids (e.g. Glooschenko et al. 1974, Bloech 1982, Depew et al. 2006). After the invasion the nearshore P_{opt} in the eastern basin of Lake Erie (2001-2002) was no longer higher than the offshore (Depew et al. 2006) and Saginaw Bay (Lake Huron) also showed a dramatic decrease (~37%) of P_{opt} in the inner, shallower part of the bay, supporting the idea that

dreissenids are capable of reducing primary production, at least in shallower waters (Fahnenstiel et al. 1995). In Lake Simcoe, a recent report estimated that the total biomass of dreissenids was 11 897 tonnes shell-free dry mass (SFDM)/m^2 and the percent of total dreissenids biomass was greatest at depth interval of 3.5-8m (32.1%) while little biomass was found in deeper areas (>20m) (Ozersky et al. 2011). The morphometry and mussel distribution in Lake Simcoe would seem likely to allow for strong mussel effects on the spatial distribution of production compared to other large lakes (e.g. the eastern basin of Lake Erie).

The nearshore shunt is a conceptual model that postulates an altered exchange of nutrients between offshore and nearshore, and retention of both offshore and external nutrients in the shallow nearshore as a consequence of the re-engineering of the lake ecosystem by dreissenids (Hecky et al. 2004). In fact, Lake Simcoe is becoming more spatially heterogeneous with dreissenids present and phytoplankton are filtered more readily at shallow, nearshore stations where they are more abundant (>80%), while deeper offshore regions such as Kempenfelt Bay remained unaffected (Guildford et al. unpublished, Young et al. 2011). Dreissenids are capable of depressing chl *a* levels as well as primary production, particularly in the shallower zone (Fahnenstiel et al. 1995), as seen in the northern part of Lake Erie (Nicholls and Hopkins 1993) and Lake Ontario (Hall et al. 2003). Somewhat contrary, in Lake Simcoe (2010-2011), the total chl *a* concentration was significantly lower in the nearshore in fall and winter but not necessarily in summer and spring. No direct observations or experiments were made on the activity of zebra mussels for this study but given that the optimal grazing temperature for *Dreissena* spp. typically range from 8 to 25 ℃ (Stanczykowska 1977), it is likely that dreissenids may have played a significant role in the spatial distribution of primary

production from late-spring (May) to fall (Sep-Nov). Dreissenids are capable of depressing phytoplankton biomass particularly under isothermal conditions as seen in Lake Michigan (Vanderploeg et al. 2002), as a result, significantly lower nearshore chl *a* seen in fall may largely be due to dreissenids actively feeding on the biomass. Unlike the isothermal conditions in fall, the formation of thermal stratification in summer (50% of the time) may have restricted mussels from accessing phytoplankton. This might lead to less of a difference in the actual chl *a* biomass between nearshore and offshore stations. In agreement with our results, in the mid-1990s (ice-free May-Oct.), there were declines in the total phytoplankton biovolume in Cook's Bay (26.4 $mm^3\ m^{-3}$/yr) and in the main basin, but no apparent decreases were found in the deeper Kempenfelt Bay (Young et al. 2011).

In addition to the effects of mussels, macrophytes can also have potential impact on nearshore phytoplankton production and chl *a*. Depew et al. (2011) found that the submerged macrophytes has increased 65% since 1987 to 2006 and 2007, and are present up to 10 m in depth. Much of their abundance is confined to shallow parts of the lake such as the Cook's Bay (Ginn 2011). Submerged macrophytes can reduce phytoplankton production by promoting shading and competition of light and nutrients (Søndergaard and Moss 1988, Depew et al. 2011). Moreover, many submerged macrophytes can release allelochemicals, interfering with phytoplankton growth (Addisie and Medellin 2012). More indirectly, macrophytes are linked to enhanced zooplankton grazing on phytoplankton because they serve as forage to zooplankton from predators (Depew et al. 2011). A rapid growth and expansion of macrophytes in the nearshore can be attributable to lower P_{int} and chl *a* in nearshore, but the future impact of macrophytes on phytoplankton primary production is still unknown for Lake Simcoe.

In some dreissenid invaded systems (e.g. Saginaw Bay, Lake Huron; Fahnenstiel et al. 1995), an increase of P^B_{max} was seen in the shallower part of the lake and attributed to enhanced nutrient cycling induced by the mussels, but this was not observed in the present study. In previous studies, differences in production between dreissenid-influenced nearshore zones and less influenced offshore zones have been attributed to differences in chl *a* concentrations and either Z_{mix} (Depew et al. 2006) or Kd_{PAR} (Fahnenstial et al. 1995). In the present study, however, the sensitivity test identified chl *a* and P^B_{max} as the main drivers, with a lower P^B_{max} nearshore. Photosynthetic parameters are affected by combinations of multiple factors, such as temperature, nutrients, species composition and cell size (Falkowski and Raven 2007). Typically, P^B_{max} is positively correlated with temperature (e.g. Fee et al. 1992; Millard et al. 1996) but during the ice-free seasons the differences in temperature between nearshore and offshore in this study were minimal. One possible reason for lower P^B_{max} in nearshore waters could be the recent reductions in TP loading, which have had greatest effect nearshore (Winter et al. 2007) and may have decreased P^B_{max} through heightened P limitation (Millard et al. 1999, Curl and Small 1965). However, the relationship between P^B_{max} and nutrients still remains controversial and is inconsistent between systems (e.g. Millard et al. 1999). There is evidence from algal culture studies (Litchman et al. 2003) that, because P deficiency depresses chl *a* contents as well as photosynthetic rates, P^B_{max} is not necessarily lower under P deficiency and may even be higher. In addition, there is evidence that nearshore phytoplankton in Lake Simcoe, as in eastern Lake Erie (North et al. 2012), are actually less P deficient than offshore.

Alternatively, spatial variation in phytoplankton species composition may have caused the differences in P^B_{max} (Smith et al. 2005). Although no samples were collected for taxonomic purposes, there were observable patterns in the ^{14}C and chl *a* size distributions. In the period of greatest expected mussel effect (late summer-fall), the production and chl a showed much more influence of larger (net and nano) classes offshore than nearshore, suggesting variability in community structure. Dreissenids are capable of filtering a wide range of size fractions (0.7-450μm) (Lavrentyev et al. 1995) but can selectively filter feed on preferred size groups, sometimes causing a shift in the phytoplankton community (Smith et al.1998; Nicholls et al. 2002; Barbiero et al. 2006; Winter et al. 2011). In the Hudson River, for instance, the seasonal variations in the phytoplankton groups changed after the establishment of mussels (Smith et al. 1998). Using diatom-based paleolimnological techniques, Hawryshyn et al. (2012) inferred a major shift in diatom species composition associated with dreissenid colonization in Lake Simcoe, consistent with "modern" sampling by Winter et al. (2011). Such a shift, Hawryshyn et al. (2012) argue, reflects a combination of climate trends, enhanced water clarity, internal P cycling and high grazing rates. To date, direct measurements of phytoplankton community composition in nearshore vs offshore zones have not been published for Lake Simcoe.

Netplankton production and biomass was greatest in fall, peaking in November, while a slight decrease was observed in the nanoplankton from September to November. The temperatures and mixing in fall should have been near-optimal for grazing activity of dreissenids. Some studies suggest that larger cells may be unpalatable to mussels, and at times the cells may be rejected as pseudofeces that are released back to the water column via the exhalant siphon. The discharged cells can survive and contribute to production and biomass (Baker et al. 1998,

Vanderploeg et al. 2001, Naddafi et al. 2007). In the dimictic Lake Erken, Naddafi et al. (2007) reported that phytoplankton size in the range of >50μm and ≤7μm were largely excreted as pseudofeces. Baker et al. (1998) noticed that in the Hudson River, diatoms were largely expelled to the water column as pseudofeces, and that the mussels filtered smaller phytoplankton more readily than the larger diatoms. However, net plankton in the current study were relatively much more abundant offshore than nearshore, especially in fall, and recent work indicates that quagga mussels are capable of ingesting and retaining large spring bloom diatoms (Vanderploeg et al. 2010). The spatial and temporal patterns of netplankton in Lake Simcoe were consistent with a similar ability of Lake Simcoe's zebra mussels to utilize the netplankton effectively and selectively reduce their abundance and productivity in the nearshore.

The general hallmark of nanoplankton is high metabolic and potential growth rates (Kalff, 2002) enabling them to proliferate especially in time of low predation. However, during open water seasons, when conditions are favourable for zooplankton and *dreissenia* spp. (8-25℃), nano-sized cells are preferentially grazed by the dreissenids (Barbiero et al. 2006). Even through mussels filter various sized particles, once they are well-fed, the dreissenids prefer particle sizes <50μm (Lavrentyev et al. 1995), a size range that may also include much of the netplankton fraction as measured in the current study. Also, food quality influences grazing selection, where the quality is defined by the content of the polyunsaturated fatty acid in algal cells (Naddafi et al. 2007). Sometimes, not only large cells but some of the small phytoplankton (e.g. *Stephanodiscus* spp.) may not be preferred by the mussels because of low polyunsaturated fatty acid content in the cells (Naddafi et al. 2007). The uptake of food by the mussels varies seasonally; dreissenids may experience low quality food in summer (cyanobacteria and chlorophytes) and high quality

food (flagellates and diatoms) in spring and autumn (Naddafi et al. 2007). The mussels may become opportunistic during times of good food quality, affecting the seasonal succession of certain phytoplankton size groups, particularly nanoplankton during fall and also spring.

Thermal structure of lakes is an important influence on phytoplankton size distributions because there is a strong association between sinking rates and the size and morphology of the cells (Wehr and Sheath 2003); smaller centric or ellipsoid diatoms enjoy advantages during thermally stratified periods compared to larger cells (Wehr and Sheath 2003). That is to say, some larger microphytoplankton (20-200µm), at least non-motile cells that lack buoyancy controls, can be lost by sedimentation from the photic zone under stable water conditions. Winter et al. (2011) and Hawryshn et al. (2012) have pointed out that shifts in the phytoplankton community structure in Lake Simcoe have connections to increasing water stability (Stainsby et al. 2011). In October to November, the resuspension of non-motile netplankton as fall mixing proceeds could enhance their biomass, while release of nutrients from the sediment and/or hypolimnion can help fuel their growth.

Seasonal and spatial dynamics of winter-spring phytoplankton

Due to the sparse winter sampling, it is difficult to capture the temporal and spatial variation of algal production and biomass. Relatively few freshwater studies are conducted outside of the conventional sampling period (late spring to late summer, Wetzel 2001) and some of these studies seem to suggest relatively low primary production and biomass during winter period (e.g. Glooschenko et al. 1974, Burns et al. 1978). Nevertheless, at times, the winter

biomass of phytoplankton is greater than summer (e.g. Straskrabova et al. 2005, Vadrucci et al. 2005) and a study done in Neusiedler See, a shallow temperate lake in Austria, showed that winter can contribute up to 10% of the annual production (Dokulil and Herzig 2009). The present results from Lake Simcoe show low production and biomass throughout winter, primarily due to light limitation. A strong, direct impact by zebra mussels may seem unlikely in this season of low temperature since they are mostly inactive during winter (Benson et al. 2013), although nearshore-offshore patterns were suggestive of mussel effects. The most important constraint on winter production, however, is the combined effect of decreased photoperiod and diminished light penetration due to snow and ice, which substantially reduce light available for photosynthesis (Wetzel 2001, Vehmaa and Salonen 2009).

The accumulation of snow is particularly important because some ice (e.g. columinar or congelation) can allow for relatively high transmission of PAR but snow cover on the ice strongly attenuates in the PAR waveband (Vehmaa and Salonen 2009). Some species of phytoplankton are capable of migrating towards the surface where light is more abundant. Smaller algae also have an advantage in such conditions because they have high surface area to volume ratios that slow sinking rates in the low-mixing environment under the ice and, with physiological modification of their buoyance, may be able to maintain themselves near the surface (Wetzel, 2001). A 'bloom' of nanoplankton was observed in mid-March with relatively high production rates. Similarly, in Lake Pääjärvi (Finland), the motile and smaller phytoplankton were observed to be most abundant under ice cover, and were able to at least partially resist mixing induced by convection during the ice growth season (Vehmaa and Salonen 2009). In Lake Simcoe, the maximum ice and snow thickness reached up to 40 cm (station E50,

3 Feb 11) and 12.7 cm (station K42, 9 Feb 11) respectively. Thicker ice and snow coverage was seen in mid-February and both nearshore and offshore production was extremely low (0.1-4.5 mg C m^{-2} d^{-1}). Once the ice and snow started to melt, however, the production increased up to four fold by March. In Lake Baikal, a population of large-celled diatoms (*Aulacoseira baicalensis*) formed under little to no snow conditions, but was greatly diminished when there was at least 10 cm of snow, attenuating 99% of light (Jewson et al. 2009). The spot measurements of irradiance in Lake Simcoe at station K42 showed only 2% and 8% of light penetrating through snow and ice in February and March, respectively, but the measurements may vary due to day-to-day weather variations. The photoperiod sets longer through winter, and the results from station K42 showed that the surface incident irradiance was 821 µE/m^2s (9 March 11) and 1820 µE/m^2s (14 Mar 11) which was up to 10 times higher than the observation from early February (177.9 µE/m^2s). The combination of increased photoperiod and reduced ice and snow thickness appeared to be the trigger for higher production and chl *a* in late-winter (March).

Additionally, the ice and snow cover can further modify the lake hydrodynamics by influencing the energy exchanges between the water and atmosphere (Assel et al. 2003, Oveisy 2012). Depending on the dynamics of the ice cover, it limits turbulence, restricts the suspension of phytoplankton in the water column, constricts the exchange of nutrients, and limits the gas exchange (Kalff 2002). Hence, the presence of ice can further prevent internal nutrient loading and sediment resuspension, thus reducing primary productivity (Nicholls, 1998). Particularly low production and biomass in February for all size fractions is likely due to the growth of ice, setting unstable conditions through convective circulation (e.g. Kiili et al. 2009). Once the ice

began to melt (mid-Mar), there may have been a period of stability that acted with the improving light environment to enhance primary production, leading to accumulation of biomass. There was in fact relatively strong inverse stratification at the time of the major offshore chl *a* maximum. Alternatively, the low sampling frequency in winter may have failed to capture an area that may have been harbouring high chl *a* biomass and production rates in nearshore waters. For instance, only one nearshore station (station E50) and two offshore stations (stations K42) were sampled in March. Nonetheless, the additional WTP samples collected in the winter do support that chl *a* concentrations were generally lower at nearshore than offshore stations.

The winter-spring phytoplankton bloom has been frequently documented across literature as seen in two of the stations in the western and central basin of Lake Erie in the 1970s (Burns et al. 1978) and also in 2007 to 2010 when a dense accumulation of *Aulacoseria islandica* (>10 µg/L chl *a*) was found below the ice under isothermal conditions (Twiss et al. 2012). Another incidence of winter bloom was recorded in Grand Traverse Bay in Lake Michigan (February and March of 1986) where the phytoplankton were concentrated in the upper 40 m under ice-cover (Vanderploeg et al. 1992). Legendre (1990) mentioned that late-winter and early spring blooms are mainly influenced by light provided that one of the proximate factors that control photosynthesis is light especially at the individual level. At the community level, however, meteorological conditions may play a larger role (Á lvarez et al. 2009). The duration of ice and snow cover is affected by meteorological conditions that can indirectly affect the primary production (Magnuson et al. 2000). The recent climate warming, for instance, has affected the ice phenology in Lake Simcoe so that Kempenfelt Bay currently experiences ice-off about 4 days earlier and ice-on about 13 days later. The total ice-free period also has been lengthened by 16

days (Hawryshyn et al. 2012). Future implications of winter primary production with respect to climate warming are hard to predict and are unknown, but reduced ice cover increases sediment resuspension and internal loading, which may enhance primary productivity (Nicholls 1998).

The importance of the spring bloom is widely documented across the literature (e.g. Gardner et al. 1990, Fahnenstiel et al. 2010, Vanderploeg et al. 2010, Sommers and Lewandowska 2011). In some low nutrient lakes, especially those situated at higher latitudes, appear to have a single spring peak that supports the pelagic food web (Sommers and Lewandowska 2011). The average production and biomass values in Lake Simcoe were lower in spring than at any other season except for winter. The ^{14}C size fractionation data show that there was a moderate increase in the nanoplankton (2-20µm) size groups and a slight increase in the netplankton (>20µm) size groups in the spring period. No apparent trends were identified in the picoplankton (0.2-2µm), contrary to some other findings in Lakes Huron and Michigan where the surface picoplankton abundances were lower during well-mixed seasons (Fahnenstiel and Carrick 1992) such as in spring. There is no direct evidence of changes in the seasonality of chl *a* and production since mussels arrived, but Hawryshyn et al. (2012) documented decreases of *Aulacoseira ambigua* before and after establishment of mussels. *Aulacoseira ambigua* is a classical spring bloom diatom and Lake Simcoe may have experienced a larger spring bloom in previous years. On the other hand, a fall maximum did occur in 1982-1992 based on the Sutton municipal water supply intake (Nicholls 1995), and the mussel veligers were not seen in Lake Simcoe until August of 1992 (Evans et al. 2011).

The spring bloom has been greatly diminished in some other large mussel-colonized lakes such as Lakes Michigan (offshore, Fahenestiel et al. 2010) and Erie (e.g. Barbiero et al. 2006). However, unlike Lake Simcoe where quagga mussels are scarce and neither zebra nor quagga mussels are abundant offshore (Ozersky et al. 2011), the aforementioned lakes have quagga mussels (*D. rostriformis bugensis*) with large populations in the profundal (offshore) as well as nearshore zones, which may allow for more impact during cold spring mixing conditions. Whether mussels are involved or not, the current study did not detect a major spring bloom in Lake Simcoe, either in total production or in netplankton. Instead, the fall was the key season for production of large and potentially fast-sinking phytoplankton. This fall peak still has potential to nourish benthos, enrich sediments, and fuel subsequent oxygen consumption but with different dynamics compared to the more classical spring bloom situation. The fate of the production generated in the fall is an important and unresolved question for Lake Simcoe. Climate changes (e.g. Sommer and Lewandowska 2011, Stainsby et al. 2011) may have diminished the importance of the Lake Simcoe spring bloom even if it did occur previously, and may also alter the processing of fall production with implications for food web production and hypolimnetic hypoxia in the next summer stratified season. The increasing air temperature trends show relatively warmer years in the recent period (Stainsby et al. 2011) which may allow for greater rates of metabolism at times of year when the processing of organic matter may formerly have been much slower. In addition, the recent increase in the *Daphnia* species due to declines in planktivourous fish (Nicholls and Tudorancea 2001) may have exerted stronger grazing pressure on phytoplankton although no direct observations of zooplankton were made.

The mass of chl *a* in winter can have implications for spring phytoplankton bloom because it may tie up the essential nutrients (e.g. dissolved P and Si) and carbon which essentially become unavailable to the spring algae while enriching the sediments as it sinks out. In Lake Erie, there is evidence of winter blooms beginning before the onset of ice cover and continuing the surface waters, diminishing silicate and perhaps available P for the spring phytoplankton (Twiss et al. 2012). In Lake Simcoe, since 1980s, spring silica concentrations have been increasing while spring TP decreased (North et al. 2012). The fate of the fall and late winter phytoplankton biomass maxima is unknown but they seem to disappear before the next spring sampling begins and may be assumed to sink, taking away nutrients, enriching sediments and fueling oxygen demand in sediments.

An inter-lake comparison of chl a:TP and SAPP:TP

A closer examination of the relationship between chl *a* and TP allows investigators to discriminate and better elucidate the possible role of dreissenids in lakes (e.g. Nicholls et al. 1999, Smith et al. 2005, Depew et al. 2006). A low chl *a*:TP ratio has been observed when zebra mussels exert high grazing rates on the phytoplankton population (Padilla et al. 1996). In the western basin station of Lake Erie, an increase in the chl *a*:TP ratio was seen when the mussel grazing decreased (MacDougall et al. 2001). Using samples from the municipal water supply intakes (May-Oct, 1976-1995) at various locations across the Laurentian Great Lakes, Ontario, Nicholls et al. (1999) reported lower chl *a*:TP in some systems coinciding with the arrival of dreissenids as seen in the nearshore of Lake Erie, western Lake Ontario and the Detroit River (Nicholls et al. 1999). In the case of Lake Erie, chl *a*:TP was found to be two to six times lower

after the invasion of dreissenids (Nicholls et al. 1999). In contrast, other sites did not show any dramatic decreases in chl *a*:TP and such sites include Lake Superior, southern Lake Huron, central and eastern Lake Ontario and the upper St.Lawrence River (Nicholls et al. 1999). Apart from the Great Lakes, the chl *a*:TP ratio in Oneida Lake remained constant before and after the establishment of zebra mussels (Idrisi et al. 2001) and there was no clear evidence that dreissenids lowered chl *a*:TP ratio in the offshore waters of some other larger lakes (Fahnenstiel et al. 1995, Nicholls et al. 1999, Smith et al. 2005). In Lake Simcoe, Young et al. (2011) showed fluctuations in the yield of chl *a*:TP from the years 1980-2008, where the ratio increased in the years 1997-2000 immediately after colonization of dreissenids and then decreased back to values similar to early 1990s and slightly increased again afterwards. Based on 2006 to 2007 samples, chl *a*:TP was lower in stations under 20 m of depth compared to deeper stations (Guildford et al. submitted). In the current results, nearshore chl *a*:TP was lower than the offshore except parts of summer (June and July). The overall mean TP was also higher in the nearshore (8.72 ±0.74 µg/L) than offshore (7.11 ±0.54 µg/L), possibly due to re-suspension of sedimented dreissenids feces, contributing to the particulate TP pool as seen in Nicholls et al. (1999). Additionally, higher TP in nearshore areas may be a result of TP inputs via tributary inflows, stormwater runoff and leaching from septic tanks (Winter et al. 2007). From 1980 to 2008, Young et al. (2011) did not find any strong association in chl *a*:TP and the establishment of dreissenids in relation to end-of summer volume-weighted hypolimnetic dissolved oxygen levels and there was an increase in the total phytoplankton biovolume based on 2008 to 2010 data, not supportive of the dreissenid grazing (North et al. 2012).

A cross-system comparison suggests that the total yield of chl *a* relative to TP in Lake Simcoe is at the low end of the range for other large lakes, falling below all trend lines (e.g. dreissenids-present,-absent, NOLSS). Within Lake Simcoe, the nearshore chl *a* was especially low compared to overall trends while offshore was in between other mussel-present and mussel-absent systems (Figure 2.10). The total TP loading into the lake has been decreasing (e.g. Eimers et al. 2005, Winter et al. 2007) but trends in ice-free TP showed no obvious trend (North et al. 2012). Despite the fact that dreissenids are capable of reducing particulate P (Higgins and Vander Zanden 2010), they can also release soluble P (Ozersky et al. 2009) reducing their impact on TP concentrations (North et al. 2012). It is also possible that sediment release of P (Nicholls 1995) is contributing to the lack of a trend in ice-free average TP concentration. However, alternatively and the likely reason for the large inter-annual variability is due to fluctuations in the annual precipitation (Young et al. 2011, North et al. 2012). In Lake Erie, there were no differences between mussel-absent and mussel-present years using similar analysis (Smith et al. 2005) but Lake Simcoe has a relatively larger area of mussel-colonized nearshore so should show more effect. However, no direct measurements are available for mussel-absent condition in Lake Simcoe to fully understand the effects of dreissenids on primary production.

The SAPP:TP analysis is modified from Smith et al. (2005) and is intended to put Lake Simcoe's primary production in context through comparisons with systems that have mussels and those which do not. Figure 2.12 supports an influence of TP on SAPP, but provides little evidence that presence or absence of dreissenids is a deciding influence on the SAPP:TP ratio in the comparison systems, which are represented mainly by measurements in offshore waters. Saginaw Bay in its dreissenid-absent years had a relatively low SAPP:TP and dreissenid-free

NOLSS lakes had very low SAPP, as noted by Guildford et al. 1994. Other dreissenid-absent systems, such as Lake Ontario and Bay of Quinte, showed high SAPP:TP ratios while the various dreissenid-present systems were not particularly low in SAPP:TP. The overall (total) and offshore values of SAPP for Lake Simcoe were relatively high and centered among other dreissenid present systems with similar TP values such as different years and basins of Lake Erie. The SAPP for nearshore Lake Simcoe, on the other hand, was on the trendline of large pre-dreissenid lakes with relatively low SAPP:TP. This further illustrates the non-uniformity of production in Lake Simcoe during this study. Millard et al. (1999) concluded that the decoupling of SAPP and TP in the nearshore of Lake Erie was largely due to declines in chl*a*:TP induced by mussel grazing because the photosynthetic efficiency was not lower. The present results suggested a different situation in Lake Simcoe as photosynthetic parameters seemed to be involved in nearshore-offshore differences.

Sensitivity analysis indicated, as found in several previous studies (Fahnenstiel et al. 1995, Millard et al. 1996, Depew et al. 2006) that chl *a* concentrations were important drivers of lower production nearshore. In the eastern basin of Lake Erie, P^B_{max} only accounted for >4% of differences in P_{int} (Depew et al. 2006); however, unlike the previous studies, P^B_{max} emerged as an additional important cause of lower nearshore SAPP in Lake Simcoe. The grand mean of P^B_{max} in Lake Simcoe determined here was 2.7 mg C·mg chl a^{-1} h^{-1}. In the data set, P^B_{max} ranged from 2.5 to 6.4 (Lake Erie) for the mussel-present lakes and 1.9 to 3 (Saginaw Bay) for the mussel absent lakes. The average value for Lake Simcoe was comparable to the range of mussel absent lakes and also higher end of NOLSS lakes (1.8 to 2.6 mg C·mg chl a^{-1} h^{-1}; late 1980s- 1990s) rather than the average P^B_{max} values for mussel present lakes. Lower P^B_{max} is commonly observed in

low-nutrient lakes (oligotrophic) provided that nutrients are likely to regulate the photosynthetic parameter (Millard et al. 1999).Despite the fact that Lake Simcoe is dreissenid-impacted, the average value of P^B_{max} was fairly low illustrating the point that the photosynthetic parameter may well be affected by the nutrient status of the lake. Furthermore, P^B_{max} is also measured between May to Oct, when most of the months were thermally stratified. The thermal stratification influences the parameter such a way that both NOLSS lakes (Guildford et al. 1994) and Lake Ontario experienced extremely nutrient deficient especially during summer stratification which was associated with low P^B_{max} (Millard et al. 1999). Although the contribution of nutrient deficiency remains controversial, different composition of phytoplankton assemblages can also influence P^B_{max}.

α^B (7.0 mg C mg$\cdot$chl a$^{-1}\cdot$mol$\cdot$quanta-$^{1}\cdot$m^{-2}) was higher than reported by Millard et al. (1999) for Lake Erie (1993 & 1994) and the Bay of Quinte (1989-1994) as documented by Millard et al. (1999). Values for α^B are sensitive to light source used, and the source used in this study tends to give higher values than those used in some other studies (Smith et al. 2005). Smith et al. (2005) measured a higher SAPP compared to other previous studies done in Lake Erie after the establishment of dreissenids and concluded that the difference was largely due to higher estimates for α^B. As the current study used the same light sources as Smith et al. (2005) it is unlikely that SAPP in the nearshore was underestimated due to erroneously low values for α^B. It is also unlikely, given the similarity of methods with Smith et al. (2005), that P^B_{max} was underestimated. However Lake Simcoe, in the year of this study, appeared to have lower nearshore SAPP driven significantly by lower light-saturated rates of photosynthesis relative to chl *a*. The implications of dreissenid presence for photosynthetic parameters may not be

consistent among lakes (Millard et al. 1999, Fahnenstiel et al. 1995) but in Lake Simcoe possible stimulation by mussel-mediated nutrient cycling did not support greater photosynthetic capacity or efficiency. The lake as a whole, and particularly the offshore, was highly efficient in translating TP into primary production. Whether that efficiency is due to indirect impacts of dreissenids or to other factors cannot be determined without further study.

Chapter 3- Deep Chlorophyll Layer (DCL) in Lake Simcoe

Overview

The deep chlorophyll layer (DCL) is a commonly documented feature in oligo- and mesotrophic lakes during the summer stratified season. If present, the DCL can be accompanied by production and biomass maxima at or close to the density gradient; as a result, the DCL is often viewed as an important feature for trophic transfer in many lakes. The current results (2010-2011) from Lake Simcoe (oligo-mesotrophic) showed that a DCL was not as frequent as expected, occurring only 28% of the time (n_{total}=18). The presence of a DCL was also temporally discontinuous, being observed in two of the summer months, May and July. For the stations with a DCL, a deep chlorophyll maximum (DCM) was detected at 13-19 m and the thickness of the DCL ranged from 8-15 m. Within the DCL, the chl *a* concentrations were 1.8-6.5 times higher than the surface mixed layer (SML) chl *a* concentrations. Profiles of percent dissolved oxygen (%) did not give clear evidence of elevated photosynthetic activity although the average subepilimnetic primary production estimates below Z_{mix} based on individual days was 55%. Assuming that the DCL often contributes significantly to the total production, it has a potential to nourish benthic filterers such as zebra mussels (*Dreissena polymorpha*). However, the present study suggests the DCL is not a strong feature in Lake Simcoe, and whether this is a consequence of feeding by the mussels themselves or other factors still requires more study.

Introduction

The deep chlorophyll layer (DCL) is widely documented in the Laurentian Great Lakes (Fahnenstiel and Scavia 1987a, Barbiero and Tuchman 2001) and other systems including oceans (Cullen 1982). In some clear oligotrophic lakes, elevated levels of primary production occurring near or above DCLs can contribute significantly to the total production which in turn, can be important for trophic transfer (Malkin et al. 2012). However, the contribution of the DCL to primary production varies widely (Millard et al. 1996); historically quite high in summer in Lake Michigan (Moll et al. 1984, Fahnenstiel and Scavia 1987b) and Superior (Moll and Stoermer 1982) but less important in the eastern basin of Lake Erie (Smith et al. 2005). Where documented in large lakes, the DCL tends to form in the early summer stratification period, deepening with the seasonal thermocline and dissipating in the late summer (Fahnenstiel and Scavia 1987b, Smith et al. 2005).

The presence of a DCL has potential to nourish consumers including benthic animals such as dreissenid mussels. In Lake Ontario, the DCL supported mussel growth at intermediate depths (10-15m) in early summer but there was no growth observed in late summer when the DCL dissipated (Malkin et al. 2012). While the DCL may be important to mussels, mussels may also affect the DCL. In some lakes with mussels, the deep chlorophyll maximum (DCM) forms deeper than recorded previously (Malkin et al. 2012). In Lake Michigan, the spring bloom has decreased greatly as mussels have spread and increased their biomass and there are indications that the DCL may also have diminished (Fahnenstiel et al. 2010). Lake Simcoe at the time of the current study had high areal mussel biomass but it was mainly in the mid-depth range (7-15m),

often below the seasonal thermocline in summer and not in the deeper offshore locations (Ozersky et al. 2011), so the implications for the DCL in Lake Simcoe not clear.

This study used vertical profiles of temperature and chlorophyll to characterize the seasonal presence, depth and chlorophyll concentrations of the DCL in Lake Simcoe. Potential productivity in the DCL was estimated using photosynthesis-irradiance (PI) modeling together with the observed chl *a* and light conditions in the DCL, while dissolved oxygen profiles were examined for evidence of DCL primary production. I hypothesized that a DCL would be observed at most offshore sites from early stratification until mid-stratification. I further hypothesized that the DCL could be a significant contributor to primary production in the early to mid stratification period but that it would become insignificant in the later stratification period. Because data on vertical chlorophyll distributions are vital to these questions, I also tested whether profiler estimates of chl *a* were consistent with estimates based on laboratory analysis of extracted chl *a*.

Methods

Sites and field sampling

Sampling was initiated from August 2010 and completed in August 2011 on a monthly basis although the winter samples (Feb-Apr 2011) were more opportunistic and inconsistent depending on field conditions. The first part of the study compares *in vivo* chl *a* obtained using a multiparameter water quality sonde (YSI-6600V2-4, YSI Inc, Yellow Spring, OH) with laboratory measurements of chl *a* in acetone extracts, in order to test whether or not the vertical profiles of chl *a* will be a good predictor for extracted chl *a*. The extracted chl *a* is not necessarily the absolute standard but it is the standard measure for the primary production estimates, so is an important reference point. All ten stations (N32, T2, E50, E51, K42, K45, M66, C6, C9, S15) were included in the analysis. The latter part of the study looks at the seasonal presence, chl *a* concentrations and potential productivity of the DCL in Lake Simcoe so, only the offshore samples (>15m; K42, K45, M66) from late-spring to late-summer (Aug-Sep 2010, May-Aug 2011) were considered. Only offshore stations from early to late-summer were considered in the second part of the study because DCL tends to develop in deeper waters during thermally stratified seasons (e.g. Fahnenstiel and Scavia 1987b). Stations were classified as "nearshore" if the Z_{max} was <15m (stations N32, T2, E50, E51, C6) and "offshore" (K42, K45, M66) if >15m in depth. Other field sampling methods and procedures were followed without deviation from chapter 2, unless stated otherwise.

Vertical water profiles

Vertical water profiles of chl *a* and the percent dissolved oxygen (%DO; up to Z_{max}) were taken with YSI for each of the stations. When comparing *in vivo* chl *a* with the extracted chl *a*, the average of *in vivo* chl *a* was made by averaging the chl *a* values to the epilimnetic sample depth, to correspond with the epilimnetic extracted chl *a* values. Vertical profiles of photosynthetically active radiation (PAR), including the surface PAR (above water), were collected using the Li-COR cosine underwater quantum sensor with Li-COR 1000 data logger (Lincoln, Nebraska). Then, the vertical attenuation coefficient (Kd_{PAR}) was calculated from the linear regression of ln (irradiance) vs. depth (Kirk 1994).

Determination of fluorometric chl a and dissolved inorganic carbon (DIC)

Extracted chl *a* was used to as a proxy for phytoplankton biomass (Cullen 1982) when estimating the primary production. To determine chl *a*, raw water was first screened through 200 µm mesh to remove larger zooplankton. Then, the screened water was filtered through a series of polycarbonate membranes (20 and 2µm). The 20 and 2µm filtrates were filtered through GF/F filters and temporarily stored in the dark at -20℃. After 18-24 h, the filters received 90% acetone for passive extraction of chl *a*, kept for another 24 h and measured using a Turner Designs 10-AU fluorometer (Turner Designs, Sunnyvale, California, USA) that had been calibrated against pure chl *a* (Smith et al. 1999, Depew et al. 2006). The Gran titration method (Gran 1952) was used to determine dissolved inorganic carbon (DIC) which was used to calculate the carbon assimilation.

Primary production estimates

For the stations that showed signs of DCL, primary production was determined as described in chapter 2 but with additional discrimination of its depth distribution. The program PSPARMS (Fee 1990) was used to construct a photosynthesis-irradiance (PI) curve (Jassby and Platt 1976) and calculate the light-saturated rate of photosynthesis (P^B_{max}) and the light utilization efficiency (α^B) where the subscript "B" denotes chl *a* normalization. One of Fee's programs, DPHOTO, was then used to calculate the daily areal and volumetric primary production based on 100% cloud-free model. Other outputs such as the mean PAR, the onset of light saturation (I_k) and the euphotic depth (Z_{eu}, 1%) were also generated along with the

production estimates. When calculating the production, chl *a* values below the surface mixed layer to Z_{max} were used; however, all other parameters (Kd_{PAR}, P^{B}_{max}, α^{b}, Z_{mix}) were assumed and kept the same as the epilimnetic samples. The % of production occurring within epilimnion was estimated by using the equation:

(1) $$(\text{Total } Z_{mix}\ P_{int}/\text{Total } P_{int})*100$$

Then the production below epilimnion (below Z_{mix}) was calculated by:

(2) $$100 - (\%\text{ production within epilimnion})$$

Statistical analysis

For the statistical analysis, model I regression was used to determine whether chl *a* obtained from YSI was a good predictor for lab extracted chl *a* (extracted). Prior to the analysis, the variables were $\log_{10}$ transformed to normalize the variances.

The model II regression was used to determine the slope of the relationship between YSI and extracted chl *a* during thermally stratified dates (except August of 2010), a data set used in latter part of the study. The analysis is similar to ordinary least squares (OLS), but OLS tends to underestimate the slope of the regression line; as a result, Major axis (MA), a type of model II regression, was chosen. MA is a useful model to use when information about the measurement errors in both of the variables is unknown and the two variables share similar measurement errors (Legendre and Legendre 1998). Moreover, this method allows one to test whether the slope is different from zero even when the two variables were measured under different

conditions (Legendre 2013). All the statistical analyses including model I regression were conducted using SYSTAT ver. 10.0 (SYSTAT Software Inc., Point Richmond, California) and the software R ver. 2.12.2 with the “lmodel2” package (Legendre 2013).

Results

Comparisons of chl a measurements

From August 2010 to August 2011, except for January, a total of 94 extracted and YSI chl *a* values were obtained in order to test whether or not *in vivo* and lab based chl *a* measurements agreed (Figure 3.1). From the model I regression, the coefficient of determination (R^2=0.61) was significant (p<0.05) and suggested a moderately strong linear relationship between $\log_{10}$ transformed YSI and extracted chl *a* (Figure 3.1). The slope of the line was close to, but less than, 1 (0.74) and the y-intercept of the line was close to zero (0.037; Table 3.1). The points were quite scattered and variable as some points deviated from the regression line (Figure 3.1, Table 3.1).

The large F-ratio in the analysis of variance indicated that some variations in the $\log_{10}$ transformed extracted chl *a* was explained by *in vivo* chl *a* (Table 3.2). Also, the hypothesis that the slope of the regression line is zero is rejected (p <0.05) where a significant linear relationship is shared between YSI and extracted chl *a* (Table 3.2).

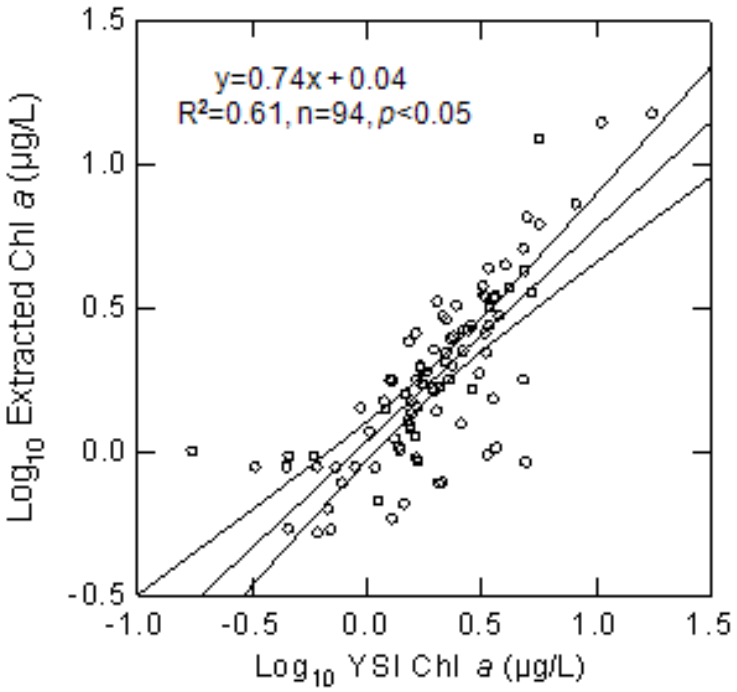

Figure 3.1 An OLS regression of extracted chl *a* vs. YSI chl *a* values for all seasons (n=94). As indicated by the *p* value on the graph, the correlation was significant and moderately strong (R^2=0.61). The middle solid line represents the slope (0.74) and the two bands around the slope are lower and upper 95% confidence interval. Prior to the analysis, the data was $\log_{10}$ transformed to stabilize the variances.

Table 3.1 Summary table of the coefficients (slope and intercept), standard error of the estimate (Std error) and 95% confidence interval from the model I linear regression of $\log_{10}$ transformed extracted and YSI chl *a*.

Effect	Coefficient	Std Error	Lower 95%	Upper 95%
Constant	0.037	0.027	-0.017	0.091
Log Extracted	0.74	0.062	0.62	0.86

Table 3.2 Analysis of variance. The parameters (sum-of-squares, degree of freedom (df), mean square, F-ratio and *p*-value) are all listed. All values were remained $\log_{10}$ transformed.

Source	Sum-of-Squares	df	Mean-Square	F-ratio	*p*-value
Regression	5.37	1	5.37	1.43×10^2	<0.05
Residual	3.45	92	0.037		

Apart from the global comparison, which included all the available chl *a* data, the winter (Feb-Mar) data were analyzed separately (n=23) by model I linear regression to further test the variability between the two measures of chl *a* in winter and whether *in vivo* chl *a* values serve as a good predictor for the extracted chl *a*. Based on the analysis, the coefficient of determination (R^2=0.72) was greater than in the global comparison and the slope of the line was closer to one (Figure 3.2, Table 3.3). There were some points that were scattered and more spread (Figure 3.2).

The results from the analysis of variance suggest that there is a significant (p= 2.8×10^{-7}) linear relationship between $\log_{10}$ transformed YSI and extracted chl *a* values in the winter. The F-ratio remained fairly high, and it seemed to suggest that YSI chl *a* still does help explaining the variances in the extracted chl *a* (p>0.05). The hypothesis that the slope of the linear regression line is zero is rejected (Table 3.4).

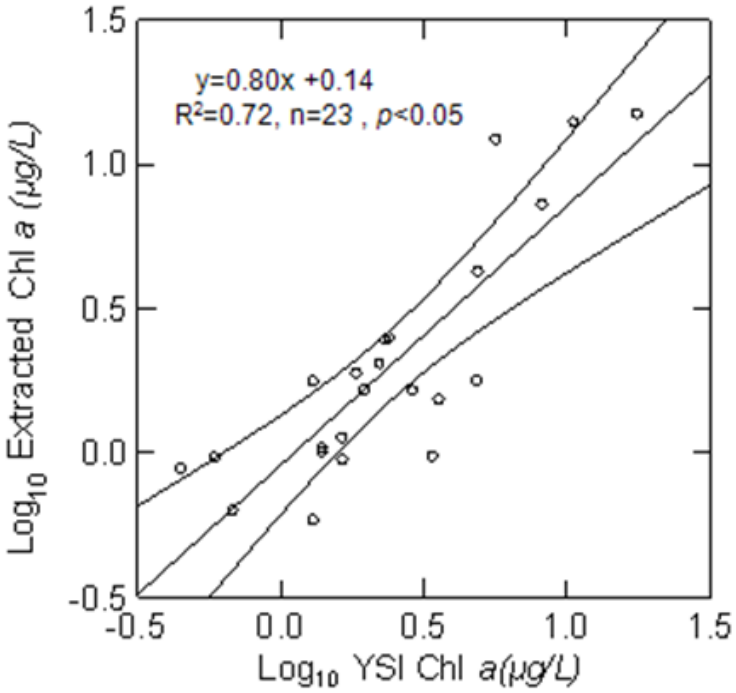

Figure 3.2 An OLS regression of $\log_{10}$ extracted and $\log_{10}$ YSI chl a (µg/L) for winter (Dec-Mar) except January. The two outer lines show upper and lower 95% confidence interval bands and the solid middle line shows the slope of the line. The regression equation of the model is y=0.80x + 0.14 where R^2 and p-value were 0.72 and <0.05 respectively.

Table 3.3 The parameters from the model I regression for the winter months only (Dec-Mar) are provided coefficient (slope (0.80); and intercept (0.14)); the std error and the lower and upper 95% of confidence interval. All of the data are $\log_{10}$ transformed prior to the analysis. No samples were collected in January.

Effect	**Coefficient**	**Std Error**	**Lower 95%**	**Upper 95%**
Constant	0.14	0.055	0.024	0.25
Log Extracted	0.80	0.11	0.58	1.03

Table 3.4 Analysis of variance for the winter (Dec-Mar) YSI and extracted chl *a* values. The parameters including sum-of-squares, degrees of freedom (df), mean-square, F-ratio as well as *p*-value are shown. All of the data is $\log_{10}$ transformed and note that no chl *a* samples were collected in January.

Source	**Sum-of-Squares**	**df**	**Mean-Square**	**F-ratio**	***p*-value**
Regression	2.43	1	2.43	54.8	2.8×10^{-7}
Residual	0.93	21	0.044		

Since the vertical chl *a* profiles of YSI will be used to examine the DCL in Lake Simcoe, it is vital to ask whether YSI chl *a* would be a good predictor for the lab extracted chl *a* during the thermally stratified period (Aug-Sept 2010 and May-Aug 2011) when a DCL could be present. There was a weak correlation between $\log_{10}$ transformed extracted and YSI chl *a*, where YSI chl *a* explained only 40% of variability of the extracted chl *a* (Figure 3.3, Table 3.5). The slope of the line was 0.50 (<1) and the points on the regression line were quite scattered and sparse (Figure 3.3, Table 3.5). Many of the values were under the lower 95% of the confidence interval and fewer points over the upper 95% confidence limit. Despite the fact that the relationship between two measured chl *a* values is weak, the null hypothesis that the slope of the regression line is zero is rejected ($p<0.05$) and there seemed to be a significant linear relationship between extracted and YSI chl *a* (Table 3.6).

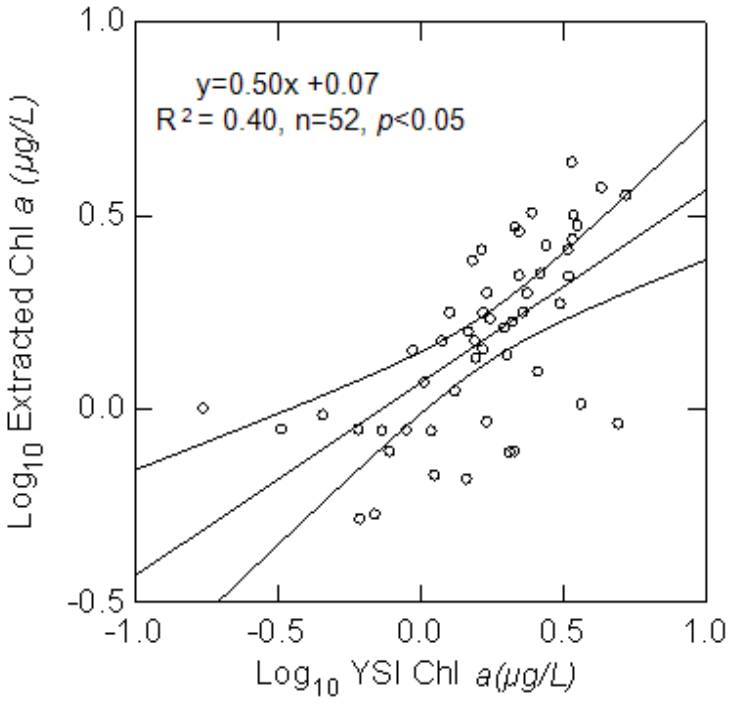

Figure 3.3 An OLS regression of extracted chl *a* vs. YSI chl *a* values for thermally stratified seasons (Aug-Sept 2010 and May-Aug 2011; n=52). As indicated by the *p* value on the graph, the correlation was significant but weak (R^2=0.40). The middle solid line is the slope (0.50) and the two bands around the slope are lower and upper 95% confidence interval. Prior to the analysis, the data was $\log_{10}$ transformed to satisfy the variances.

Table 3.5 The parameters from the model I regression for the thermally stratified months only (Aug-Sep 2010 and May-Aug 2011). These parameters include the coefficient (slope (0.50) and intercept (0.07)), the std error and the lower and upper 95% of confidence interval. All of the data is $\log_{10}$ transformed prior to the analysis.

Effect	Coefficient	Std Error	Lower 95%	Upper 95%
Constant	0.068	0.032	0.0036	0.13
Log Extracted	0.50	0.086	0.33	0.67

Table 3.6 Analysis of variance of YSI and extracted chl *a* values for the thermally stratified period (Aug-Sep 2010 and May-Aug 2011). The parameters include sum-of-squares, degrees of freedom (df), mean-square, F-ratio as well as *p*-value. All of the data is $\log_{10}$ transformed.

Source	Sum-of-Squares	df	Mean-Square	F-ratio	*p*-value
Regression	1.12	1	1.12	33.5	0.000
Residual	1.68	50	0.034		

Previous regression analysis (Figure 3.3, Table 3.5 and 3.6) included all of the available data from summer 2010; however, August 2010 chl *a* values were removed from analysis because of high variability in the data where lab extracted chl *a* values were seemingly low and underestimated. Once the data from August 2010 were excluded from the regression, the linear relationship between $\log_{10}$ transformed YSI chl *a* and extracted values improved so that YSI chl *a* explained 70% of the variability in the extracted chl *a*. The slope of the line was also closer to one (Figure 3.4, Table 3.7). The outcome of this analysis suggests that the null hypothesis is rejected and there is a significant relationship between the extracted and YSI chl *a* where YSI chl *a* is a good predictor for the extracted chl *a* (Table 3.8).

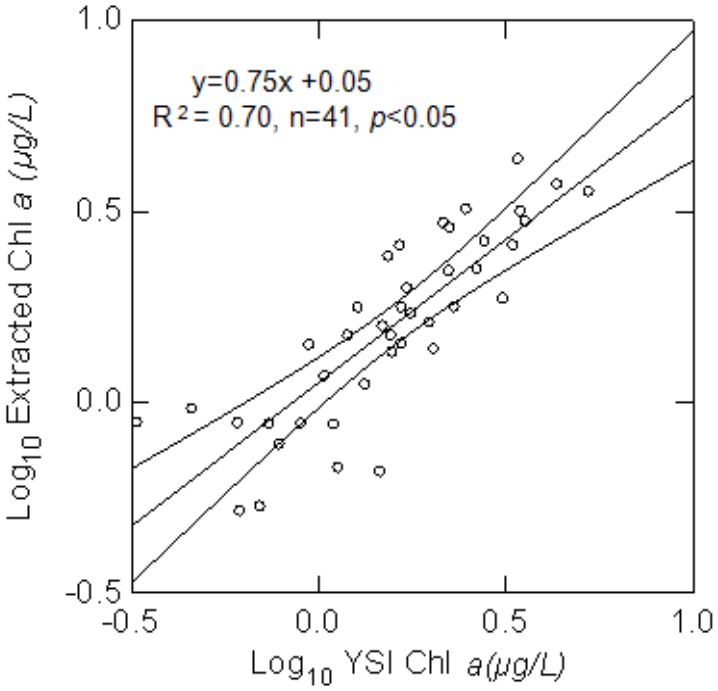

Figure 3.4 An OSL regression of extracted chl *a* vs. YSI chl *a* values from Sep 2010 and May-Aug 2011 (n=41). As indicated by the *p* value on the graph, the correlation was significant (<0.05) and moderately strong (R^2=0.70). The middle solid line represents the slope (0.75) and the two bands around the slope are lower and upper 95% confidence interval. Prior to the analysis, the data was $\log_{10}$ transformed to normalize the variances. An outlier was detected and removed from the analysis.

Table 3.7 The parameters from the model I regression for the thermally stratified months excluding August 2010 (Sep 2010 and May-Aug 2011). The coefficients (slope (0.75) and intercept (0.052)), the std error and the lower and upper 95% of confidence interval are provided. All of the data is $\log_{10}$ transformed. One outlier was omitted from the analysis.

Effect	Coefficient	Std Error	Lower 95%	Upper 95%
Constant	0.052	0.026	0.00	0.11
Log Extracted	0.75	0.079	0.59	0.91

Table 3.8 Analysis of variance of YSI and extracted chl *a* values for the thermally stratified period from Sep 2010 and May-Aug 2011. The parameters include sum-of-squares, degrees of freedom (df), mean-square, F-ratio as well as *p*-value. All of the data is $\log_{10}$ transformed. Also, an outlier was taken out from the analysis.

Source	Sum-of-Squares	df	Mean-Square	F-ratio	*p*-value
Regression	1.64	1	1.64	90.6	0.000
Residual	0.71	39	0.018		

Table 3.9 Major axis, a type of model II regression was used to test the significance of slope based on the model log(y)=blog(x)+*a* where *a*=intercept, b= slope of the line and x=dependent variable (YSI chl *a*) and y=independent variable (extracted chl *a*). The coefficient of determination (R^2) and the lower and upper 95% confidence intervals of the OLS (ordinary least squares) and MA slopes and intercepts are provided below.

Months*	Type of regression	R^2	Intercept	Slope	Intercept		Slope	
					Lower 95% CI	Upper 95% CI	Lower 95% CI	Upper 95% CI
Aug 2010-2011	OLS	0.61	0.04	0.74	-0.02	0.09	0.62	0.86
	MA		-0.02	0.94	-0.07	0.02	0.80	1.10
Winter (Dec-Mar 2011)	OLS	0.72	-0.04	0.90	-0.18	0.09	0.65	1.15
	MA		-0.11	1.07	-0.24	-0.005	0.81	1.42
Aug-Sept 2010 & May-Aug 2011	OLS	0.40	0.07	0.50	0.004	0.13	0.33	0.67
	MA		0.03	0.69	-0.04	0.07	0.47	0.96
Sept 2010 & May-Aug 2011	OLS	0.70	0.05	0.75	0.0	0.11	0.59	0.91
	MA		0.03	0.88	-0.01	0.06	0.71	1.09

*Includes all the specified months except for January

As OLS tends to underestimate the slope when the independent variable is measured with error, MA regression is also used for the analysis. The results from MA regression showed that the slope was closer to one and the intercept was closer to zero compared to the results from OLS (Table 3.9). Based on the MA regression, the intercepts were not different from zero and the slopes were also not significantly different from 1 except for one data set from Aug-Sept 2010 & May-Aug 2011 (Table 3.9).

Deep Chlorophyll Layer (DCL)

In this study, the deep chlorophyll layer (DCL) was defined as a region below or at thermocline where chl *a* was more than 2 times of the epilimnion concentration. Then, within this layer, the deep chlorophyll maximum (DCM) was the depth maximal of the chl *a*. During the late-spring to summer (Aug-Sept 2010, May-Aug 2011), 18 offshore samples (from stations K42, K45 and M66) were collected (Table 3.10). The average temperature for offshore epilimnetic samples in May was <8℃ (e.g. Figure 3.5) but as months progressed, the average temperature (Jul-Aug) increased to about 21-23℃ (e.g. Figure 3.6). For the months considered, all of the stations developed stable thermal stratification except in May, when a weak stratification was present.

A DCL was only detected 28% (n=5) of the time. Among the five occasions, three stations were in May (stations K42, K45, M66) and two in July (stations K45 and M66). Otherwise, a DCL was not detected for the rest of the season. For the stations that showed a DCL, the photic zone depth Z_{eu} (1% light level) was greater than Z_{mix} (Table 3.10). In May, the Z_{mix}

ranged from 5-10m and the top of the DCL was often approximately 10m with a thickness of 10-15m (Table 3.10). The average depth of the DCM was about 16m (Table 3.11). In July, the average Z_{mix} was 8.6m and the average depth of the DCM was 16.5m, similar to the DCM depth observed in May but the thickness of the DCL lessened to 8-10m, with the top depth starting at 10m (Table 3.11).

Table 3.10 Summary of all offshore stations (K42, K45 and M66) sampled from Aug-Sept 2010 and May-Sept 2011. The seasonal thermocline was defined as >1.0 C m^{-1} temperature gradient and the Z_{eu} (m) is the depth of photic zone (1% light level). DCL:SML is the ratio of average chl *a* concentration measured in DCL and SML.

Station	Month	Seasonal thermocline	Z_{mix} (m)	Z_{eu} (m)	Z_{max} (m)	DCL and DCM	SML (µg/L)	DCL:SML
K42	August 2010	Yes	9	14.5	36	No	3.4	N/A*
K45	August 2010	Yes	9.5	16.6	27	No	1.7	N/A
M66	August 2010	Yes	11	14.6	31	No	2.1	N/A
K42	September 2010	Yes	12	11.1	37.5	No	5.3	N/A
K45	September 2010	Yes	12	10.1	27	No	3.5	N/A
M66	September 2010	Yes	13	10.8	30	No	3.3	N/A
K42	May 2011	Weakly stratified	8	18.9	36.5	Yes	1.8	1.8
K45	May 2011	Weakly stratified	5	22	28.6	Yes	1.2	2.9
M66	May 2011	Weakly stratified	10	22.4	30.5	Yes	1.0	2.7
K42	June 2011	Yes	5.3	17.1	38	No	1.6	N/A
K45	June 2011	Yes	14.3	21.2	31.9	No	1.5	N/A
M66	June 2011	Yes	13.6	16.2	31	No	1.2	N/A
K42	July 2011	Yes	10.7	17.4	38.6	No	0.71	N/A
K45	July 2011	Yes	8.6	15.5	32.7	Yes	0.17	6.5
M66	July 2011	Yes	8.6	18.6	31.7	Yes	0.61	2
K42	August 2011	Yes	11	16.5	38.9	No	1.5	N/A
K45	August 2011	Yes	12.5	12.5	32.2	No	2.2	N/A
M66	August 2011	Yes	13.5	15.2	31.3	No	2.2	N/A

*N/A: Not available. DCL and DCM was not found

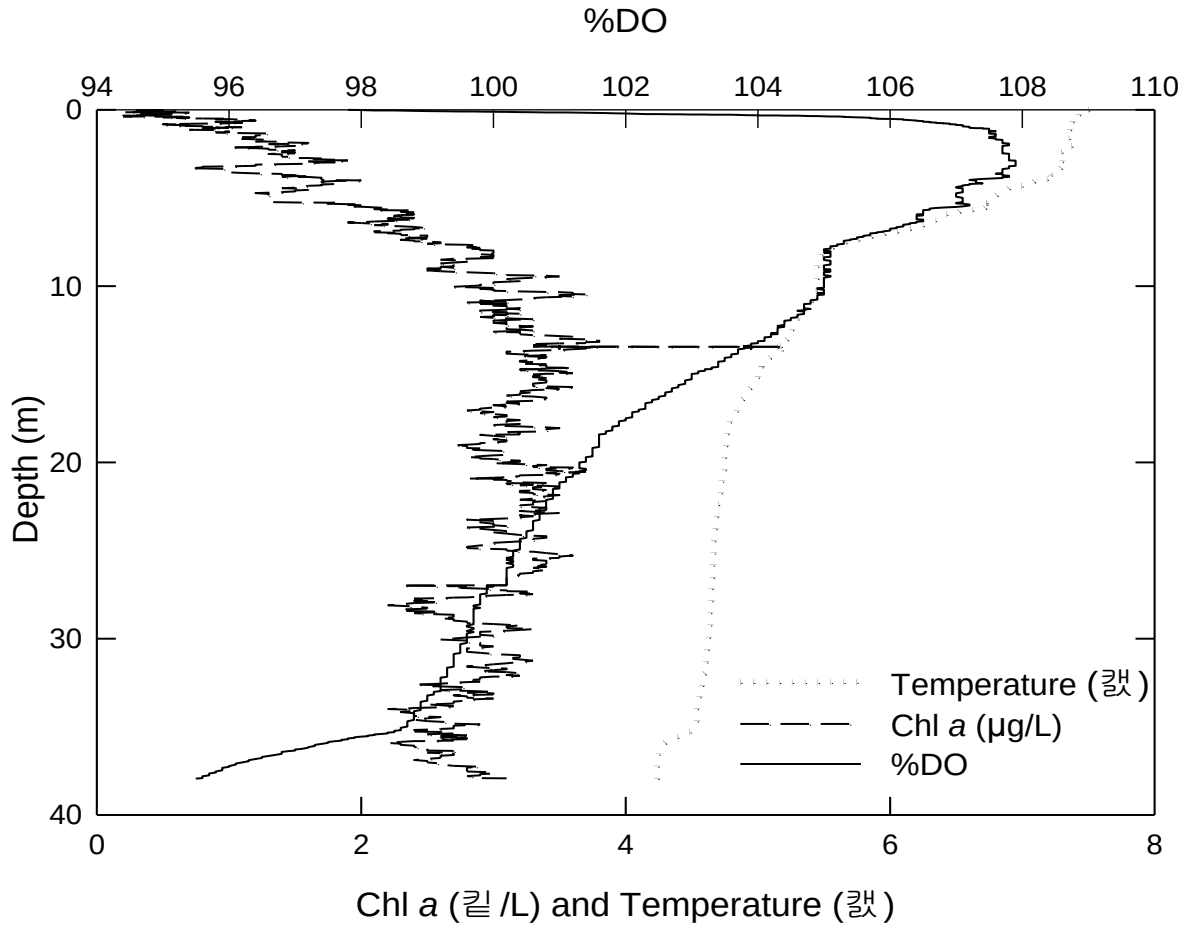

Figure 3.5 Vertical distribution of dissolved oxygen (% saturation; solid line), chl *a* (µg/L; long-dash line) and temperature (°C; short-dash line) over depth (m) for station K42 May 2011.

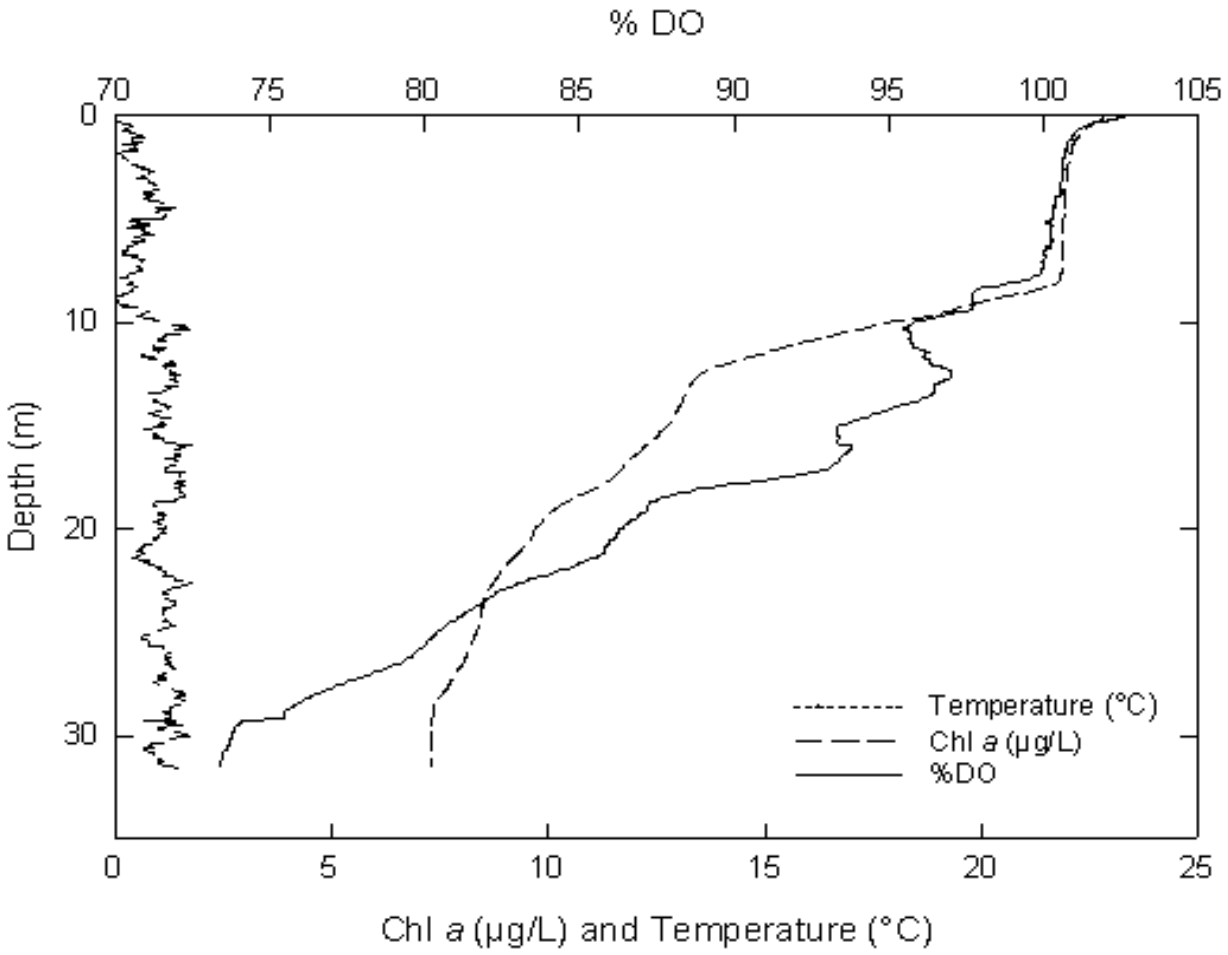

Figure 3.6 Vertical distribution of % dissolved oxygen (% DO; solid line), chl *a* (µg/L; long-dash line) and temperature (°C; short-dash line) over depth (m) for station M66 July 2011.

Table 3.11 The offshore stations (Z_{max}= >15m; Aug-Sept 2010 and May-Aug 2011) with DCL identified by vertical water column profiles using YSI. The surface mixed layer (SML) chl *a* represents the average epilimnetic chl *a* (µg/L) taken from YSI vertical profiles of chl *a*. The top depth of DCL (m) is the starting depth at which the subsurface chl *a* levels exceed two times of epilimnetic concentrations, usually below or at thermocline. The bottom depth of DCL (m) is the depth where DCL no longer exists (SML chl *a* ≥DCL chl *a*). Then, the chl *a* concentration in DLC is determined by averaging the chl *a* over the depth in which DCL is present, and the DCM is the maximum average chl *a* concentration (µg/L) over a meter found within DCL. The percentage of dissolved oxygen (%DO) is also included in the table, as taken from YSI.

Stations	**Date**	**Z_{mix} (m)**	**SML chl *a* (µg/L)**	**Top depth of DCL(m)**	**Bottom depth of DCL(m)**	**DCL chl *a* (µg/L)**	**DCM chl *a* (µg/L)**	**Depth of DCM (m)**	**%DO DCL**	**%DO DCM**
M66	10-May-11	10	1.0	10	25	2.7	3.7	18.5	102	101
K42	10-May-11	8	1.8	10	25	3.3	5.2	13	103	104
K45	10-May-11	5	1.3	10	20	3.5	4.3	16.6	104	103
K45	14-Jul-11	8.6	0.2	10	20	1.1	1.6	17	92	88
M66	14-Jul-11	8.6	0.6	10	18	1.2	1.8	16	95	94

The average *in vivo* chl *a* concentrations within the surface mixed layer (SML) from May and July ranged from 0.2 to 1.8 µg/L whereas the chl *a* concentration found within the DCL ranged from 1.1 to 3.5 µg/L. The average of SML and DCM chl *a* concentrations over the two months when the DCL was present (May and July) were 1 µg/L and 3.3 µg/L respectively; so the ratio between DCM and SML was 3. The average *in vivo* SML chl *a* concentration was particularly low in July, ranging from 0.2 to 0.6 µg/L and, at times, the ratio between chl *a* concentration in DCL to SML reached up to 6.5 times (station K42, Table 3.11).

The vertical distribution of the percent dissolved oxygen (%DO) may indicate elevated levels of primary production in the water column. Over 100% oxygen saturation was found within DCL depths in May. In July, on the other hand, the %DO was lower, just below 100% (92 and 95%, Table 3.11). However, throughout the study, there were no elevated levels of %DO observed near or at DCL for any stations relative to the SML (Table 3.11, Figure 3.5 and 3.6).

Epilimnetic P_{int} ranged from 14-69% for the stations that had DCL (Table 3.12). The average P_{int} occurring below Z_{mix} was estimated to be 55% of the total production in the water column for these stations, but the estimates were highly variable varying from 31% (July station M66) to 86% (May station K45).The mean PAR below Z_{mix} ranged from 21.8-59.6 µEin m^{-2} sec^{-1} and the I_k (1.6-5.5 µmol m^{-2} sec^{-1}) seemed to be generally higher in the stations where a DCL was detected (Table 3.12). At stations without a DCL, epilimnetic P_{int} was >80% of the total for the water column.

Aside from a DCL as usually defined, there seem to be some subsurface chl *a* maxima in the shallower waters in Lake Simcoe based on *in vivo* fluorescence. For example, one nearshore station (Z_{max}=5m; station N32) sampled in August of 2010 showed a subsurface chl *a* peak at a depth of 2.5m accompanied by elevated levels of % DO (113-114%; Figure 3.7).

Table 3.12 Using the Fee model, P_{int} (mg C m^{-2}) and P_{avg} (mg C m^{-3}) for offshore stations (Z_{max}= >15m; Aug-Sept 2010 and May-Aug 2011) were estimated based on 100% theoretical cloud free condition. All the parameters were kept the same as the epilimnetic samples and chl *a* values were entered below surface mixed layer to Z_{max}. Percent Epilimnion (% Epi) is the percent of daily primary production occurring in the epilimnion. The outputs from the model also include mean PAR (µEin m^{-2} sec^{-1}) up to and below Z_{mix} and the onset of light saturation (I_k, µmol m^{-2} sec^{-1}).

				P_{int} (mg C m^{-2})			**P_{avg} (mg C m^{-3})**			**Mean PAR(µEin m^{-2} sec^{-1})**		
Station	**Month**	**Z_{samp} (m)***	**Z_{eu} (m)**	**Total**	**To Z_{mix}***	**%Epi***	**Total**	**To Z_{mix}***	**%Epi**	**To Z_{mix}**	**Below Z_{mix}**	**I_k (µmol m^{-2} sec^{-1})**
K42	August 2010	0-10	14.5	746.9	690.2	~92.4	87.0	76.7	88	200.4	16.7	1.1
K45	August 2010	0-8	16.6	573.8	486.2	85	63.5	51.2	81	216.5	19.6	1.7
M66	August 2010	0-10	14.6	197.6	187.8	95	19.8	17.1	86	171.6	11.9	1.4
K42	September 2010	0-10	11.1	1224.7	1224.7	100	110.3	110.3	100	111.3	0.0	1.9
K45	September 2010	0-10	10.1	756.8	756.8	100	75.0	75.0	100	111.4	0.0	1.5
M66	September 2010	0-10	10.8	713.8	713.8	100	66.3	66.3	100	111.3	0.0	1.4
K42	May 2011	0-10	18.9	522.0	327.0	63	54.7	32.7	60	232.9	22.4	2.7
K45	May 2011	0-10	22	488.1	69.0	14	38.5	13.8	36	385.3	59.6	5.5
M66	May 2011	0-10	22.4	583.9	264.1	45	52.2	26.4	50	263.7	28.9	2.7
K42	June 2011	0-4	17.1	698.0	253.5	36	85.4	47.8	56	360.6	49.2	2.3
K45	June 2011	0-10	21.2	790.1	648.4	82	66.0	45.3	69	207.6	15.9	1.5

M66	June 2011	0-10	16.2	66.5	62.9	95	6.0	4.6	77	171.6	10.8	1.3
K42	July 2011	0-9	17.4	395.2	350.2	89	39.5	32.7	83	218.2	18.4	1.3
K45	July 2011	0-7	15.5	762.9	269.9	35	103.1	31.4	30	236.7	21.8	5.2
M66	July 2011	0-7	18.6	592.4	408.8	69	65.8	47.5	72	272.4	29.3	1.6
K42	August 2011	0-10	16.5	1096.2	997.8	91	108.8	90.7	83	178.8	13.9	1.9
K45	August 2011	0-10	12.5	954.7	951.9	~100	275.8	76.2	28	126.4	128.6	1.3
M66	August 2011	0-10	15.2	914.8	903.3	~99	73.9	66.9	91	140.7	8.5	1.1

*%Epi was calculated by: (To Z_{mix} /To)*100

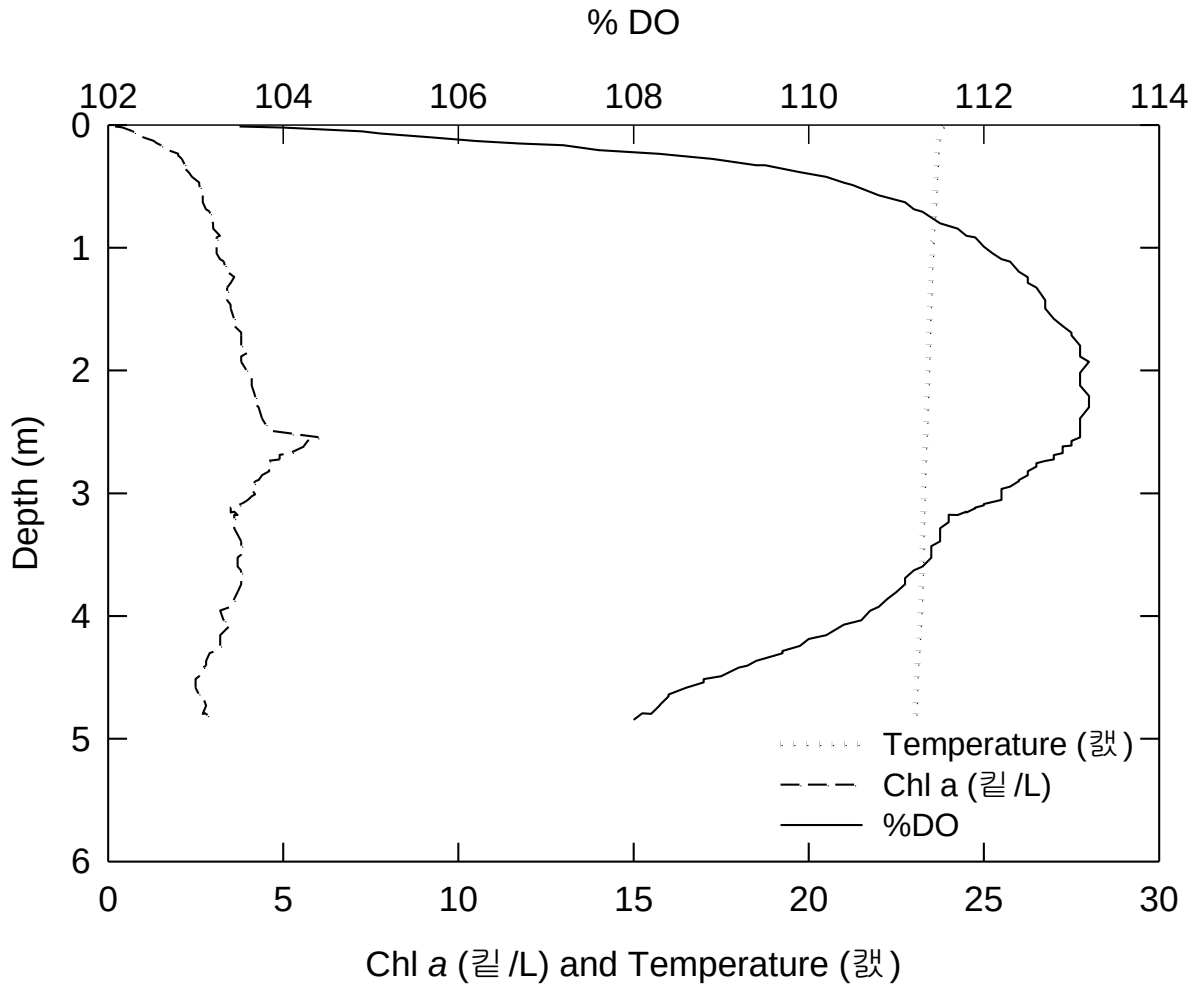

Figure 3.7 An example of subsurface chl *a* maximum in well-mixed shallow water. Vertical profiles of % dissolved oxygen (% DO; solid line), chl *a* (µg/L; long-dash line) and temperature (℃; short-dash line) over depth (m) is shown for station N32 August 2010.

Discussion

Comparison of chl a measurements

In vivo fluorescence is widely used to estimate vertical distribution of chl *a* in natural aquatic systems (Mignot et al. 2011). Although in vivo fluorescence is popular and favored among many investigators to measure chl *a* with depth, the method sometimes has difficulty in converting the fluorescence signal into an accurate estimate of chl *a* because of environmental variations such as the community assemblage, light and nutrients (Cullen et al. 1982, Mignot et al. 2011). For instance, even though the fluorescence is directly proportional to the chl *a* in the water, other pigments may interfere and affect the measurements. Nonetheless, in the current results, the model I linear regression showed that the *in vivo* florescence estimates of chl *a* were consistently correlated with the extracted chl *a* estimates. When the model II regression (MA) was applied, the slope of best fit and intercepts were closer to one and zero respectively. For the global, winter and stratified months data sets, the slope and intercept was not significantly different one and zero respectively, implying that YSI and extracted chl *a* measurements share 1:1 predictive relationship.

Although the relationship between YSI and lab-based chl *a* was significant in Aug-Sept 2010 and May-Aug 2011 data based on OLS, the slope of the predictive relationship was less than one suggesting that YSI has a tendency to underestimate chl *a* at low concentrations and overestimate at higher concentrations. This could happen if the YSI is not calibrated properly because YSI is dependent on temperature (YSI environmental 2006), where chl *a* estimates tends to increase as the temperature decreases. However, this is unlikely to have largely affected the

results because the instrument was calibrated with the natural lake water before the measurements were taken. Instead, once the August 2010 data were removed from the analysis due to high variability and underestimation, the relationship was much stronger where YSI chl *a* explained 70% of the variability in extracted chl *a*, compared to 40% variation. The slope and intercept was not significantly different from one and zero respectively, suggesting that both YSI and extracted chl *a* values agree with each other.

Deep chlorophyll layer (DCL) in Lake Simcoe

The development and persistence of DCMs can depend on the trophic status of lakes (Moll and Stoermer 1982) and can be important in oligo- and mesotrophic lakes, especially when there is sufficient light and nutrients to support the sub-epilimnetic community (Moll and Stoermer 1982, Fahnenstiel and Scavia 1987b, Malkin et al. 2012). Historically, DCMs were identified in many parts of the Great Lakes including Lakes Superior (Moll and Stoermer 1982), Michigan (e.g. Fahnenstiel and Scavia 1987b), Erie (e.g. Depew et al. 2006) and Ontario (e.g. Malkin et al. 2012), but reports on DCMs have not been made for Lake Simcoe yet. Based on the 2010-2011 data (May-Sept) a DCL was found only 28% of the time (n_{to}= 18) in Lake Simcoe which is very different from Lake Superior where the DCM is believed to be more frequent and a common feature of the deeper waters (Barbiero and Tuchman 2004). Most of the offshore stations (>15m; M66, K45, K42) that showed some indications of DCL were from May (weak stratification) and July (stable stratification). If found, the DCM in Lake Simcoe was centered at 13-19 m (Table 3.11) whereas DCMs were found deeper in Lakes Superior and Michigan, located at 25 m and 22 m respectively (Moll and Stoermer 1984) although both lakes were

sampled in August when DCM may have deepened. No DCM was detected in Lake Simcoe in August. For the stations with a DCL observed, chl *a* was 1.8 fold or higher (up to 6.5 fold) compared to the epilimnetic chl *a* samples. On average, DCL chl *a* was 3 fold higher than epilimnetic chl *a*, which is comparable to Lake Superior (3-3.5 fold; Moll and Stoermer 1982) but higher than some parts of Lake Erie (2-2.5 fold; Barbiero and Tuchman 2001 and 1.8 fold; Depew et al. 2006).

The subepilimnetic production occurring within or a few meters above the DCL can significantly contribute to total primary production and can be important for trophic transfer, as seen in the deeper waters of Lake Michigan (Fahnenstiel and Scavia 1987b) and also in the coastal zone of Lake Ontario (Barbiero and Tuchman 2004, Malkin et al. 2012). In Lake Michigan (mid-July), phytoplankton biomass was not only accumulated on the thermocline but they were also actively photosynthesizing, with an average of 69% of total production occurring between 5-50m of depth (Moll and Stoermer 1984). Large contributions from the DCL were also made in the eastern basin of Lake Erie (2001-2002) where subepilimnetic production on individual days contributed up to 67% of the total primary production in the water column and up to 19% of total seasonal areal primary production (SAPP) (Depew et al. 2006). The production within the DCL yielded even higher SAPP estimates for Lake Michigan where subepilimnetic production constituted approximately 30% (annual) and 50% (summer-only) to the total SAPP (Fahnenstiel and Scavia 1987a). Among the stations that had DCL in Lake Simcoe, the percentage of areal primary production on individual days occurring below Z_{mix} was >30%, but was highly variable between individual stations. The average subepilimnetic production below Z_{mix} was approximately 55%, which was higher than Lake Michigan (30%;

Fahnenstiel and Scavia 1987a) but lower than the eastern basin of Lake Erie (65%; Depew et al. 2006). However, unlike the other studies, the associated parameters including P^B_{max}, α^B and Kd_{PAR} were kept the same as the epilimnetic samples because separate discrete samples from DCL were not collected. Instead, chl *a* values obtained from the YSI were entered into the production program below Z_{mix} to Z_{max}. This is likely to influence the production estimates because the model DPHOTO (Fee 1990) assumes uniformity in the distribution of parameters in the water column unless specified (Depew et al. 2006). In fact, Depew et al. (2006) found that P^B_{max} and I_k values from the DCL were lower than the epilimnetic samples although α^B values were sometimes higher than the epilimnetic samples. However, the fact that Z_{eu} (1% light level) exceeded Z_{mix} throughout the study does indicate that there is light available for photosynthesis in the metalimnion. As of now, there seems to be some variability in Lake Simcoe, but not many demonstrations of significant deep production and biomass maxima as seen in other lakes.

Other than the estimates from the Fee model, a % dissolved oxygen peak may indicate elevated levels of production. In the vertical oxygen profiles, the percent oxygen saturation was >100% at all of the offshore stations collected in May (K42, K45, M66; Table 3.11) but there were no apparent %DO peak coincident to DCL (e.g. Figure 3.5). Instead, high %DO saturation levels in May may be a result of the seasonal heating of the lake as much, or more, than photosynthetic oxygen production (e.g. Wang et al. 2012). The relatively cold water in the metalimnion (4~6℃) may also have experienced some effect from warming, but to a lesser degree. Often a DCL is accompanied by production and biomass maxima (Fahnenstiel and Scavia 1987b) but some studies show that accumulations of chl *a* in the thermocline can form a DCL without high production or biomass (Cullen 1982, Barbiero and Tuchman 2001). Likewise,

the absence of sharp %DO peak in May could have been attributed to spring surface biomass sinking to the metalimnion. At times, surface phytoplankton may sink out into the metalimnion as nutrients become depleted in the epilimnion (Moll and Stoermer 1982). In Lake Michigan, for instance, the presence of spring diatoms in the epilimnion above the DCL significantly decreased after the onset of thermal stratification suggesting that there was biomass sinking as well as, or rather than, *in situ* growth driving the DCL dynamics (Fahnenstiel and Scavia 1987b). Although identifying phytoplankton species was not pursued in the present study, seasonal patterns of phytoplankton size classes from the epilimnetic samples suggest that there were decreases in the larger phytoplankton (>20µm) in May (see chapter 2). Likewise, Fahnenstiel and Scavia (1987c) suggested that the increase in the subepilimnetic biomass during the early stratification period (primarily June) when the epilimnetic temperatures were less than 15°C could have been the remnant of large, non-buoyant blooms of spring diatoms. Similar to the May samples, an oxygen peak was not detected within the depths of the DCL in July and the %DO was about 10% lower in July than May (>88%, Table 3.11). However, contrary to the observations from the vertical profiles of %DO, the production estimates from the Fee model predicted up to 65% (station K54, Table 3.12) of subepilimnetic production to the total production in July.

The extent to which the dreissenids affect the development of the DCL and the rates of subepilimnetic production is still poorly understood in lakes, including Lake Simcoe, but possibly with the exception of Lake Michigan (Depew et al. 2006). A study conducted in Lake Michigan showed that the size of DCL in recent years (2007-2008) was similar to or smaller than the previous years (1983-1987 and 1995-1998) mainly due to a shift in phytoplankton composition (net diatoms) caused by the quagga mussel (*Dreissena rostriformis bugensis*)

(Fahnenstiel et al. 2010). In contrast, in other lakes such as Lake Erie, increased water clarity was observed coincident to the arrival of dreissenids and this enhancement may have encouraged offshore subepilimnetic production (Millard et al. 1996). Similarly, a more recent study in Lake Michigan related the increase in DCL size to water transparency (Barbiero et al. 2009). After the invasion of mussels water clarity changes did occur in Lake Simcoe but they were inconsistent between years and areas (North et al. 2012). Whether the zebra mussels are capable of impacting the size of the DCL remains unsolved in Lake Simcoe. The mussels may be less likely to exert an impact on the DCL since they remain low in the offshore waters and the quagga mussels are still at low numbers throughout the lake (Ozersky et al. 2011a). However, the mechanisms by which mussels can impact the DCL in large lakes, where they do not have good direct access to the DCL phytoplankton in the deep offshore waters, are still not well known. It is possible that the large mussel populations at intermediate depths can strongly influence the DCL in Simcoe as water masses are advected between nearshore and offshore, much as long-range effects are speculated to operate in Lake Michigan (Vanderploeg et al. 2010).

As much as dreissenids affect DCL, DCL has the potential to nourish the mussels. In the coastal zone of Lake Ontario, for instance, DCM frequently intersected the mussels where the mussels were often nourished (Malkin et al. 2012). In the case of Lake Simcoe, zebra mussels that are largely present at 7-15m of depth suffer from food-limitation during early to mid thermal stratification period (Schwalb et al. submitted). However, zebra mussels are still at low numbers in offshore waters (Ozersky et al. 2011). The extent to which a DCL intersects the mussels and serves as potential food source during thermally stratified period still remains unresolved, but the

present study suggests that the DCL as measured by chl *a* is not a strong or persistent feature in Lake Simcoe.

Whether or not DCM has ecological significance remains controversial and varies between systems (Millard et al. 1996, Barbiero and Tuchman 2004). Millard et al. (1996) reported that DCM does not contribute significantly to the total primary production in Lake Erie while others concluded that the DCM can be biologically active and can have ecological significance in the system (e.g. Moll and Stoermer 1982, Fahnenstiel and Scavia 1987b). The question of ecological relevance still remains unclear in Lake Simcoe, and further assessment of DCL biomass and primary production in the future may help elucidate its significance.

Chapter 4- Conclusion

Lake Simcoe is the largest lake in the southern Ontario, excluding the Laurentian Great Lakes. The lake is of value to the province providing water to eight municipalities and attracting tourists and locals for recreational pursuits. However, since European settlement in the late 1700s, the lake has been degraded. During the 1970s, a rapid growth of urbanization and changing agricultural practices in the watershed led to increases in total phosphorus (TP) inputs into the lake, mainly through tributaries and outputs from sewage water treatment plants (Nicholls 1997, Young et al. 2011). Phosphorus (P) is regarded as the key limiting nutrient in lakes, and excessive P loading often stimulates phytoplankton and macrophyte biomass, which is often associated with degradation of water quality and hypoxia (Eimers et al. 2005). Hypoxia is a major concern in Lake Simcoe because it has a detrimental impact on the recruitment of native cold-water fish. The cold-water fishery has an important economic value, as it is one of the most popular recreational pursuits in Lake Simcoe generating over $200 million of annual revenue (LSEMS 2008).

In the late 1970s, oxygen depletion was estimated to be occurring over >33% of the lake surface area, totaling 20% of the lake volume (Neil 1990). The low oxygen levels led to recruitment failure of relatively high oxygen demanding cold water fish species such as lake whitefish (*Coreoonusclupeaformis*) and lake trout (*Salvelinus namaycush*; Winter et al. 2007). Since then, heightened concerns have prompted the Lake Simcoe Environmental Management Strategy (LSEMS) to attempt to remediate and restore cold-water fisheries by reducing TP loading into the lake and meeting the target of end-of-summer volume-weighted hypolimnetic

dissolved oxygen (MVWHDO) concentrations of 7 mg/L (Eimers et al. 2005), which is the minimum oxygen requirement for lake trout. Although TP levels have been reduced (Winter et al. 2007) and substantial improvements on the MVWHDO have been made (Young et al. 2011), the lake is still below (5mg/L) the recommended target.

The main objective of chapter 2 is to characterize the temporal and spatial patterns of phytoplankton primary production and biomass in Lake Simcoe. Phytoplankton production and biomass is linked to hypoxia, because much of the phytoplankton production that is not immediately consumed (e.g. by planktivous fish, zooplankton) settles out into deeper waters where it decomposes, consuming oxygen in the process. The results (2010-2011) from chapter 2 indicate that there is significant primary production occurring in the late summer to fall, contrary to the classical phytoplankton seasonal pattern for temperate dimictic lakes. In connection to hypoxia, this late summer to fall production and biomass maxima has the potential to nourish benthos, enrich sediments and fuel subsequent oxygen consumption. Deposition of particulate organic matter in fall can have adverse effects on the recruitment of some cold-water fish species such as lake whitefish because they typically spawn in the fall (Nov-Dec) and their eggs remain in the spawning grounds until spring (Apr-May) when they hatch (Fisheries and Oceans Canada, 2010). On the other hand, one possible scenario can be that much of the organic matter can be burned-off before the next summer commences, resulting in diminished hypoxia in summer. Filtration by zebra mussels and rapid colonization of macrophytes (3.1 kg m^{-2} in 2008; Ginn 2011) can also retain much of the organic materials and compete with phytoplankton for resources, thereby reducing the severity of oxygen depletion over time.

Whether or not Lake Simcoe experienced larger spring peaks in past years still remains an open question. The importance of the phytoplankton spring bloom has not been highlighted in the past for Simcoe, but for other large lakes such as Lake Michigan, spring blooms play a large role in supporting secondary producers (Fahnenstiel et al. 2010). Even if the bloom did not occur previously, the absence of spring bloom in Lake Simcoe could be a result of a large phytoplankton biomass found in winter (mid-March) tying up much of the essential nutrients (e.g. silica) which essentially becomes unavailable to the spring phytoplankton while enriching the sediments as it sinks out. Research on other comparable lakes such as Lake Erie has shown that winter and early spring phytoplankton have the potential to deliver organic matter and fuel oxygen-depletion in the hypolimnion (Twiss et al. 2012). Similarly, Lake Simcoe is ice-covered for most of winter and the large phytoplankton bloom observed in mid-March may have the potential to enrich sediments, leading to subsequent oxygen depletion in summer. Furthermore, reduction of ice cover due to climate warming could also contribute to a larger diatom bloom in the future, which could potentially lead to earlier and more severe hypoxia in the summer.

The interaction of multiple stressors (e.g., dreissenids, nuisance macrophytes, and climate) and a lack of historical data make the seasonal production pattern even harder to predict in Lake Simcoe. For instance, stressors such as climate warming were linked to changes in the diatom assemblages in Lake Simcoe itself (Rühland et al. 2012) but the effects on primary production remain unknown. In the longer run, sampling beyond the conventional time (winter, spring and fall) is necessary to characterize the seasonal and spatial patterns of production and biomass. Having robust and long term data can help to elucidate some of the possible mechanisms of hypoxia and suggest ways to control phytoplankton production and biomass more effectively.

For instance, mid-September is the end of the set-date for monitoring MVWHDO levels because the water temperature starts to cool down and the mixed depth extends below 18m. However, the MVWHDO levels have been decreasing beyond the set date of mid-September and continue to decline to the end of month, largely due to prolonged fall turnover (Stainsby et al. 2011, Young et al. 2011). The results from chapter two show that fall (Sep-Nov) seems to be an important season for production and biomass, suggesting that longer monitoring dates for MVWHDO may be necessary in the future.

Lake Simcoe is relatively small compared to the also mussel-infested Great Lakes, with over 50% of its area being less than 20 m deep. The nearshore of the lake is not only important for tourism and recreational pursuits, but also supports warm-water fish. The offshore of the lake, on the other hand, serves as habitat for cold-water fish including lake trout. For most of the time, primary production and chl *a* was lower in the nearshore than in the offshore. The greatest spatial differences were evident during fall mixing when zebra mussels may have had greater access to phytoplankton in the nearshore, exerting higher grazing pressure on phytoplankton. The SAPP (May-Oct) also was lower in the nearshore than in the offshore, which was quite productive in comparison to other similar large lakes. The direct impact of zebra mussels on the primary production still remains unsolved, although some of the results do support effects of mussels. For instance, selective decreases in phytoplankton size fractions in the nearshore community, particularly when mussels are thought to be active, do support preferential feeding by zebra mussels. The chl *a*:TP was also significantly lower nearshore than offshore, consistent with grazing impacts from the large nearshore dreissenid mussel community (e.g. Nicholls et al. 1999). Despite the fact that Lake Simcoe shows some of the "symptoms" listed under the nearshore

shunt hypothesis (Hecky et al. 2004, North et al. 2012), the processes by which mussels are re-engineering the lake seem to operate somewhat differently from other comparable mussel-invaded lakes (e.g. North et al. 2012). Moreover, since zebra mussels graze on phytoplankton and remove them from the water column, macrophyte biomass has the potential to grow, especially under nutrient-rich and enhanced light conditions (Ginn 2011). Although macrophytes can be beneficial (e.g. fish habitat), excessive growth of macrophytes can reach undesirable levels, which can be economically costly and consume more oxygen. Phytoplankton production and biomass can therefore be used as environmental markers to compare changes over time (Ginn 2011) and predict the state of the ecosystem function.

A deep chlorophyll *a* maximum (DCM) was only found 28% of the time for this study. Nonetheless, the average subepilimetic primary production occurring within DCM was estimated to be 55%. From the management perspective, it is imperative to examine the DCM in the future because it can be important for trophic transfer as seen in other Great lakes, including Lake Michigan (Fahnenstiel and Scavia1987b) and Lake Ontario (Malkin et al. 2010) as the DCM has the potential to nourish benthic filterers such as zebra mussels. Combinations of wind-driven horizontal currents and internal wave activity in Lake Simcoe (Bouffard and Boegman 2012) may also allow DCM to be available to the mussels residing in waters that are much shallower (Schwalb et al. submitted). However, at this point, the lack of data on DCMs makes it difficult to predict the extent to which DCMs overlap with the mussels and also the mechanism and ecological relevance of DCM in Lake Simcoe.

In the future, studies of phytoplankton primary production and biomass will help understand the contribution of fall and winter production and provide guidance to site-specific phosphorus and oxygen remediation. Moreover, characterizing temporal primary production can help understand the changes in other stressors such as climate change. In order to effectively design management strategies and to extrapolate some of the possible future outcomes of interactions between multiple stressors in a lake ecosystem, consistent long term data are crucial since important ecological changes and processes occur over a decade or longer, depending on the lake (Magnuson 1990**,** Fahnenstiel et al. 2010). The absence of long term data can lead to ineffective and misguided management practices, which in return can be costly (Magnuson 1990, Fahnenstiel et al. 2010**)**. In Lake Simcoe, apart from the introduction of mussels, combinations of other stressors such as the climate changes and urbanization make it even harder to predict the possible ecological outcomes (Hawryshyn et al. 2012). Before investing in future costly management changes, monitoring and research should be continued to determine what changes will have the greatest impact.

References

Addisie, Y., and Medellin, A.C. Allelopathy in aquatic macrophytes: Effects on growth and physiology of phytoplanktons. 2012. J. of Plant Sci. **6**(10):270-276.

Akerman, J.D., Loewen, M.R., and Hamblin, P.F. 2001. Benthic-pelagic coupling over a zebra mussel reef in western Lake Erie. Limnol. Oceanogr. **46**:892-904.

Á lvarez, E., Nogueira, E., Acuña, J.L., López- Á lvarez, M. and Sostres, J.A. 2009. Short-term dynamics of late-winter phytoplankton blooms in a temperate ecosystem (Central Cantabrian Sea, Southern Bay of Biscay). J. Plankton Res. **31**(6):601-607.

Arnott, D.L., and Vanni, M.J. 1996. Nitrogen and phosphorus recycling by the zebra mussel (*Dreissena polymorpha*) in the western basin of Lake Erie. Can. J. Fish. Aquat. Sci. **53**:646-659.

Assel, R. A., Cronk, K. and D.C. Norton. 2003. Recent trends in Laurentian Great Lakes ice cover. Climate Change. **57**:185-204.

Baker, S.M., Levinton, J.S., Kurdziel, J.P., and Shumway, S.E. 1998. Selective feeding and biodeposition by zebra mussels and their relation to changes in phytoplankton composition and seston load. J. Shellfish Res. **17**(4):1207-1213.

Barbiero, R.P. and Tuchman, M.L. 2001. Results from the U.S. EPA's biological open water surveillance program of the Laurentian Great Lakes: II. Deep chlorophyll maxima. J. Great Lakes Res. **27**(2):155-166.

Barbiero, R.P. and Tuchman, M.L. 2004. The deep chlorophyll maximum in Lake Superior. J. Great Lakes Res. **30**:256-268.

Barbiero, R.P., Rockwell, D.C., Warren, G.J., and Tuchman, M.L. 2006. Changes in spring phytoplankton communities and nutrient dynamics in the eastern basin of Lake Erie since the invasion of *Dreissena* spp. Can. J. Fish. Aquat. Sci. **63**(7):1549-1563.

Barbiero, R.P., Balcer, M.D., Rockwell, D.C. and Tuchman, M.L. 2009. Recent shifts in the crustacean zooplankton community of Lake Huron. Can. J. Fish. Aquat. Sci. **66**:816–828.

Beardall, J., Ihnken, S., and Quigg, A. 2009. Gross and net primary production: closing the gap between concepts and measurements. Aquat Microb Ecol. **56**:113-122.

Bender, M., Orchardo, J., Dickson, M.L., Barber, R., and Lindley, S. 1999. In vitro O_2 fluxes compared with ^{14}C production and other rate terms during the JGOFS Equatorial Pacific experiment. Deep Sea Research Part I. **46**:637-654.

Benson, A. J., Raikow, D., Larson, J. and Fusaro, A. 2013. *Dreissena polymorpha*. USGS Nonindigenous Aquatic Species Database, Gainesville, FL.

Bjorkman, K.M. and Karl, D.M. 2003. Bioavailability of dissolved organic phosphorus in the euphotic zone at Station ALOHA, North Pacific Subtropical Gyre. Limnol. Oceanogr. **48**:1049-1057.

Bloesch, J. 1982. Inshore-offshore sedimentation differences resulting from re-suspension in the eastern basin of Lake Erie. Can. J. Fish. Aquat. Sci. **39**:748-759.

Bocaniov, S.A. and Smith, R.E.H. 2009. Plankton metabolic balance at the margins of very large lakes: temporal variability and evidence of dominance of autochthonous processes. Freshwater Biol. **54**:345-362.

Bouffard, D., Boegman, L. 2012. Basin-scale internal waves. In: Bengtsson, L., Herschy, R.W., Fairbridge, R.W., editors. Encyclopedia of Lakes and Reservoirs. New York (NY): Springer.

Boegman, L., Loewen, M.R., Hamblin, P.F., and Culver, D.A. 2008. Vertical mixing and weak stratification over zebra mussel colonies in western Lake Erie. Limnol. Oceanogra. **53**(3):1093-1110.

Bolker, B.M., Brooks, M.E., Clark, C.J., Geange, S.W., Poulsen, J. R, Stevens, M. H. H. and White, J. S. 2009. Generalized linear mixed models: a practical guide for ecology and evolution. Trends in Ecology and Evolution. **24**(3):127-135.

Boney A.D. 1989. Phytoplankton. Edward Arnold, Great Britain.

Burns, N.M., Rosa, F. Gedeon, A. 1978. Lake Erie in mid-winter. J. Great Lakes Res. **4**(2):134-141.

Carrick, H., Barbiero, R.P., and Tuchman, M. 2001. Variation in Lake Michigan plankton: temporal, spatial, and historical trends. J. Great Lakes Res. **27**(4):467-485.

Cha, Y.K., Stow, C.A. and Bernhardt, E.S. 2012. Impacts of dreissenid mussel invasions on chlorophyll and total phosphorus in 25 lakes in the USA. Freshwater biol. 15.

Charlton, M.N., Le Sage, M.N. and Milne, J.E. 1999. Lake Erie in transition: the 1990's. In *state of Lake Erie: Past, Present and Future*. M. Munawar, T. Edsall, and I.F. Munawar, eds., pp.97-124. Leiden, The Netherlands:Backhuys Publishers.

Cole, J.J. and Pace, M.L. 1995. Why measure bacterial production? A reply to the comment by Jahnke and Craven. Limnol. Oceanogra. **40**:441-444.

Conroy, J.D., Kane, D.D., Dolan, D.M., Edwards, W.J., Charlton, M.N., and Culver, D.A. 2005. Temporal trends in Lake Erie plankton biomass: roles of external phosphorus loading and dreissenid mussels. J. Great Lakes Res. **31**:89-110.

Cullen, J.J. 1982. The deep chlorophyll maximum: comparing vertical profiles of chlorophyll *a*. Can. J. Fish. Aquat. Sci. **39**:791-803.

Curl, H., and Small, L.F. 1965. Variations in photosynthetic assimilation ratios in natural phytoplankton communities. Limnol. Oceanogr. **10**:67-73.

De Stasio, B.T., Schrimpf, M.B., Beranek, A.E., and Daniels, W.C. 2008. Increased chlorophyll *a*, phytoplankton abundance, and cyanobacteria occurrence following invasion of Green Bay, Lake Michigan by dreissenid mussels. Aquat. Invasion **3**(1):21-27.

Depew, D.C., Guildford, S.J. and Smith, R.E.H. 2006. Nearshore-offshore comparison of chlorophyll a and phytoplankton production in the dreissenid-colonized eastern basin of Lake Erie. Can. J. Fish. Aquat. Sci. **63**:1115-1129.

Depew, D.C., Houben, A.J., Ozersky, T., Hecky, R.E. and Guildford, S.J. 2011. Submerged aquatic vegetation in Cook's Bay, Lake Simcoe: Assessment of changes in response to increased water transparency. J. Great Lakes Res. **37**:72-82.

Dokulil, M.T. and Herzig, A. 2009. An analysis of long-term winter data on phytoplankton and zooplankton in Neusiedler See, a shallow temperate lake, Austria. Aquat. Ecol. **43**(3):715-725.

Eimers, M.C., Winter, J.G., Scheider, W.A., Watmough, S.A. and Nicholls, K.H. 2005. Recent changes and patterns in the water chemistry of Lake Simcoe. J. Great Lakes Res. **31**:322-332.

Essington, T.E., and Carpenter, S.R. 2000. Nutrient cycling in Lakes and Streams: Insights from a comparative analysis. Ecosystem. **3**:131-143.

Evans, D.O., Nicholls, K.H., Allen, Y.C., and McMurtry, M.J. 1996. Historical land use, phosphorus loading, and loss of fish habitat in Lake Simcoe, Canada. *Cam. J. Fish. Aquat. Sci.* **53**:194-218.

Evans, D.O., Skinner, A.J., Allen, R., and McMurtry, M.J. 2011. Invasion of zebra mussel, *Dreissena polymorpha*, in Lake Simcoe. J. Great Lakes Res. **37**:36-45.

Fahnenstiel, G.L. and Carrick, H.J. 1992. Phototrophic picoplankton in Lakes Huron and Michigan: abundance, distribution, composition, and contribution to biomass and production. Can. J. Fish. Aquat. Sci. **49**:379-388.

Fahnenstiel, G.L. and Scavia, D. 1987a. Dynamics of Lake Michigan phytoplankton: primary production and growth. Can. J. Fish. Aquat. Sci. **44**: 499-508.

Fahnenstiel, G.L., and Scavia, D. 1987b. Dynamics of Lake Michigan phytoplankton: the deep chlorophyll layer. J. Great Lakes Res. **13**(3):285-295.

Fahnenstiel, G.L., Lang, G.A., Nalepa, T.F., and Johengen, T.H. 1995. Effects of zebra mussel (*Dreissena polymorpha*) colonization on water quality parameters in Saginaw Bay, Lake Huron. J. Great Lakes Res. **21**(4):435-448.

Fahnenstiel, G.L., Pothoven, S., Vanderploeg, H., Klarer, D., Nalepa, T. and Scavia, D. 2010. Recent changes in primary production and phytoplankton in the offshore region of southeastern Lake Michigan. J. Great Lakes Res. **36**:20-29.

Falkowski, P.G. and Raven, J.A. 1997. Aquatic Photosynthesis. Blackwell Science. Malden, MA.

Falkowski, P.G. and Raven, J.A. 2007. Aquatic Photosynthesis. 2nd edition. Princeton University Press, Princeton.

Fee, E.J. 1990. Computer programs for calculating *in situ* phytoplankton photosynthesis. Can. Tech. Rep. Fish. Aquat. Sci.No. 1740.

Fee, E.J., and Hecky, R.E. 1992. Introduction to the Northwest Ontario Lake Size Series (NOLSS). Can. J. Fish. Aquat. Sci. **49**:2434-2444.

Fee, E.J., Shearer, A., DeBruyn, E.R., and Schindler, E.U. 1992. Effects of lake size on phytoplankton photosynthesis. Can. J. Fish. Aquat. Sc*i*. **49**:2445-2459.

Fisheries and Oceans Canada. 2010. Ontario-Great Lakes Area Fact Sheets. Available at: http://www.dfo-mpo.gc.ca/regions/central/pub/factsheets-feuilletsinfos-ogla-rglo/lakewhitefish-grandcoregone-eng.htm

Fishman, D.B., Adlerstein, S.A., Vanderploeg, H.A., Fahnenstiel, G.L., and Scavia, D. 2009. Causes of phytoplankton changes in Saginaw Bay, Lake Huron, during the zebra mussel invasion. J. Great Lakes Res. **35**:482-495.

Fishman, D.B, Adlerstein, S.A., Vanderploeg, H.A., Fahnenstiel, G.L. and Scavia, D. Phytoplankton community composition of Saginaw Bay, Lake Huron, during the zebra mussel (*Dreissena polymorpha*) invasion: A multivariate analysis. J. Great Lakes Res. **36**:9-19.

Gardner, W.S., Quigley, M.A., Fahnenstiel, G.L., Scavia, D., Frez,W.A., 1990. *Pontoporeia hoyi*—a direct trophic link between spring diatoms and fish in Lake Michigan. In: Tilzer, M.M., Serruya, C. (Eds.), Large Lakes: Structural and functional properties. Springer, pp. 632–644.

Ginn, B.K. Distribution and limnological drivers of submerged aquatic plant communities in Lake Simcoe (Ontario, Canada): Utility of macrophytes as bioindicators of lake trophic status. J. Great Lakes Res. **37**:83-89.

Glooschenko, W.A., Moore, J.E., Munawar, M., and Vollwenweider, R.A. 1974. Primary production in Lakes Ontario and Erie: a comparative study. J. Fish. Res. Board of Canada. **31**:253-263.

Guildford, S.J., Hendzel, L.L., Kling, H.J., and Fee, E.J. 1994. Effects of lake size of phytoplankton nutrient status. Can. J. Fish. Aquat. Sci. **51**:2769-2783.

Guildford, S.J., Hecky, R.E., Smith, R.E.H., Taylor, W.D., Charlton, M.N., Barlow-Busch, L., North, R.L. 2005. Phytoplankton nutrient status in Lake Erie in 1997. J. Great Lakes Res. **72**:72-88.

Hall, S.R., Pauliiukonis, N.K., Mills, E.L., Rudstam, L.G., Schneider, C.P., Lary, S.J., and Arrhenius, F. 2003. A comparison of total phosphorus, chlorophyll *a*, and zooplankton in embayment, nearshore and offshore habitats of Lake Ontario. J. Great Lakes Res. **29**:54-69.

Halsey, K.H., Milligan, A.J., and Behrenfeld, M.J. 2010. Physiological optimization underlies growth rate-independent chlorophyll-specific gross and net primary production. Photosynth Res. **103**:125-137.

Hawryshyn, J., Rühland, K.M., Quinlan, R., and Smol, J.P. 2012. Long-term water quality changes in multiple-stressor system: a diatom-based paleolimnological study of Lake Simcoe (Ontario, Canada). Can. J. Fish. Aquat. Sci. **69**:24-40.

Hecky, R.E., Kling, H.J., and Brunskill, G.J. 1986. Seasonality of phytoplankton in relation to silicon cycling and interstitial water circulation in large, shallow lakes of central Canada. Hydrobiologia. **138**:117-126.

Hecky, R.E., Smith, R.E.H., Barton, D.R., Guildford, S.J., Taylor, W.D., Charlton, M.N., and Howell, T. 2004. The nearshore phosphorus shunt: a consequence of ecosystem engineering by dreissenids in the Laurentian Great Lakes. Can. J. Fish. Aquat. Sci. **61**: 1285-1293.

Higgins, S.N., and Vander Zanden, M.J. 2010. What a difference a species makes: a meta-analysis of Dreissenid mussel impacts on freshwater ecosystems. Ecol. Monographs. **80**(2): 179-196.

Hiriart, V. P., B. M. Greenburg, S. J. Guildford, and Smith R. E. H. 2002. Effects of ultraviolet radiation on rates and size distribution of primary production by Lake Erie phytoplankton. Can. J. Fish. Aquat. Sci. **59:** 317–328.

Idrisi, N., Mills, E.L., Rudstam, L.G., and Stewart, D.J. 2001. Impact of zebra mussels (*Dreissena polymorpha*) on the pelagic trophic levels of Oneida Lake, New York. Can. J. Fish. Aquat. Sci. **58**: 1430–1441.

Jassby, A.D., and Platt, T. 1976. Mathematical formulation of the relationship between photosynthesis and light for phytoplankton. Limnol. Oceanogr. **21**(4):540-547.

Jewson, D.H., Granin, N.G., Zhdanov, A.A., and Gnatovsky, R.Y. 2009. Effect of snow cover on under-ice growth of planktonic diatoms in Lake Baikal. Aquat. Ecol. **43**.

Kalff, J. 2002. Limnology. Prentice-Hall, Upper Saddle River, NJ.

Karatayev, A.Y., Burlakova, L.E., and Padilla, D.K. 1997. The effects of *Dreissena polymorpha* (pallas) invasion on aquatic communities in Eastern Europe. J. Shellfish Res. **16:**187-203.

Kiili, M., Pulkkanen, M. and Salonen, K. 2009. Distribution and development of under-ice phytoplankton in 90-m deep water column of Lake Päijänne (Finland) during spring convection. Aquat. Ecol. **43**:707-713.

Kirk, J.T.O. 1994. Light and photosynthesis in aquatic ecosystems. Oxford University Press, Oxford, UK.

Klaumeier, C.A., Litchman, E. 2001. Algal games: the vertical distribution of phytoplankton in poorly mixed water columns. Limnol. Oceanogr. **46**:1998-2007.

Kwiatkowski, R.E. 1984. Comparison of 1980 Lake Huron, Georgian Bay and North Channel surveillance data with historical data. Hydrobiol. **118**:255-266.

Lavrentyev, P.J., Gardner, W.S., Cavaletto, J.F., and Beaver, J.R. 1995. Effects of the zebra mussel (*Dreissena polymorpha* Pallas) on protozoa and phytoplankton from Saginaw Bay, Lake Huron. J. Great Lakes Res. **21**:545-557.

Lawlor, D.W. 2001. Photosynthesis: Molecular, Physiological and Environmental Processes. Bios Scientific Pub Ltd, USA.

Legendre, L. 1990. The significance of microalgal blooms for fisheries and for the export of particulate organic carbon in oceans. J. Plankton Res. **12**:681-699.

Legendre, P. 2013. Model II regression user's guild, R edition. Available at cron.r-project.org. Accessed March 10th, 2013.

Legendre, P and Legendre L. 1998. Numerical Ecology. The Netherlands.

Li, W.K.M., and Maestrini, S.Y. 1993. Measurement of Primary Production from the Molecular to the Global Scale. Copenhagen, ICES.

Lindeman, R. 1942. The trophic-dynamic asepect of ecology. Ecol. **23:**399-418.

Litchman, E., Steiner, D., and Bossard, P. 2003. Photosynthetic and growth responses of three freshwater algae to phosphorus limitation and daylength. Freshwater Biol. **48**:2141-2148.

LSEMS. 2008. Lake Simcoe basin wide report. Available at: http://www.lsrca.on.ca/pdf/reports/lsems/basin_wide_report.pdf#search="long term monitoring"

MacDougall, T.M., Benoit, H.P., dermott, R., Johansson, O.E., Johnson, T.B., Millard, E.S., and Munawar, M. 2001. Lake Erie 1998: Assessment of abundance, biomass and production of the lower trophic levels, diets of juvenile yellow perch, and trends in the fishery. Can. Tech. Rpt. Fish. Aquat. Sci. 2376.

MacIssac, H.J., Johansson, O.E., Ye, J., Sprules, W.G., Leach, J.H., McCorquodale, J.A., and Grigorovich, I.A. 1999. Filtering impacts of an introduced bivalve (*Dreissena polymorpha*) in a shallow lake: application of a hydrodynamics model. Ecosystems. **2**:338-350.

Magnuson, J.J. 1990. Long-term ecological research and the invisible present. Bioscience. **40**:495-501.

Magnuson, J.J., Robertson, D.M., Benson, B.J., Wynne, R.H., Livingstone, D.M., Arai, T., Assel, R.A., Barry, R.G., Card, V., Kuusisto, E., Granin, N.G., Prowse, T.D., Steward, K.M. and

Makarewicz, J.C., Lewis, T.W., and Bertram, P. 1999. Phytoplankton composition and biomass in the offshore waters of Lake Erie: pre- and post-*Dreissena* introduction (1983-1993). J. Great Lakes Res. **25**:135-148.

Malkin, S.Y., Silsbe, G.M., Smith, R.E.H., and Howell, E.T. 2012. A deep chlorophyll maximum nourishes benthic filter feeders in the coastal zone of a large clear lake. Limnol. Oceanogr. **57**(3):735-748.

Mignot, A., Claustre, H., D'Ortenzio, F., Xing, X., Poteau, A. and Ras, J. 2011. From t he shape of the vertical profile of in vivo fluorescence to Chlorophyll-*a* concentration. Biogeosciences Discuss., **8**:3697-3737.

Mills, E.L., J.H. Leach, J.T. Carlton, and Secor C.L. 1993. Exotic species in the Great Lakes: a history biotic crises and anthropogenic introductions. J. Great Lakes Res. **19**: 1-54.

Mills, E.L., Rosenberg, G., Spidle, A.P., Ludyanskiy, M., Pligin, Y., and May, B. 1996. A review of the biology and ecology of the quagga mussel (*Dreissena bugensis*), a second species of freshwater Dreissenid introduced to North America. American Zoologist. **36**:271-286.
Millard, E.S., Myles, D.D., Johansson, O.E., and Ralph, K.M. 1996. Phytoplankton photosynthesis at two index stations in Lake Ontario 1987-1992: assessment of the long-term response to phosphorus control. Can. J. Fish. Aquat. Sci. **53**:1092-1111.

Millard, E.S., Fee. E.J., Myles, D.D., and Dahl, J.A. 1999. Comparison of phytoplankton photosynthesis methodology in Lakes Erie, Ontario, the Bay of Quinte, and the Northwest Ontario Lake Size Series. In *State of Lake Erie: Past, Present and Future.* M. Munawar, T. Edsall, and I. F. Munawar, eds., pp. 441-468. Leiden, The Netherlands: Backhuys Publishers.

Moll, R.A. and Stoermer, E.F. 1982. A hypothesis relating trophic status and subsurface chlorophyll maxima of lakes. Arch. Hydrobiol. **94**(4):425-440.

Moll, R.A., Brahce, M.Z. and Peterson, T.P. 1984. Phytoplankton dynamics within the subsurface chlorophyll maximum of Lake Michigan. J. plankton res. **6**(5):751-766.

Naddafi, R., Pettersson, K., and Eklöv, P. 2007. The effect of seasonal variation in selective feeding by zebra mussels (*Dreissena polymorpha*) on phytoplankton community composition. Freshwater Biol. **52**(5):823-842.

Nalepa, T.P., Fanslow, D.L., Pothoven, S.A. 2010. Recent changes in density, biomass, recruitment, size structure, and nutritional state of *Dreissena* populations in southern Lake Michigan. J. Great Lakes Res. Res. **36** (supplement3):5-19.

Neil, J. 1990. Lake Simcoe hypolimnion aeration- an assessment of the potential for direct treatment of oxygen depleted hypolimnetic waters in Lake Simcoe. Available at: http://www.lsrca.on.ca/pdf/reports/lsems/hypolimnion_aeration.pdf#search="oxygen"

Nicholls, K.H. 1995. Some recent water quality trends in Lake Simcoe, Ontario: implications for basin planning and limnological research. J. Can. Water Resources. **20**(4).

Nicholls, K.H. 1997. A limnological basis for a Lake Simcoe phosphorus loading objective. J. Lake Reservoir Manage. **13**:189-198.

Nicholls, K.H. and Hopkins, G.J. 1993. Recent changes in Lake Erie (North Shore) phytoplankton: cumulative impacts of phosphorus loading reductions and the zebra mussel introduction. J. Great Lakes Res. **19**:637-647.

Nicholls, K.H., Hopkins, G. J., and Standke S.J. 1999. Reduced chlorophyll to phosphorus ratios in nearshore Great Lakes waters coincide with the establishment of dreissenid mussels. Can. J. Fish. Aquat. Sci. **56**:153-161.

Nicholls, K.H., Heintsch, L. and Carney, E. 2002. Univariate step-trend and multivariate assessments of the apparent effects of P loading reductions and zebra mussels on the phytoplankton of the Bay of Quinte, Lake Ontario. J. Great Lakes Res. **28**:15-31.

Nicholls, K.H. and Tudorancea, C. 2001. Species-level and community-level data analyses reveal spatial differences and temporal change in the crustacean zooplankton of a large Canadian lake (Lake Simcoe, Ontario). J. Limnol. **60**:155-170.

North, R.L., Barton, D., Crowe, A.S., Dillon, P.J., Dolson, R.M.L., Evans, D.O., Ginn, B.K., Hakanson, L., Hawryshyn, J., Jarjanazi, H., King, J.W., La Rose, J.K.L., León, L., Lewis, C.F.M., Liddle, G.E., Lin, Z.H., Longstaffe, F.J., Macdonald, R.A., Molot, L., Ozersky, T., Palmer, M.E., Quinlan, R., Rennie, M.D., Robillard, M.M., Rodé, D., Rühland, K.M., Schwalb, A., Smol, J.P., Stainsby, E., Trumpickas, J.J., Winter, J.G., and Young, J.D. 2012. The state of Lake Simcoe (Ontario, Canada): the effects of multiple stressors on phosphorus and oxygen dynamics.

Odum, E. 1959. Fundamentals of ecology. Saunders, Philadelphia.

Oveisy, A., Boegman, L. and Imberger, J. 2012. Three-dimensional simulation of lake and ice dynamics during winter. Limnol. Oceangr. **57**(1):43-57.

Ozersky, T., Malkin, S., Barton, D. and Hecky, R. 2009. Dreissenid phosphorus excretion can sustain *C. glomerata* growth along a portion of Lake Ontario shoreline. J. Great Lakes Res. **35**:321-328.

Ozersky, T., Barton, D.R., Depew, D.C., Hecky, R.E., and Guildford, S.J. 2011b. Effects of water movement on the distribution of invasive dreissenid mussels in Lake Simcoe, Ontario. J. Great Lakes Res. **37**:46-54.

Padilla, D.K., Adolph, S.C., Cottingham, K.L., and Schneider, D.W. 1996. Predicting the consequences of Dreissenid mussels on pelagic food web. Ecological Modelling. **85:**129-144.

Palmer, M.E., Winter, J.G., Young, J.D., Dillon, P.J., and Guildford, S.J. 2011. Introduction and summary of research on Lake Simcoe: Research, monitoring, and restoration of a large lake and its watershed. J. Great Lakes Res. **37**:1-6.

Pinheiro, J.C., and Bates, D.M. 2000. Mixed-effects models in S and S-PLUS. Springer, New York, USA.

Platt, T., Gallegos, C.L. and Harrison, W.G. 1980. Photoinhibition of photosynthesis innatural assemblages of marine phytoplankton. J. Mar. Res. **38**:687-701.

Rousar, D.C. 1973. Seasonal and spatial changes in primary production and nutrients in Lake Michigan. Water Air Soil Pollut. **2**:497-514.

Rühland, K.M., Quinlan, R., Smol, J. P. 2012. Long-term water quality changes in a multiple-stressor system: a diatom-based paleolimnological study of Lake Simcoe (Ontario, Canada). Canadian J. of Fisheries and Aquat. Sci. **69**(1):24-40.

Schindler, D.W. 1977. Evolution of phosphorus limitation in lakes. Science. **195**:260-267.

Schneider, D.W. 1992. A bioenergetics model of zebra mussel, *Dreissena polymorpha*, growth in the Great Lakes. Can. J. Fish. Aquat. Sci. **49**:1406-1416.

Smith, T.E., Stevenson, R.J., Caraco, N.F., and Cole, J.J. 1998.Changes in phytoplankton community structure during the zebra mussel (*Dreissena polymorpha*) invasion of the Hudson River (New York). J. Plankton Res. **20**(8):1567-1579.

Smith, R.E.H. Furgal, J.A., Charlton, M.N., Greenberg, B.M.H., Hiriart, V.P., and Marwood, C.A. 1999. The attenuation of ultraviolet radiation in a large lake with low dissolved organic matter concentrations. Can. J. Fish. Aquat. Sci. **56**:1351-1361.

Smith, R.E.H., Hiriart-Baer, V.P., Higgins, S.N., Guildford, S.J., and Charlton. M.N. 2005. Planktonic primary production in the offshore waters of dreissenid-infested Lake Erie in 1997. J. Great Lakes Res. **31**(Suppl. 2):50-62.

Sommer, U., and Lewandowska, A. 2011. Climate change and the phytoplankton spring bloom: warming and overwintering zooplankton have similar effects on phytoplankton. Glob. Chang. Biol. **17**(1): 154-162.

Søndergaard, M., and Moss, B. 1998. Impacts of submerged macrophytes on phytoplankton in shallow freshwater lakes. In: Jeppesen, E., Søndergaard, M., Søndergaard, M., Christoffersen, K. (Eds.), The structuring role of submerged macrophytes in lakes. Springer-Verlag, New York, pp. 115-132.

Stainsby, E.A., Winter, J.G., Jarjanazi, H., Paterson, A.M., Evans, D.O., and Young, J.D. 2011. Changes in the thermal stability of Lake Simcoe from 1980 to 2008. J. Great Lakes Res. **37**:55-62.

Stanczykowska, A. 1977. Ecology of *Dreissena polymorpha* (Pall.) (Bivalva) in Lakes. Pol. Arch. Hydrobiol. **24**:461-530.

Starkweather, J. n.d. Linear Mixed Effects Modeling using R. Available at: http://www.unt.edu/rss/class/Jon/Benchmarks/LinearMixedModels_JDS_Dec2010.pdf

Straskrábová, V., Izmest'eva, L. R., Maksimova, E. A., Fietz, S., Nedoma, J., Borovec, J., Kobanova, G.I., Shchetinina, E.V. and Pislengina, E.V. 2005. Primary production and microbial activity in the euphotic zone of Lake Baikal (Southern Basin) during late winter. Glob. Planet. Chang. **46**: 57–73.

Twiss, M.R., McKay, R.M.L., Bourbonniere, R.A., Bullerjahn, G.S. Carrick, H.J., Smith, R.E.H., Winter, J.G., D'souza, N.A., Furey, P.C., Lashaway, A.R., Saxton, M.A., Wilhelm, S.W. 2012. Diatoms abound in ice-covered Lake Erie: An investigation of offshore winter limnology in Lake Erie over the period 2007 to 2010. J. Great Lakes Res. **38**:18-30.

Vanderploeg, H.A., Gardner, W.S., Parrish, C.C., Liebig, J.R., and Cavaletto, J.F. 1992. Lipids and the life-cycle strategy of a hypolimnetic copepod in Lake Michigan. Limnol. Oceanogr. **37**:413-424.

Vanderploeg, H. A., Liebig, J. R., Carmichael, W. W., Agy, M. A., Johengen, T. H., Fahnenstiel, G. L. and Nalepa, T. F. 2001. Zebra mussel (*Dreissena polymorpha*) selective filtration promoted toxic *Microcystis* blooms in Saginaw Bay (Lake Huron) and Lake Erie. *Can J. Fish. Aquat. Sci.* **58**: 1208-1221.

Vanderploeg, H.A., Nalepa, T.F., Jude, D.J. et al. 2002. Dispersal and emerging ecological impacts of Ponto-Caspian species in the Laurentian Great Lakes. Can. J. Fish. Aquat. Sci. **59**(7):1209-1228.

Vanderploeg, H.A., Liebig, J.R., Nalepa, T.F., Fahnenstiel, G.L. and Pothoven, S.A. 2010. *Dreissena* and the disappearance of the spring phytoplankton bloom in Lake Michigan. J. Great Lakes Res. **36**:50-59.

Vehmaa, A. and Salonen, K. 2009. Development of phytoplankton in Lake Pääjärvi (Finland) during under-ice convective mixing period. Aquat Ecol. **43**:693-705.

Vuglinski, V.S. 2000. Historical trends in lake and river ice cover in the Northern Hemisphere. Science. **289**(5485):1743-1746.

Wang, J., Bai, X., Hu, H., Clites, A., Colton, M., and Lofgren, B. 2012. Temporal and spatial variability of Great Lakes ice cover, 1973-2010. J. Climate. **25**:1318-1329.

Wehr, J.D. and Sheath, R.G. 2003. Freshwater algae of North America: Ecology and classification. Academic Press, San Diego, Calif.

Wetzel, R.G. 1990a. Land-water interfaces:Metabolic and limnological regulators. Verh. Internat. Verein. Limnol. **24**:6-24.

Wetzel, R.G. 2001. Limnology: lake and river ecosystems. Academic Press, San Diego, Calif.

Wetzel, R. G. and Likens, G. E. 1991. Limnological analyses. Springer-Verlag, New York.

Williams, W.D. 1993. Worldwide occurrence and limnological significance of falling water-levels in large, permanent saline lakes. Verg. Int. Ver. Limnol. **25**: 980-983.

Winter, J.G., Eimers, M.C., Dillon, P.J., Scott, L.D., Scheider, W.A., and Willox, C.C. 2007. Phosphorus inputs to Lake Simcoe from 1990 to 2003: Declines in tributary loads and observations on lake water quality. J. Great Lakes Res. **33**:381-396.

Winter, J.G., Young, J.D., Landre, A., Stainsby, E., and Jarjanazi, H. 2011. Changes in phytoplankton community composition of Lake Simcoe from 1980 to 2007 and relationships with multiple stressors. J. Great Lakes Res. **37**:63-71.

Wright, R. T. 1964. Dynamics of a phytoplankton community in an ice-covered lake. Limnol. Oceanogr. **9**:63-178.

YSI environment. 2006. *In vivo* measurement of Chlorophyll and the YSI 6025 wiped chlorophyll sensor. YSI Inc. 1-4.

Young, J.D., Winter, J.G., and Molot, L. 2011. A re-evaluation of the empirical relationships connecting dissolved oxygen and phosphorus loading after dreissenid mussel invasion in Lake Simcoe. J. Great Lakes Res. **37**:7-14.

Appendix I

Appendix Table 1.1. Summary of linear mixed effects model output of different variables (Aug 2010-Jul 2011). The bolded numbers indicate significance ($P<0.05$).

			Pairwise comparisons						
Variable	**Interaction**	**Season**	**Zone***	**1:2****	**1:3****	**1:4****	**2:3****	**2:4****	**3:4****
P_{int}	0.85	**< .0001**	**0.012**	**0.02**	**0.0004**	**0.0016**	0.51	**< .0001**	**< .0001**
P_{avg}	0.92	**< .0001**	1	**0.0007**	**0.0002**	0.13	**< .0001**	**0.0004**	**< .0001**
P_{opt}	0.058	**< .0001**	**0.011**	0.13	**< .0001**	0.53	**< .0001**	0.35	**< .0001**
Kd_{PAR}	0.80	**0.0065**	0.36	0.12	**0.0022**	**0.014**	**< .0001**	0.35	**< .0001**
Mean PAR[a]	**0.016**	**< .0001**	**< .0001**	0.69	0.29	0.88	**0.033**	0.53	0.34
			Offshore	**0.0058**	0.32	0.89	**0.0071**	**0.0016**	0.33
Chl *a*[b]	**0.012**	**0.031**	**0.015**	0.065	0.059	0.71	0.98	0.12	0.11
			Offshore	0.047	0.97	0.28	**0.0044**	**0.0002**	0.14
Chl *a*:TP	0.19	**0.016**	**0.0084**	0.92	**0.061**	**0.077**	**0.0059**	**0.016**	0.88
P^B_{max}	0.76	**0.0027**	0.37	0.11	**0.032**	0.37	0.25	0.36	0.078
$\alpha^{B\,c}$	0.98	**0.0070**	0.36	0.53	**0.016**	0.76	**0.012**	0.28	**0.0016**

14C size fractionation* **									
Net (>20 µm)	0.92	**0.0065**	**0.00014**	0.52	**0.023**	0.73	**0.025**	0.23	**0.001**
Nano (2-20 µm)	0.82	**0.00096**	**0.0062**	0.21	**0.0012**	0.43	**0.0044**	0.63	**0.0021**
Pico (0.2-2 µm)	0.93	0.16	0.18	N/A	N/A	N/A	N/A	N/A	N/A
Chl *a* size fractionation* **									
Net (>20 µm)	0.10	**0.0073**	**0.0014**	0.86	**0.014**	0.16	**0.0012**	0.10	0.34
Nano (2-20 µm)	0.40	0.063	**0.023**	0.29	0.68	0.28	**0.044**	**0.011**	0.36
Pico (0.2-2 µm)	0.13	**< .0001**	**0.0068**	**0.0011**	**< .0001**	0.88	**< .0001**	**0.0004**	**< .0001**

*Zone: Statistical difference between the average nearshore and offshore stations
**Pairwise comparisons of 1-Spring, 2-Summer 3-Fall 4-Winter
***^{14}C and chl *a* size fractions include data from August 2011
[a]Mean PAR: the average difference in mean PAR when comparing offshore to nearshore for spring (p=**< .0001**), summer (p=0.058), fall (p**< .0001**) and winter (p**< .0001**)
[b]Chl *a*: the average difference in chl *a* when comparing offshore to nearshore- spring (p=0.06), summer (p=0.26), fall (p=**0.0035**) and winter (p=**0.0001**)
[c]One outlier was identified and excluded from the data (α^B=95.1 mg C mg chl a^{-1} mol quanta^{-1} $\cdot$ m^{-2} , Station K45 July 2011)

Appendix Table 1.2 Summary of predicted production (P_{int} and P_{avg}) for Beaverton water treatment plant (WTP) based on the incident irradiance, theoretical 75%- and 100% cloud-free model. Photosynthesis-irradiance (PI) parameters were generated using the program PSPARMS; however, other parameters (Kd_{PAR}, Z_{mix}) were based on other stations ("assumed station", E50, E51, T2) located close to WTP that were sampled within the same month. Throughout the calculation, the production model assumed that the extracted chl *a* values from the WTP samples were same throughout the depth. Also, the Z_{max} for WTP was assumed to be 7.6m. Otherwise, the units for the variables are: α^B (mgC/(mg chl Ein m-2)); P^B_{max} (mgC/(mg chl hr)); chl *a* (µg/L); P_{int} (mg C m^{-2}); P_{avg} (mg C m^{-3}).

					Incident Irradiance				**75% cloud-free model**				**100% cloud-free model**			
WTP	**PI parameters**				**P_{int}**		**P_{avg}**		**P_{int}**		**P_{avg}**		**P_{int}**		**P_{avg}**	
Assumed station	**WTP Sample Dates**	**α**	**P^b_{max}**	**Chl *a***	**To****	**To Z_{mix}**	**To**	**To Z_{mix}**	**To**	**To Z_{mix}**	**To**	**To Z_{mix}**	**To**	**To Z_{mix}**	**To**	**To Z_{mix}**
E50 Feb	11/01/11	4.2	0.71	0.31	0.2	0.2	0.0	0.0	11.9	10.7	2.7	1.6	12.6	11.2	3.0	1.7
E50 Feb	01/02/11	1.2	0.23	0.51	0.9	0.9	0.1	0.1	7.2	6.5	1.6	1.0	7.7	6.8	1.8	1.0
E50 Mar	08/03/11	4.2	0.82	4.1	243.1	201.5	59.3	33.6	268.5	214.5	69.1	35.7	276.5	219.1	72.0	36.5
E50 Mar	22/03/11	0.51	0.07	1.9	10.8	8.9	2.7	1.5	12.2	9.6	3.2	1.6	12.4	9.7	3.3	1.6
T2 Apr	05/04/11	0.82	0.13	2.4	24.5	24.5	3.2	3.2	26.5	26.5	3.5	3.5	27.0	27.0	3.5	3.5
T2 Apr	13/04/11	2.7	0.61	2.8	126.7	126.7	16.6	16.6	141.3	141.3	18.5	18.5	145.4	145.4	19.1	19.1
T2 Apr	19/04/11	2.7	1.04	1.2	76.6	76.6	10.0	10.0	96.2	96.2	12.6	12.6	101.6	101.6	13.3	13.3
E50 May*	03/05/11	4.4	1.6	0.93	65.8	65.8	8.6	8.6	134.0	134.0	17.6	17.6	137.8	137.8	18.1	18.1
E51 May	03/05/11	4.4	1.6	0.93	125.4	125.4	16.5	16.5	133.4	133.4	17.5	17.5	137.4	137.4	18.0	18.0
E50 Jun	07/06/11	3.5	1.8	1.3	111.9	76.3	29.4	20.1	221.2	117.9	58.1	31.0	232.4	120.9	61.0	31.8
E50 Jul	05/07/11	6.2	4.8	0.69	227.5	227.5	29.9	29.9	241.7	241.7	31.7	31.7	267.3	267.3	35.1	35.1
E51 Jul	05/07/11	6.2	4.8	0.69	134.1	134.1	17.6	17.6	246.1	246.1	32.3	32.3	271.3	271.3	35.6	35.6

*In some cases, two production estimates were generated using variables from two different stations
**'To' stands for total production

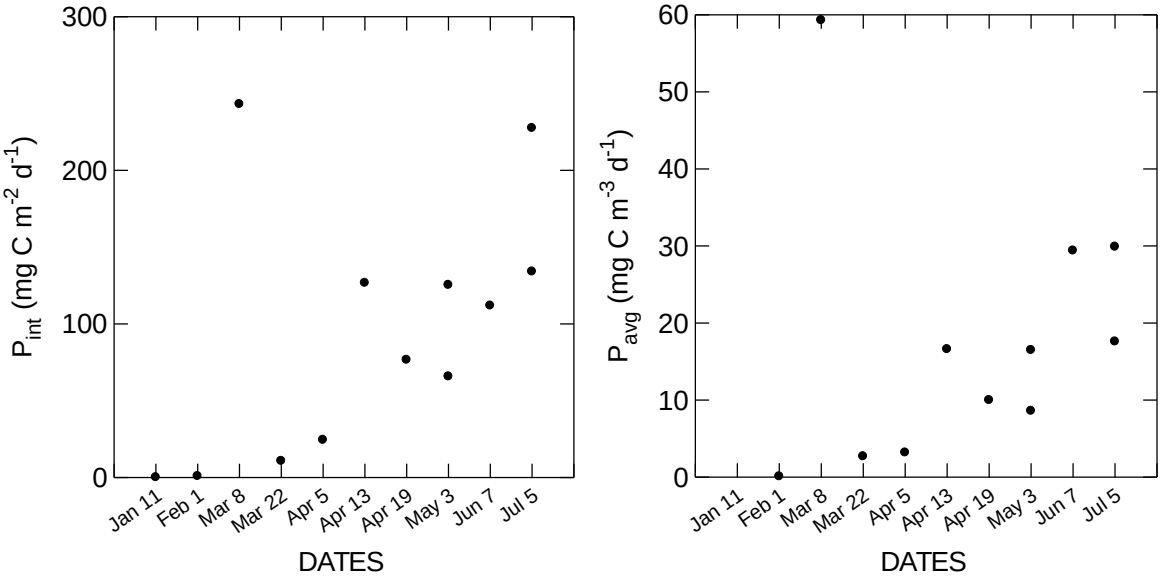

Appendix Figure 1.1 A plot of predicted P_{int} (mg C m^{-2} d^{-1}) and P_{avg} (mg C m^{-3} d^{-1}) for the WTP samples. Most of the samples were sampled on a monthly basis except for March (n_{Mar}=2) and April (n_{Apr}=3). A total of 12 WTP samples were collected over the course of the study.

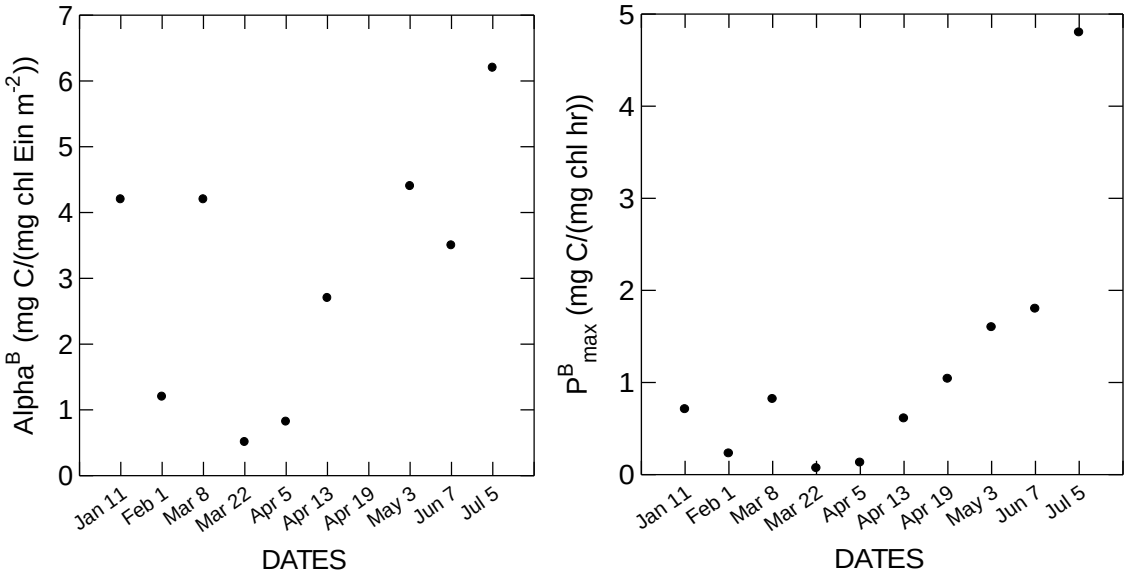

Appendix Figure 1.2 WTP PI parameters. a) The left figure shows light utilization efficiency (α^B; (mgC/(mg chl Ein m-2)) plotted against the sampled date b) The right figure shows the rate of light saturation (P^Bmax; mgC/(mg chl hr)) versus the sampled date. The PI parameters were derived using the program, PSPARMS.

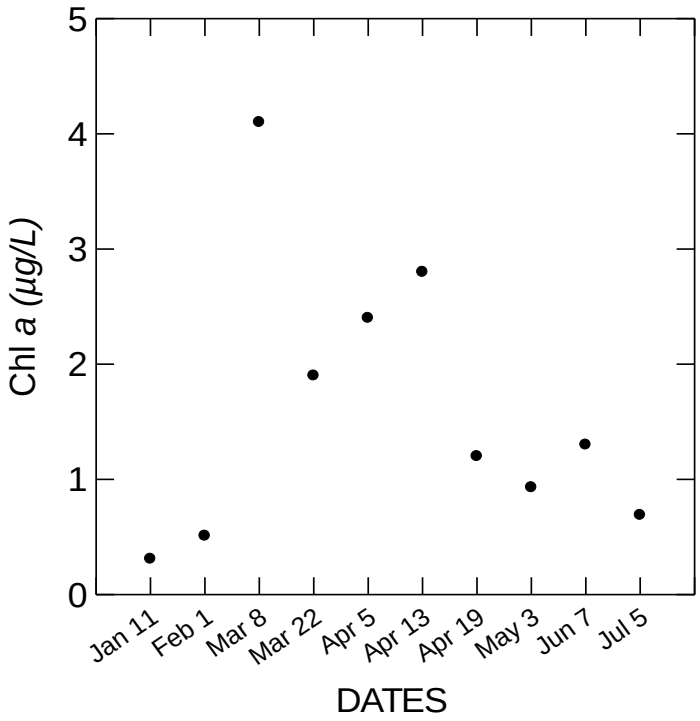

Appendix Figure 1.3 Extracted chl *a* (µg/L) values for WTP across the sampled dates.

Appendix Table 1.3 Daily areal and volumetric productions for transitional site (~15m; S15, C9). The production estimates were based on the incident irradiance, theoretical 75%- and 100% cloud-free model. The programs DTOTAL and DPHOTO were used to generate P_{int} (mg C m^{-2} d^{-1}) and P_{avg} (mg C m^{-3} d^{-1}). The production was calculated using the integrated epilimnetic samples except in February (station C9) and March (station S15) when the sampled were collected within a meter from the surface ('surface'). The units for the variables were: Z_{samp} (m); Z_{mix} (m); α^B (mgC/(mg chl Ein m-2)); P^B_{max} (mgC/(mg chl hr)); chl *a* (µg/L).

							Incident Irradiance				**75% cloud-free model**				**100% cloud-free model**			
					PI parameters		**P_{int}**		**P_{avg}**		**P_{int}**		**P_{avg}**		**P_{int}**		**P_{avg}**	
Station	**Date**	**Z_{samp} (m)**	**Z_{mix} (m)**	**Chl*a***	**α**	**P^b_{max}**	**To**	**To Z_{mix}**	**To**	**To Z_{mix}**	**To**	**To Z_{mix}**	**To**	**To Z_{mix}**	**To**	**To Z_{mix}**	**To**	**To Z_{mix}**
S15	05/08/10	0-8	19	2.6	4.6	1.0	293.2	293.2	21.1	21.1	312.4	312.4	22.4	22.4	340.8	340.8	24.5	24.5
C9	05/08/10	0-10	8	2.4	6.9	2.4	768.7	575.3	102	71.9	615.2	508.4	80.3	63.6	686.6	544.0	90.3	68.0
S15	02/09/10	0-10	12	3.1	6.5	1.5	234.6	234.6	22.2	22.2	354.2	354.2	33.5	33.5	388.6	388.6	36.8	36.8
C9	02/09/10	0-10	12	3.6	6.5	2.8	782.6	769.9	79.6	77.0	934.4	908.3	96.3	90.8	1017	978.5	106	97.9
S15	10/11/10	0-10	19	3.3	4.7	1.8	333.0	333.0	23.7	23.7	270.1	270.1	19.2	19.2	315.7	315.7	22.5	22.5
C9	10/11/10	0-10	16	3.3	6.1	2.5	374.3	374.3	30.5	30.5	275.2	275.2	22.4	22.4	328.6	328.6	26.8	26.8
S15	03/12/10	0-10	14	1.8	3.9	1.2	115.5	115.5	8.2	8.2	142.9	142.9	10.2	10.2	161.5	161.5	11.5	11.5
C9	03/12/10	0-10	14.5	2.2	4.0	1.4	73.4	73.4	5.1	5.1	157.6	157.6	11.0	11.0	136.3	136.3	9.5	9.5
C9 **	08/02/11	Surface	-	1.1	2.9	0.42	0.5	0.5	0.0	0.0	40.8	40.8	2.9	2.9	44.2	44.2	3.2	3.2
S15	01/03/11	2	-	0.9	8.8	1.7	184.8	177.3	16.1	12.7	154.9	151.3	12.5	10.8	169.8	164.6	14.2	11.8

S15	10/05/11	0-10	19.6	0.94	7.8	3.0	426.9	426.9	21.8	21.8	452.7	452.7	23.2	23.2	528.5	528.5	27.0	27.0
C9	10/05/11	0-10	16.1	1.6	6.4	2.2	341.9	341.9	24.1	24.1	328.6	328.6	23.2	23.2	373.4	373.4	26.4	26.4
S15	14/07/11	0-8	10.7	0.5	13	8.2	614.4	512.0	64.1	47.9	523.6	456.2	53.3	42.6	453.4	407.7	45.3	38.1
C9	14/07/11	0-8	10.3	1.3	7	4.7	820.1	706.3	85.8	68.6	616.2	564.9	62.6	54.8	708.4	633.0	72.9	61.5

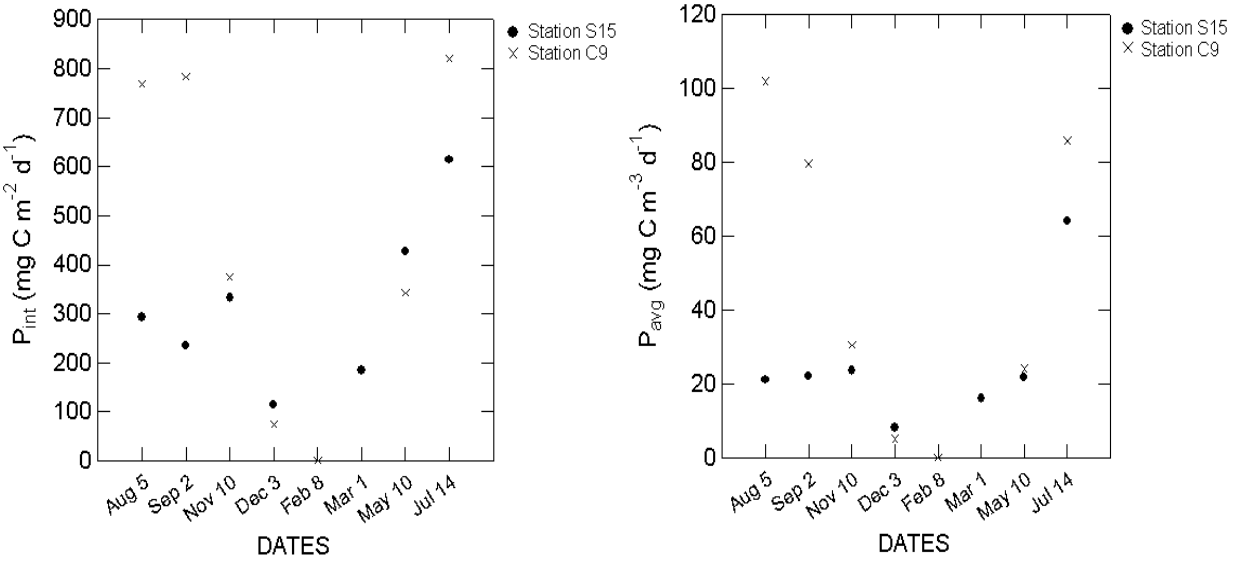

Appendix Figure 1.4 A plot of P_{int} (mg C m^{-2} d^{-1}) and P_{avg} (mg C m^{-3} d^{-1}) for transitional sites (S15 and C9). The station S15 (•) was collected throughout the study period (n_{S15}=7) except October, January, April, June and August. Similarly, station C9 (x) was sampled 7 times over the course of the study except October, January, March, April, June and August.

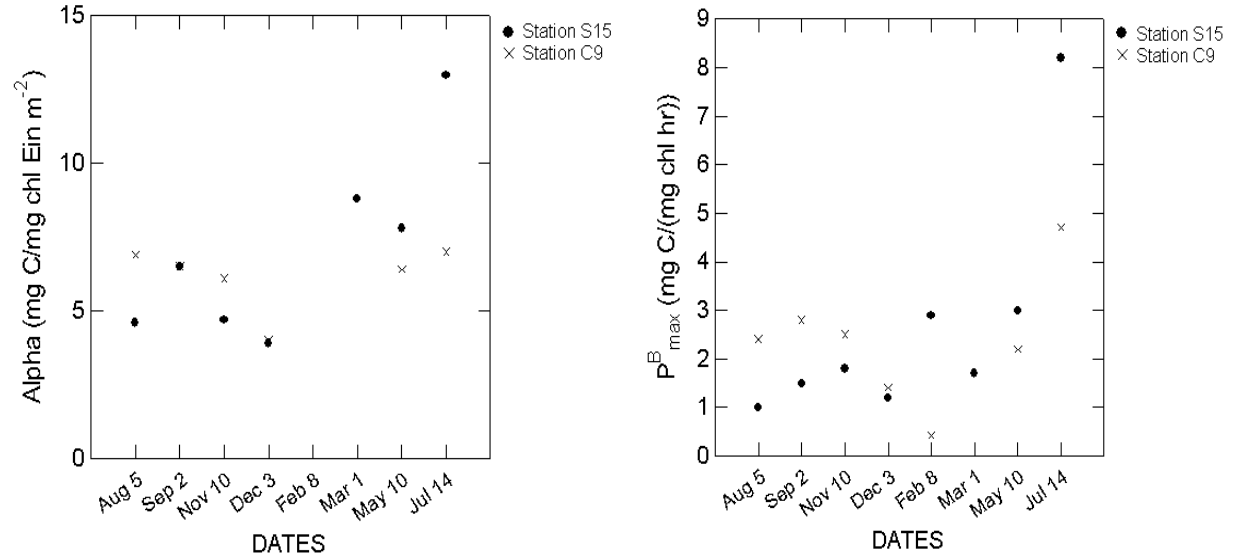

Appendix Figure 1.5 PI parameters for transitional stations a) The left figure shows light utilization efficiency (α^B; (mgC/(mg chl Ein m-2)) against the sampled date b) The right figure shows the rate of light saturation (P^Bmax; mgC/(mg chl hr)) against the sampled date. The PI parameters were generated using the Fee program (1990), PSPARMS. Station S15 was represented by the solid dot (•) and the station C9 as "x".

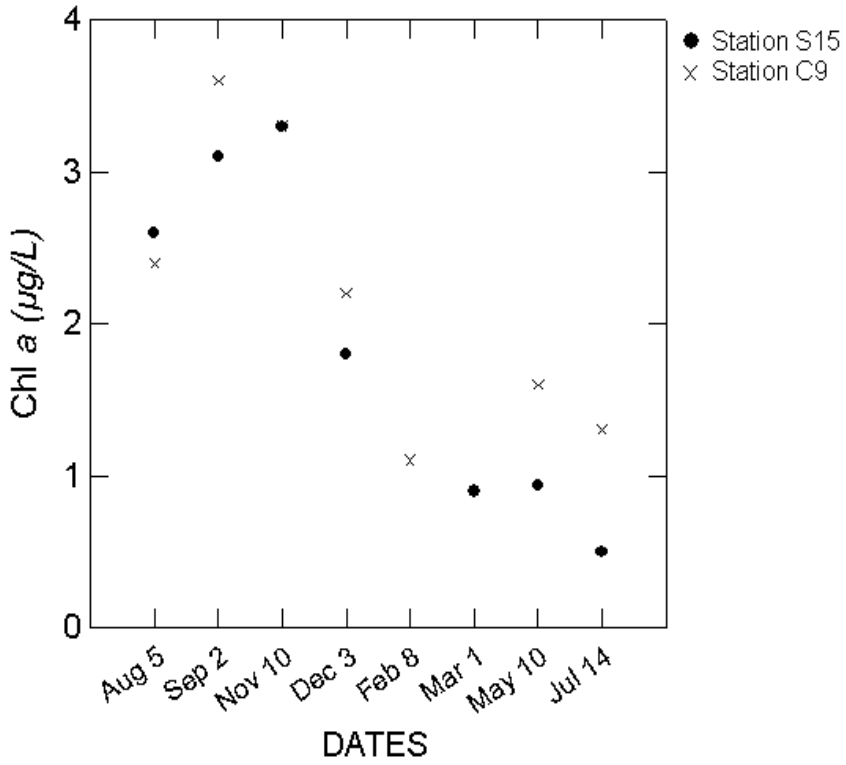

Appendix Figure 1.6 Extracted chl *a* values (µg/L) for transitional sites- C9 (•) and S15 (x).

Appendix II

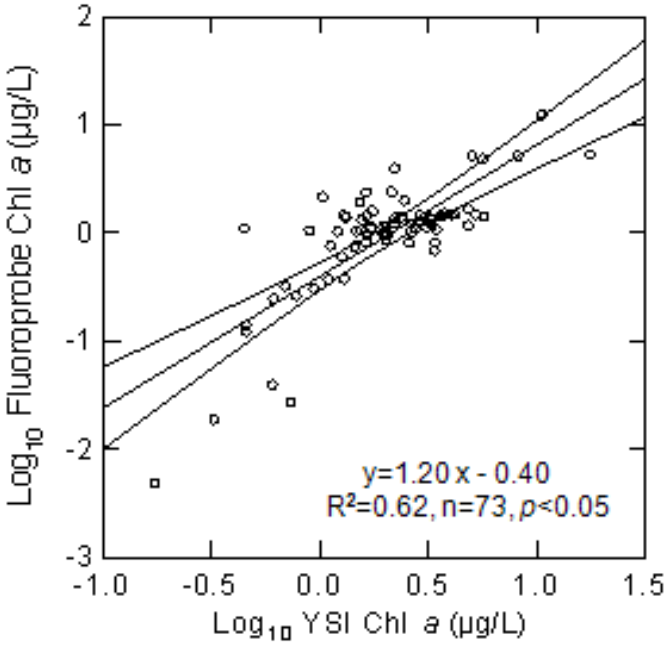

Appendix Figure 2.1 A plot of $\log_{10}$ transformed fluoroprobe chl *a* vs. YSI chl *a* (µg/L) for all the available seasons (n=73). The equation of the line is y=1.20x-0.40 and the R^2 is 0.62. The middle line represents the slope and the other two lines show upper and lower 95% confidence interval. The *p*-value that the slope of the regression line is zero was <0.05.

Appendix Table 2.1 Summary table of the coefficients (slope and intercept), standard error of the estimate (Std error) and 95% confidence interval from the model I linear regression of log_{10} transformed fluoroprobe and YSI chl *a*. Two outliers were identified and were removed from the analysis.

Effect	Coefficient	Std Error	Lower 95%	Upper 95%
Constant	-0.40	0.051	-0.50	-0.30
Log_Extracted	1.22	0.11	0.99	1.44

Appendix Table 2.2 Table of analysis of variance. The list of parameters (sum-of-squares, degree of freedom (df), mean square, F-ratio and *p*-value) are summarized. All values remained log_{10} transformed. Two outliers were omitted from the analysis.

Source	Sum-of-Squares	df	Mean-Square	F-ratio	*p*-value
Regression	12.7	1	12.7	1.15E+02	0.00
Residual	7.85	71	0.11		

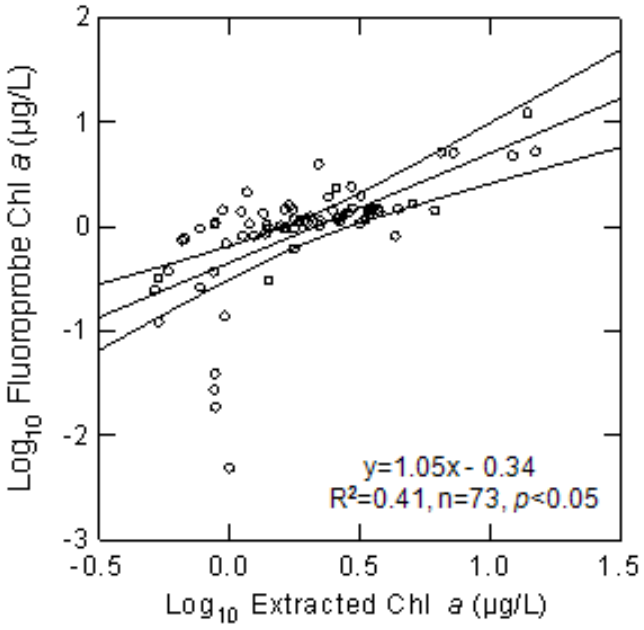

Appendix Figure 2.2 The model I linear regression of $\log_{10}$ transformed fluoroprobe and extracted chl *a* (n=73). The slope is 1.05 and the y-intercept is -0.34 (y=1.05x-0.34). The R^2 was 0.41 and the significance of the slope of the regression line being zero was $p<0.05$.

Appendix Table 2.3 Table of coefficients (slope and intercept), standard error of the estimate (Std error) and 95% confidence interval from the model I linear regression of $\log_{10}$ transformed fluoroprobe and extracted chl *a*. Two outliers were excluded from the analysis.

Effect	**Coefficient**	**Std Error**	**Lower 95%**	**Upper 95%**
Constant	-0.34	0.0641	-0.47	-0.21
Log_YSI	1.05	0.15	0.75	1.34

Appendix Table 2.4 Analysis of Variance**.** The list of parameters (sum-of-squares, degree of freedom (df), mean square, F-ratio and *p*-value) are summarized. The values remained $\log_{10}$ transformed. Also, two outliers were omitted from the analysis.

Source	**Sum-of-Squares**	**df**	**Mean-Square**	**F-ratio**	***p*-value**
Regression	8.45	1	8.45	49.6	0.00
Residual	12.1	71	0.17		